DEPARTMENT OF CHEMICAL ENGINEERING
UNIVERSITY OF CAMBRIDGE

# Micro-Mechanical Testing of Interfacially Adsorbed Protein Networks


DANIEL BRIAN JONES
CHURCHILL COLLEGE

A DISSERTATION SUBMITTED FOR THE DEGREE OF DOCTOR OF PHILOSOPHY
MARCH 2002

## Preface

This dissertation describes work carried out at the Department of Chemical Engineering of the University of Cambridge, for the degree of Doctor of Philosophy. This work was conducted between October 1998 and November 2001 under the supervision of Dr. Anton P. J. Middelberg. It is my original work except where stated in the text and includes nothing that has been submitted for any degree, diploma or other qualification at any other university. This dissertation contains 44 992 words and 55 figures in 163 pages. Parts of this work have been (or are going to be) presented elsewhere:

Refereed Journal Articles

Jones, D.B.; Middelberg, A.P.J. *"Direct determination of the mechanical properties of an interfacially-adsorbed protein film."* Chemical Engineering Science, in press.

Jones, D.B.; Middelberg, A.P.J. *"Micro-mechanical testing of interfacial protein networks demonstrates ensemble behaviour characteristic of a nano-structured biomaterial."* Submitted to Langmuir, January 2002.

Jones, D.B.; Middelberg, A.P.J. *"Influence of interfacial protein networks on droplet breakup in simple shear flow."* Submitted to AIChE Journal, February 2002.

Refereed Conference Papers

Jones, D.B.; Middelberg, A.P.J. *"Mechanical properties of peptides and proteins adsorbed at the air-water interface."* 6th World Congress of Chemical Engineering, Melbourne, Australia, September 2001.

*Daniel Jones*
*Churchill College*
*University of Cambridge*
*March 2002*

## Acknowledgements

Firstly, I would like to thank my supervisor Dr. Anton Middelberg for his support and guidance during the course of my research to date. I am particularly pleased that we will continue to work together in the future and I look forward to working in the Bioproducts and Bioprocessing group as a Post-Doctoral Research Associate.

I would also like to thank the Engineering and Physical Sciences Research Council for providing financial support for this work in the form of a Research Studentship and Research Grant for the project.

Special thanks must go to all my friends and colleagues in the Bioproducts and Bioprocessing group who have made contributions through discussion and feedback on all aspects of my work. Mostly, however, I simply wish to thank them for the friendship that has enriched my time in Cambridge so greatly. In alphabetical order: Adam, Alex, Allessandro, Andre, Chew Tin, Christoph, Daniel, David, Giacomo, Heikki, Jason, Jemma, Mark, Nicole, Rene, Wen Bin, Woo Seok. Particular thanks must go to Jemma for help proof-reading this document.

I would like to thank members of the Chemical Engineering and Engineering workshops (Paul, Lee, Andy, Dave) for help building equipment and making later modifications. Thanks are also due to Chris Lomax for help with some experiments presented in Chapter 6 and to Dr. Wilson for allowing use of his Laser Particle Sizer.

I am also grateful to the members of the Chemical Engineering Department at Nottingham University for providing me with a solid foundation in the area and nurturing my enthusiasm for the subject. Particular thanks in this regard are due to Prof. Azzopardi and Dr. Jones.

Finally my very special thanks must go to my family, Eve, Brian, Abby and Hannah for their unfailing love and support. Their presence at my side through all the highs and lows of my life has been a source of great comfort and inspiration.

*Daniel Jones*

*March 2002*

## Summary

Droplet breakup is a key step in emulsion processing and manufacture. An ability to predict droplet disruption in a known flow field is essential to allow emulsion product formulation with the optimal droplet size, minimise energy input during manufacture and to reduce shear damage of the surface-active species. Conventional theories for predicting droplet disruption are based upon interfacial energy alone and fail when a protein emulsifier is present at moderate concentration. This is because the protein forms an interfacial network having mechanical strength.

New equipment, the Cambridge Interfacial Tensiometer (CIT), was designed and constructed to directly determine the mechanical properties of protein films adsorbed at the air-water and oil-water interfaces. The technique is an interfacial two-dimensional analogy of conventional materials testing methodology, but is conducted with high spatial resolution and requires the measurement of micro-Newton forces. Interfacial elasticity modulus values were of order 200 mN/m for β-lactoglobulin networks at the air-water interface, consistent with a calculated ensemble average estimated using Atomic Force Microscopy derived data on the unfolding of individual protein molecules†. Interfacial elasticity modulus increased with protein concentration, although a 31% enhancement in the maximum stress transmitted through the protein film resulted when sub-interfacial β-lactoglobulin concentration was reduced from 1.0 mg/mL to 0.01 mg/mL. Reduced competition for interfacial space at lower protein concentrations is believed to result in greater conformational change, and hence entanglement, on adsorption to the interface from dilute solution. Importantly, this study suggests that network mechanical response is determined by residual protein tertiary structure, and that adsorbed networks should therefore be analysed as nano-structured biomaterials. The mechanical properties of adsorbed layers of *de novo* peptides were determined with the CIT. The peptides were shown to exhibit the extremes of protein behaviour previously observed, demonstrating the possibility of controlling product form and functionality through combined hydrodynamic and molecular specification.

This is the first study to establish the mechanical properties of an adsorbed protein film using conventional stress-strain approaches to high material deformations. The work demonstrates that droplets surrounded by interfacially adsorbed protein should be viewed as deformable capsules or cells enclosed within a stress-transmitting network. Deformation and disruption could then be predicted by existing theories for such systems, using the constitutive data provided by the CIT stress-strain tests. Such an approach is expected to be superior to existing methods based solely on interfacial energy.

† Data from Carrion-Vazquez *et al.* (1999) and Best *et al.* (2001).

# Table of Contents

## List of Figures

## List of Tables

## Notation

| | | |
|---|---|---|
| $A$ | Area | [ $m^2$ ] |
| $E$ | Young's Modulus of Elasticity | [ Pa ] |
| $G$ | Shear rate | [ $s^{-1}$ ] |
| $P$ | Pressure | [ Pa ] |
| $Pr$ | Probability | [ - ] |
| $r$ | Radius | [ m ] |
| $R$ | Molar ratio | [ - ] |
| $t$ | Interfacial film thickness | [ m ] |
| $V$ | Volume | [$m^3$] |

*Greek letters*

| | | |
|---|---|---|
| $\varepsilon$ | Interfacial dilatational modulus | [ N/m ] |
| $\phi$ | Phase angle | [ deg. ] |
| $\gamma$ | Interfacial tension | [ N/m ] |
| $\mu$ | Shear modulus | [ N/m ] |
| $\eta$ | Viscosity | [ Pa.s ] |
| $\lambda$ | Viscosity ratio | [ - ] |
| $\pi$ | Interfacial pressure ($\gamma_{\text{clean interface}} - \gamma_{\text{emulsifier}}$) | [ N/m ] |
| $\Omega$ | Capillary number | [ - ] |
| $\Omega_{crit}$ | Critical capillary number | [ - ] |

*Superscripts*

| | | |
|---|---|---|
| ' | Elastic response | [ - ] |
| " | Viscous response | [ - ] |

*Subscripts*

| | | |
|---|---|---|
| $C$ | Continuous phase | [ - ] |
| $D$ | Dispersed phase | [ - ] |

# 1. Introduction

The breakup of droplets in an inhomogeneous flow is a key process in emulsion manufacturing and manipulation, and has long been a subject of interest in both chemical engineering and fluid dynamics (Janssen *et al.*, 1994). An early example of an "engineered" emulsion product is homogenised milk, produced by Gaulin with his first high-pressure homogeniser and drunk at the World's Fair in Paris in 1900 (Becher, 1991).

Emulsion droplet size controls the functionality of products and the efficiency and reproducibility of a range of processes. For example, interfacial area determines the productivity of some biocatalytic transformations (Hickel *et al.*, 1999), the storage stability of drug emulsions (Zurowska-Pryczkowska *et al.*, 1999), and the form and functionality of food products comprising multiple phases (Dickinson, 1992). Optimal emulsion functionality may be achieved at some optimum droplet volume as this determines the rates of settling or creaming (Walstra, 1996), and also the specific surface area available for adsorption of surface-active species. Therefore, the ability to predict droplet disruption in a given flow field is required to allow emulsion formulation with optimal droplet size, minimise energy input required for emulsification, and reduce the potential for damage of surface-active species in zones of excessive shear (Wolf *et al.*, 1996). In emulsion processing, the presence of a protein layer having mechanical strength affects both the ease of initial droplet disruption (Williams *et al.*, 1997) and the subsequent emulsion stability during storage (Dickinson *et al.*, 1988).

Emulsification can be broadly defined as the breakup of large droplets of one liquid in another immiscible liquid. The average droplet size is usually in the range of 0.2 μm – 50 μm. The interfacial area in a concentrated emulsion can be as high as 5000 $m^2$ (~1 football pitch) per litre of dispersed liquid. The structure, total area and mechanical properties of the interface can impact on many aspects of the emulsion system. For example the oil phase volume, droplet size distribution and interfacial properties can all influence the stability, rheology and flow properties of emulsion based products. For these reasons characteristics such as interfacial energy and

interfacial rheology are important areas of study when dealing with emulsion systems. A liquid droplet behaves as if it were surrounded by an imaginary "skin" which tends to shrink the interface to the smallest possible area. This is the called the surface or interfacial tension and has units of $J/m^2$ or N/m. Classical mechanics indicates that the interfacial tension is the work required to increase the area by a unit amount. Free energy and reversible work are equivalent in thermodynamics so surface tension is more accurately termed interfacial free energy. Examples of the minimisation of interfacial free energy surround us in everyday life: the sphericity of raindrops and soap bubbles, capillary rise in thin tubes and the ability of insects such as water beetles to "walk" on a pond interface. In the literature "surface" and "interface" are often used interchangeably. For this work "interface" is preferred for a fluid-fluid boundary and "surface" used where a fluid is in contact with a solid phase. Exceptions are made when quoting or analysing existing literature where the original terminology is kept.

The large excess free energy associated with the high interfacial area of emulsions requires the input of large amounts of energy to create an emulsion with a sufficiently small size distribution to render it dynamically stable. Most practical uses of emulsions depend on the possibility of controlling and manipulating their droplet size and stability by the judicious addition of emulsifiers (Lucassen-Reynders, 1996). The two major classes of interfacially active molecules are proteins and low molecular weight surfactants. Both play a vital role in the creation and stabilisation of the product microstructure. Important aspects regarding potential interfacially active molecules are: their capability to lower the interfacial tension and the rate of lowering; the adsorbed amount; their ability to desorb; the possibility of conformational change during and after adsorption; the thickness of the adsorbed layer; the interaction between the adsorbed molecules; and their lateral mobility (Bos and van Vliet, 2001).

Low molecular weight surfactants are simple amphiphilic molecules, generally consisting of a hydrophobic tail and a hydrophilic head group. Such molecules self-associate at interfaces, with the appropriate part of the molecule located within the hydrophilic or hydrophobic fluid phase, forming a fluid adsorbed layer. Proteins, however, are much larger and more complicated macromolecules consisting of a

folded chain of amino acids with varying degrees of hydrophobicity. Protein molecules adsorb at the interface but then proceed to unfold and expose more hydrophobic groups to the non-aqueous phase (Figure 1-1). As a result of the molecular unfolding, the protein molecules develop strong interactions with their neighbouring protein molecules, and effectively form a network at the interface, albeit a very thin structure (~5 nm thick, see next chapter for further details).

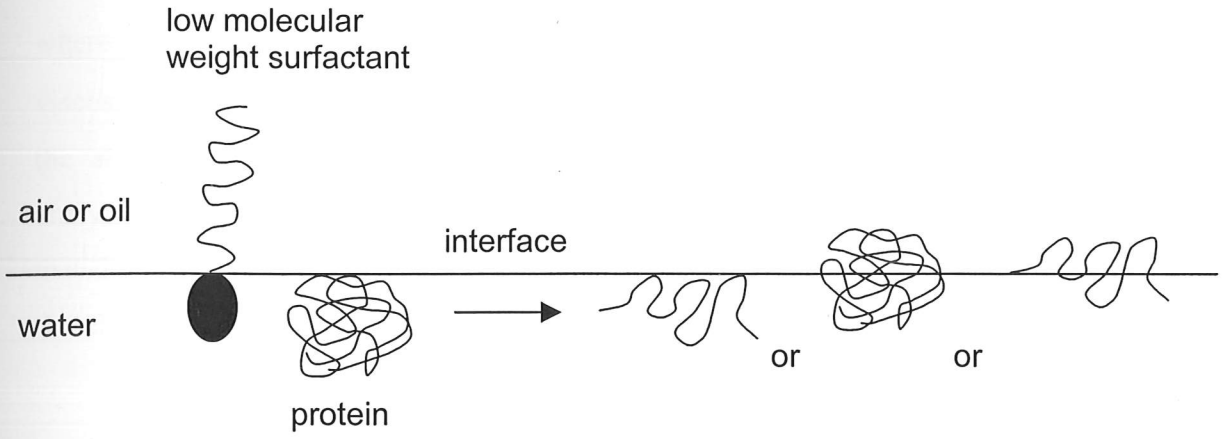


**Figure 1-1** **Conformation of a low molecular weight and a macromolecular emulsifier at a fluid-fluid interface (not to scale). The two drawings on the right apply to oil-water interfaces. Reproduced from Bos and van Vliet (2001).**

Important product characteristics, such as stability, viscosity, consistency, texture, shelf life, reaction time, distribution and release of active components, colour and taste are all decisively influenced by the particle size distribution. The objective of every emulsifying technique is, therefore, to attain a specific droplet size distribution. The aim of engineers and scientists involved in the production of emulsion based products is to predict the functionality and performance of emulsions from the structure and dynamics of the components, which allows the manipulation of ingredients or processing conditions to create a product with the required properties.

A commonly encountered approach to predict droplet disruption is the use of a plot of dimensionless capillary number *($\Omega$)*, or laminar Weber number, versus viscosity ratio of the dispersed and continuous phases *($\lambda$)*. Such a plot is shown in Figure 1-2. The

capillary number represents the ratio of the viscous forces causing droplet deformation and the stabilising Laplace (interfacial tension) forces,

$$\Omega = \frac{\eta_C . G}{\gamma / r} \tag{1.1}$$

$$\lambda = \frac{\eta_D}{\eta_C} \tag{1.2}$$

where $\gamma$ = interfacial tension, $G$ = shear rate, $r$ = droplet radius, $\eta_D$ = dispersed phase viscosity, $\eta_C$ = continuous phase viscosity. This type of generalised plot works well in the absence of any interfacially active species. However, such a hydrodynamic analysis makes two implicit assumptions about the behaviour of the interface. Firstly that the interfacial tension is constant and uniform around the droplet, and secondly that the interface has negligible elasticity and viscosity.

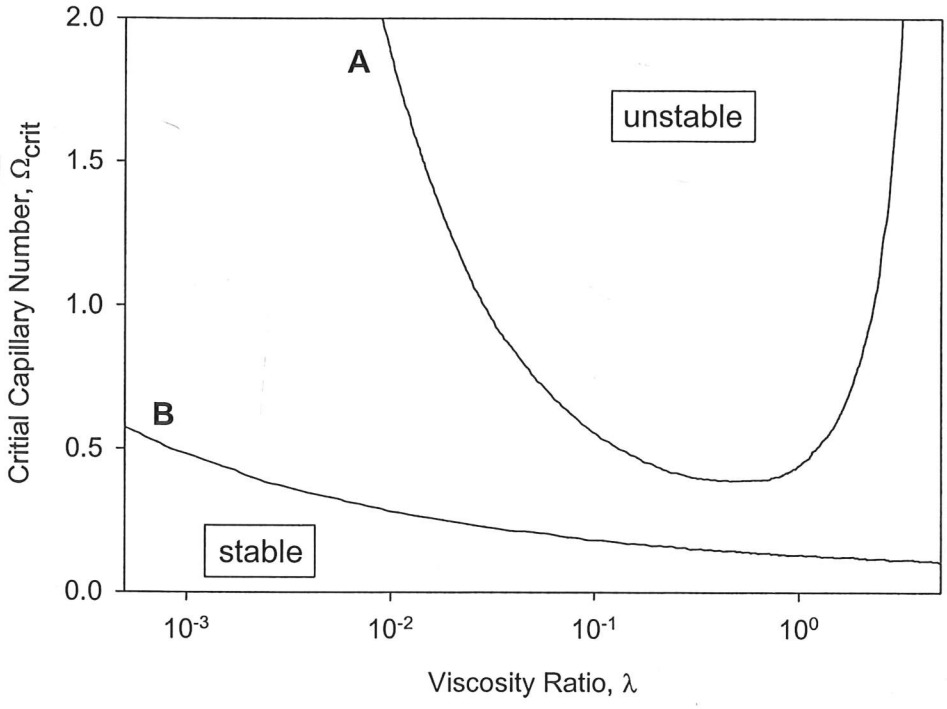


**Figure 1-2** **Critical capillary number as a function of viscosity ratio for surfactant free systems. Simple shear flow A, plane hyperbolic flow B. After data by Grace (1982) and Bentley and Leal (1986).**

In the case of an interfacially adsorbed emulsifier the critical capillary number for breakup can deviate from that indicated by the plot shown in Figure 1-2. Janssen *et al.* (1994) studied the effect of low molecular weight (non-protein) emulsifiers on droplet breakup. The results showed that the droplets were always at least as stable as expected from capillary number predictions. In certain cases a greater shear rate (higher capillary number) was required, and this effect was phenomenologically characterised using an empirical interfacial tension greater than the equilibrium value. A correlation was developed using a single fit parameter and the resistance of the interface to expansion, which was measured experimentally. The authors attributed the increased droplet stability to interfacial viscoelasticity, caused by the presence of an emulsifier, making droplet breakup more difficult.

In contrast, the work of Williams *et al.* (1997) has shown that the capillary number plot and the modifications proposed by Janssen *et al.* (1994) fail when a moderate concentration (> 0.01 mg/mL) of the globular protein β-lactoglobulin is present in the aqueous phase. The result is a droplet that is smaller than that predicted from the equilibrium interfacial tension using conventional theories. This indicates a droplet destabilising mechanism that results in disruption at a lower shear rate than expected from interfacial energy correlations. In contrast, another commonly used milk-protein emulsifier (β-casein) did not result in deviations from the results predicted from the capillary number plot. Therefore, whilst protein interfacial adsorption has been extensively studied, our ability to predict emulsion droplet size in even simple shear flow is lacking when certain proteins are adsorbed at moderate concentration.

In a review of the static and dynamic aspects of protein behaviour at interfaces Walstra and De Roos (1993) concluded that "most effects of adsorbed proteins on the various kinds of physical instability of emulsions and foams are semiquantitatively understood, but that the variation among proteins in the production of small droplets and bubbles during emulsification and foaming, respectively, still largely defies explanation". The inability of existing theories to enable a prediction of droplet size suggests that a radical re-think of our view of emulsification is required. Such emulsions might, for example, be better considered as cells or as membrane-bound capsules. Such a view is not inconsistent with very early studies, such as those of

Ascherson (1840), which drew analogies between cells and protein-stabilised emulsions.

If successful predictions of droplet disruption cannot be made from the interfacial tension alone then more sophisticated experimental techniques are required to measure other interfacial properties when adsorbed protein molecules are present at the interface. Workers studying the interfacial rheology of protein and surfactant solutions have devised a host of different experimental techniques and analysis methods (Miller *et al.*, 1996). Experimental difficulties and limitations more often determine the approach taken than rational selection of the optimal testing method. The dynamic response of an interfacial film can provide insight into the degree of inter- and intra- molecular bonding, competition for interfacial space, and the extent of conformational changes in the protein molecules. Interfacial dilatational rheology is determined by measuring the change in interfacial tension, due to a specific change in interfacial area. This is a measure of the resistance to compression and expansion of the interface. Interfacial shear rheology, on the other hand, can be a direct measure of the mechanical strength of the adsorbed layer. Usually in this type of test the interface is subjected to a shear stress, and the measured strain is recorded. The most accurate and reproducible results tend to come from methods that utilise small, reversible applied stresses or strains, thus minimising any disruption or damage to the interfacial layer. Therefore, such data are invariably limited to the low strain regime. The theory of interfacial rheology is two-dimensional as the stresses and strains are measured in the plane of the interface. However, in reality a three-dimensional film with a thickness of the order of a few nanometers is being experimentally investigated. An interfacial stress (units mN/m) and a dimensionless interfacial strain are defined. By analogy with three-dimensional systems Newtonian interfacial flow and Hookean interfacial elasticity can then be represented. A major problem in the current literature base is that the published information is highly fragmented and uses different equipment on widely varying protein systems, making the task of providing overarching conclusions in this area extremely difficult. This is an inevitable consequence of a research field lacking a clearly defined testing method and no universal "standard" result with which to calibrate new techniques or test alternative theories.

Variations in interface age, method of formation, degree of deformation and measuring technique make the extraction of accurate and meaningful relationships between protein structure, inter- or intra- molecular bonding and film strength very difficult. There are many conflicting results in the reported behaviour of protein films adsorbed at both the air-water and oil-water interfaces. One of the few consistent patterns to emerge is that globular proteins show higher resistance to interfacial shear and dilation at low deformation (Graham and Phillips, 1980a, 1980b; Williams and Prins, 1996; Faergemand *et al.*, 1997; Faergemand and Murray, 1998). However, the degree of deformation for the quoted shear modulus is often not quantified or is defined differently by each research group. Creep tests at constant shear stress obviously yield a slightly different type of information and are highly sensitive to the constant shear stress used. For the case of an interfacial network with mechanical strength, most techniques for the determination of interfacial rheology are flawed because they are invasive procedures that partly destroy the network that they seek to measure, unless the degree of deformation is vanishingly small. In these small deformation experiments, the material properties measured are usually assumed to be in the initial linear elastic regime. Many studies have provided results for the shear modulus of adsorbed protein films, but the dilatational modulus is reported much more rarely. The measured interfacial rheological response is often assumed to be either perfectly viscous or perfectly elastic to avoid isolating the recoverable and non-recoverable components of the energy input. Therefore, interpretation of the results from some techniques is highly subjective.

For the study of droplet breakup it is most desirable to have information on the mechanical properties of protein layers adsorbed at the oil-water interface. However, due to the technical difficulties involved in performing experiments at the oil-water interface there is much more information available regarding the air-water interface. Apart from this lack of information for the oil-water interface, it is far from clear how the results from interfacial rheology experiments should be interpreted to help predict droplet disruption. In the case of an adsorbed protein network the dilatational modulus presumably measures a combination of the change in interfacial tension and the effects of stresses transmitted directly through the network. This would explain the lower level of sensitivity to protein conformation and structure of interfacial dilatational experiments compared with shear-based methods. However, interpretation

of interfacial shear data is fraught with difficulties due to the large variations in the experimental procedures reported in the literature. For example, creep-compliance tests at constant stress, continuously straining techniques and experiments performed with low amplitude oscillations where the amplitude can be set differently by each group of workers.

The technical problems outlined here and in the Literature Review (Chapter 2), coupled with the confusing and sometimes conflicting results, clearly establish the need for a new experimental technique. A technique capable of operating over a wide range of total deformation and strain rate would enable more insightful interpretation and unification of the existing body of literature. Such a technique should not be limited to small deformation studies and must not require any assumptions about the behaviour of the interfacial material under test to enable truly objective analysis of the experimental results.

Novel equipment, the Cambridge Interfacial Tensiometer (CIT), will be developed in this study to directly measure the mechanical properties of interfacial protein networks. The instrument will be designed to try to avoid the some of the major problems with existing equipment for measuring interfacial rheology. Specifically, the need of many low-strain shearing techniques to make *a priori* assumptions about the material behaviour (e.g. linear response to a pre-defined strain). The CIT should be capable of providing more detailed information about the interfacial network mechanical properties to fully describe the material behaviour up to the failure point, rather than simply reporting an initial elasticity modulus. The instrument will, therefore, have to been significantly different from existing equipment designed to subject the interface to shear, or dilatational approaches producing a $\pi$-$A$ diagram analogous to a $P$-$V$ isotherm.

Detailed data available from CIT tests will be used to investigate the reasons for failure of the capillary number correlation and allow more accurate prediction of the droplet size resulting from exposure to a known flow regime. The CIT should have the ability to create full stress-strain curves for the adsorbed film that could be used for the generation of a material constitutive equation. Such detailed information on

the film behaviour would allow *a priori* computational modelling of droplet deformation and breakup, and indicate the validity of predicting droplet size using a plot of critical capillary number versus viscosity ratio. Detailed information on the mechanical properties of adsorbed proteins or peptides could be used to optimise emulsion processing conditions, or to facilitate the design of biomolecules having the most favourable characteristics for the creation and stabilisation of emulsion-based products. This approach would enable emulsion product optimisation through the combined processes of molecular design and hydrodynamic specification.

At present, engineers can specify the shear environment an emulsion droplet will experience though control of the hydrodynamic environment. However, current droplet disruption models fail in the presence of commonly used protein emulsifiers. Therefore, the primary aim of this work is to provide detailed information on the mechanical properties of the interface under such conditions, that can be used in fundamental modelling techniques with true predictive capacity. The secondary aim is to design the interfacial properties to provide control in the formulation of emulsion based products through both hydrodynamic and molecular specification. To satisfy these aims, four major objectives must be reached. The first objective is the detailed design, construction and validation of the CIT. The instrument must be validated and tested to ensure the results are truly representative of the interfacial test material. These tests are all performed at the air-water interface. The next objective is to link the interfacial mechanical properties to the molecular structure and mechanisms of intermolecular interaction. Having performed multiple tests at the air-water interface the CIT must be refined to operate at the oil-water interface. The third objective is, therefore, to use the CIT to obtain detailed constitutive relationships for protein networks bound at the oil-water interface and correlate these data with changes in droplet disruption mechanism. The secondary aim requires the demonstration of an ability to control the interfacial mechanical properties. Therefore, the final objective is to select and design peptide systems capable of showing the extremes of protein behaviour found in previous experiments.

Prediction of droplet disruption is usually based on engineering correlations employing empirical fits based on various dimensionless groupings. The work of Williams *et al.* (1997) clearly showed that the presence of an interfacial protein

network caused a destabilising effect that could not be explained through calculations based solely on interfacial energy. Therefore, a review of the protein interfacial rheology literature was conducted and is presented in the following chapter. This review highlights certain deficiencies in the existing knowledge base and the difficulties in interpreting such data to provide insights into droplet disruption.

New equipment was developed to test the mechanical properties of interfacial networks, inspired by conventional materials testing techniques and the desire to produce a constitutive equation for the interfacially adsorbed material. The equipment design, construction and modes of operation are discussed in the Materials and Methods section (Chapter 3). Having constructed the new equipment it was vital to test for correct operation and check that the results are truly representative of the material adsorbed at the interface. More specifically, to check that the results are a function of material mechanical properties rather than equipment design or operating parameters. Chapter 4 is concerned with this equipment validation. For ease of operation all tests were performed at the air-water interface. The work presented in Chapter 5 aims to demonstrate a link between the mechanical properties of the interface and the molecular structure, and to provide further insight into the mechanisms of protein-protein interaction for the adsorbed species. The influence of hydrophobic and disulfide bonding is considered, as well as the relationship between the ensemble network properties measured using the CIT and studies on the unfolding of individual protein molecules by Atomic Force Microscopy (AFM).

The work presented in Chapter 6 involves refinement of the CIT design and test procedures for operation at the oil-water rather than the air-water interface. In addition, a device to produce simple shear flow was designed, constructed and employed to disrupt oil droplets surrounded by a network of adsorbed β-lactoglobulin, to confirm the failure of the capillary number correlation as a predictive method under such conditions. The more advanced CIT design and the knowledge gained from Chapter 5 was then combined with this technique for disrupting oil droplets in a well-defined flow field to demonstrate the value of the CIT as a tool in the prediction of droplet disruption. Further investigations into the molecular origins of the strength of the protein networks, and the desire to control interface mechanical properties,

resulted in the decision to use peptides of clearly defined secondary structure as models of commonly occurring protein structural motifs. This work (presented in Chapter 7) led to the eventual design of a *de novo* peptide, specifically created to form rigid interfacial networks of adsorbed peptide. The aim of generating peptide-based structures through rational molecular design allows a host of exciting design possibilities for the creation of novel bioproducts and bioprocesses to be considered. Chapter 8 draws conclusions from the work completed and suggests important areas for further investigation such as modifications to the CIT and scope for synergistic benefits through combination with other techniques capable of providing information on the interfacial molecular structure in real time. This final chapter concludes with potential strategies for further molecular design.

# 2. Literature Review

## 2.1. Emulsification

Emulsification is the dispersion of liquid droplets in a second continuous phase. The phases are immiscible and the size of the dispersed droplets is usually in the range 0.2 μm – 50 μm (Lucassen-Reynders, 1996). Emulsions are usually termed oil-in-water if the non-polar phase is distributed in the aqueous phase and water-in-oil for the reverse. Emulsions are important in the broad areas of food technology, nutritional and pharmaceutical sciences as well as the chemical and detergent industries.

Emulsification agents are required in many foods containing fats. Obvious examples include margarine and salad dressings. They are frequently used in products such as ice cream and cheese spreads to lower the calorie content by removing fat and substituting with water to maintain the food bulk. Emulsion formation is important in many reactions occurring at or across the oil-water interface to increase the interfacial area, and hence bulk rate of reaction. Many biocatalysts, such as the enzyme lipase, are water-soluble yet catalyse reactions involving the oil phase, and thus require the presence of both an oil and water phase. Lipase catalyses the breakdown of triacylglycerols to mono or di-acylgylcerols and fatty acids, which may be of use in both the food and pharmaceutical industries (Stryer, 1995). An emulsion can be used to dilute and deliver a highly concentrated oil-soluble product such as a pesticide or drug, with a less valuable aqueous bulk phase. The use of peptide emulsifiers, with simpler secondary and tertiary structure than proteins, should enable a better understanding of the mechanisms of droplet breakup when protein and peptide are present at the oil-water interface. This is particularly valuable as existing theories fail under certain conditions, and an improved understanding may ultimately lead to the creation of more accurate correlations with a wider range of applicability.

### *2.1.1. Emulsifier Efficacy*

The job of an emulsifier or surfactant is twofold: firstly to lower the interfacial tension to enable drops to be disrupted, and secondly to stabilise the resulting emulsion droplet against coalescence (Walstra, 1993). An emulsion droplet is stabilised by its

Laplace pressure, $\gamma/r$, where $\gamma$ is the interfacial tension and $r$ is the droplet radius (Grace, 1982). The droplet will be disrupted when deformation forces arising from the fluid flow overcome the stabilising Laplace pressure. It follows that droplets of a given size can be formed at a lower shear rate, and hence energy input to the system, if the interfacial tension can be reduced. Alternatively, smaller droplets can be formed in an item of emulsification equipment at normal operating conditions.

To maintain emulsion stability it is necessary to understand the mechanisms by which destruction of an emulsion can occur. There are four main mechanisms: Oswald ripening, creaming, aggregation and coalescence (Walstra, 1996). Oswald ripening is the diffusion of material from a small droplet to a larger one, increasing the average droplet size of the emulsion. It results from an increase in chemical potential of the dispersed phase due to the Laplace pressure. The Laplace pressure is greater in a small droplet than a large one, so the difference in chemical potential provides the driving force for diffusion of the dispersed phase material from the smallest drops to the largest. Oswald ripening can be retarded under several conditions. The most obvious being when the dispersed phase has minimal solubility in the continuous phase, although it is also retarded if the surfactant is unable to desorb from the oil-water interface (Dickinson, 1992; Walstra, 1996). The second condition occurs for insoluble surfactants or for very highly surface-active species. Due to the irreversible nature of protein adsorption, it is not thought that this method is a significant issue in protein stabilised emulsions.

Creaming or settling is simply a result of a density difference between the continuous and dispersed phases. This effect is much greater for large particles. Therefore, the rate can be reduced by retarding other destabilising effects. Creaming effects can also be reduced by increasing the continuous phase viscosity or by attempting to form a macromolecular network in the phase surrounding the droplets (Dickinson, 1992). The two important roles of a surfactant are to reduce the interfacial tension allowing an emulsion to be formed, and then to stabilise the emulsion against coalescence. Coalescence of emulsion droplets will always be thermodynamically favourable due to the increased interfacial energy of such a system. Therefore, methods to stabilise emulsions must provide an energy barrier against aggregation and coalescence. For

emulsion droplets to coalesce, the film of continuous phase liquid between them must drain to a thickness where it will collapse. Fisher and Mitchell (1988) observed the draining film between approaching droplets in aqueous protein solution. They found that β-casein behaved as a conventional surfactant with the film draining to some critical thickness. However, with lysozyme present at the interface the film drained to a metastable distance and then remained at this separation for a time varying from minutes to hours, depending upon the film thickness and age. The authors suggested that the chance of draining film collapse is related to the mechanical properties of the adsorbed protein film. However, care is required in the interpretation of these experimental results due to the large size of the droplets (~1.2 mm). Real emulsion droplets are likely to be about three orders of magnitude smaller and as mentioned above, the coalescence stability is a strong function of droplet size. Dickinson *et al.* (1988) also found that lysozyme adsorbed at the oil-water interface substantially increased the stability of emulsion-sized droplets, although their work was conducted at a planar interface.

Small molecule surfactants are able to stabilise emulsions due to their mobility in the interface. A momentary imbalance of surfactant distribution will cause diffusion towards the region of surfactant depletion or high interfacial tension. In this way the interface can resist any deformation that will result in a gradient in the interfacial tension and provides a kind of "self-healing" mechanism for the interface. This is known as the Marangoni effect. The simplest way to express this resistance to deformation is the Gibbs Elasticity.

$$\varepsilon = \frac{d\gamma}{d(\ln A)} \qquad (2.1)$$

where $2\varepsilon$ = Gibbs Elasticity (the original definition proposed by Gibbs was for a two-sided soap bubble) and $A$ = interfacial area. The Gibbs Elasticity is thought to be a crucial parameter in maintaining the stabilisation of a thin film against rupture for such surfactants (Walstra, 1996). The effect is likely to be greatly reduced for proteins and crosslinked peptides that are adsorbed at the interface, due to their lower mobility. However, such molecules may form interfacial networks that have a degree of

elasticity resulting from their structure rather than the Marangoni effect discussed above. The two stabilisation mechanisms are, therefore, provided through mutually exclusive interfacial behaviour (Enser *et al.*, 1990; Clark *et al.*, 1994; Mackie *et al.*, 1999).

Adsorbing polymers can create very stable emulsions due to the steric repulsion of the polymer chains. This is a form of entropic stabilisation caused by the loss of mobility of the polymer chains and can act over relatively large distances. However, a non-adsorbing polymer can have a deleterious effect on emulsion stability. This is because the centre of the polymer molecule cannot approach the droplet closer than the radius of the coil. The result is a depletion layer surrounding the droplet with a lower osmotic potential. Overlap of depletion layers of adjacent droplets decreases the overall depletion volume, which is energetically favourable and results in droplet aggregation. Generally, proteins have exposed hydrophobic patches, providing a mechanism to anchor the molecule to an air-water or oil-water interface. Therefore, proteins have the potential to provide steric interaction and stabilisation if a long, water soluble, peptide chain can be extended into the aqueous environment.

### 2.1.2. Predicting Droplet Breakup

In the absence of any surface-active species, droplet breakup in a steady, simple shear flow can be predicted from a plot of viscosity ratio *($\lambda$)* against capillary number *($\Omega$)*. A generalised plot for droplet disruption in simple shear and plane hyperbolic flow is presented in Figure 2-1.

$$\lambda = \frac{\eta_D}{\eta_C} \tag{2.2}$$

$$\Omega = \frac{\eta_C . G}{\gamma / r} \tag{2.3}$$

where $\eta_D$ = dispersed phase viscosity, $\eta_C$ = continuous phase viscosity, $\lambda$ = viscosity ratio, $r$ = undeformed droplet radius, $G$ = shear rate and $\gamma$ = interfacial tension. The capillary number is the ratio of the viscous stresses exerted by the outer fluid on the

droplet ($\eta_c.G$) divided by the stabilising Laplace pressure ($\gamma/r$). When the viscous forces deforming the droplet exceed the Laplace pressure, the critical capillary number ($\Omega_{crit}$) is reached and droplet breakup occurs (Janssen *et al.*, 1994, 1997).

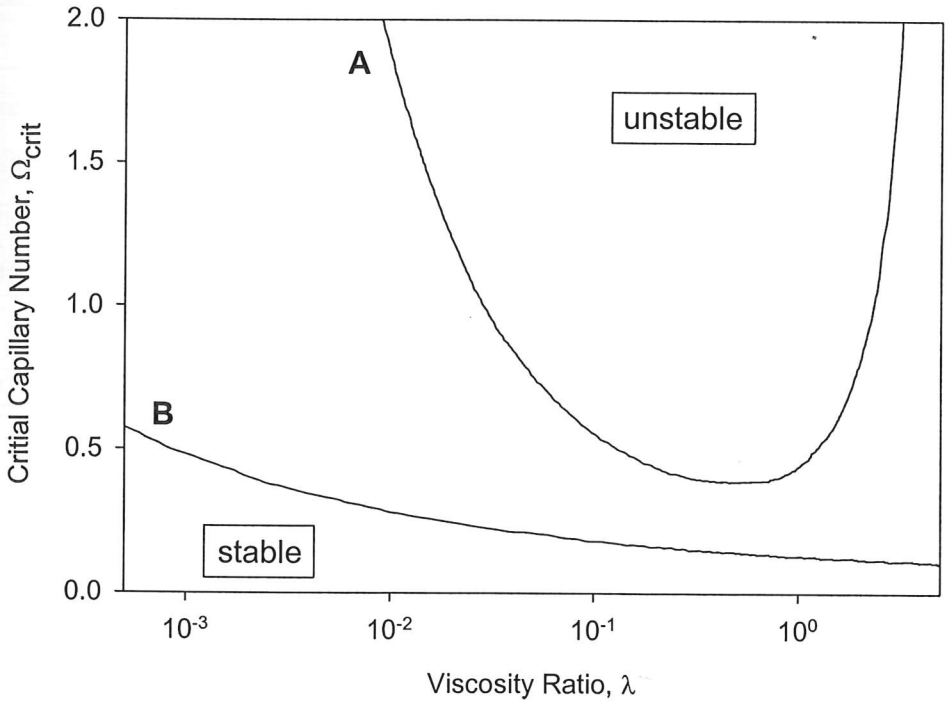


**Figure 2-1** **Critical capillary number as a function of viscosity ratio for surfactant free systems. Simple shear flow A, plane hyperbolic flow B. After data by Grace (1982) and Bentley and Leal (1986).**

It can be seen from the capillary number definition that as the interfacial tension is reduced, the capillary number rises at a given shear rate. Therefore, the capillary number is more likely to exceed the critical value. If the above approach is followed, then the only property of an emulsifier or surfactant that is considered in the theory is an ability to reduce interfacial tension. Most current hydrodynamic treatments of droplet breakup neglect the effects of emulsifiers other than their direct impact on the stabilising Laplace pressure. If such theories accurately reflected the behaviour of real systems, then one would expect the size of emulsion droplets to vary linearly with interfacial tension, i.e. breakup occurs at a constant value of the critical capillary number. This is clearly not the case and has been shown in many studies. The

divergence between experiment and theory is caused by making implicit assumptions about the system which are not true. Firstly, that the interfacial tension is constant and uniform, and secondly, that the interface transmits tangential stresses undiminished (Lucassen-Reynders, 1996). The second assumption is equivalent to negligible interfacial elasticity and viscosity. This is clearly not the case in a situation where a protein film having mechanical strength is created.

Janssen *et al.* (1994) showed that a surfactant increasing the viscoelasticity of the interfacial layer can make breakup more difficult. The ratio of actual critical capillary number to critical capillary number for the system with constant and uniform interfacial tension was always greater than 1. A correlation was suggested for this ratio in terms of the interfacial dilatational elasticity modulus, equilibrium interfacial tension and a fit parameter.

Williams *et al.* (1997) investigated the effect of β-lactoglobulin and β-casein on droplet breakup by using a Couette device and aqueous droplets suspended in silicone oil. A Couette type device can be used to generate an approximation to simple shear flow. The apparatus consists of two concentric cylinders rotating in opposite directions. Neglecting the curvature of the cylinders, which is small compared to the gap between them, a region of simple shear flow is created. Not only is the shear regime well characterised but also it can be easily calculated from the relative speeds of the two cylinders. This is an important system to study because other flow regimes can often be broken down into elements of simple shear flow. "Frequently, the local flow experienced by the drop is a (quasi-) simple shear flow." (Janssen *et al.*, 1994). Williams *et al.* (1997) found that the critical value of $\Omega$ is lower than that predicted from $\gamma$ at undisturbed conditions. The experiment showed an interesting effect that when the β-lactoglobulin concentration exceeded $10^{-2}$ mg/mL, droplet breakup suddenly became much easier (Figure 2-2). It is thought that this is a result of conformational changes in the β-lactoglobulin which allows an interfacial network, that limits the degree of droplet deformation, to be formed (Williams and Prins, 1996). This violates the second assumption of the capillary number approach mentioned above. The droplet was shown to exhibit solid-body like behaviour, breakup was unaffected by the viscosity of the dispersed phase and the internal

circulation rate was low. The authors suggest that under certain conditions the maximum stable droplet size could be decreased by a factor of around 200 from that predicted by $\gamma$ alone in this solid-body type regime. In summary, the capillary number approach fails when a protein capable of forming a strong interfacial network is present.

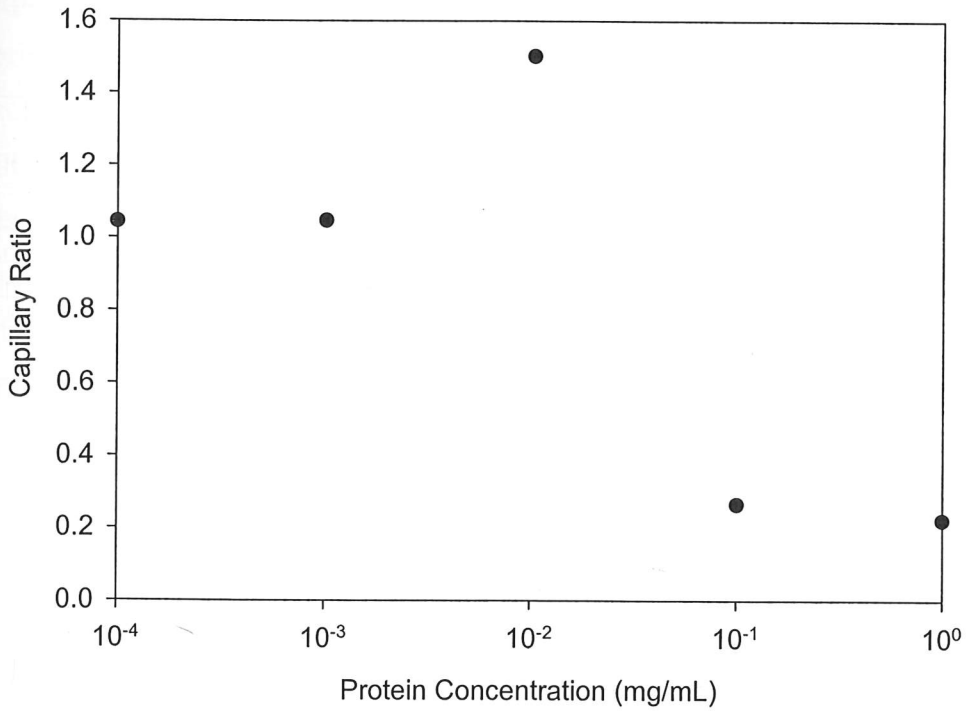


**Figure 2-2** **Capillary ratio as a function of β-lactoglobulin concentration. Reproduced from Williams *et al.* (1997). Capillary ratio denotes observed value of capillary number over that predicted from a plot of capillary number versus viscosity ratio.**

## 2.2. Interfacial Protein Networks

Literature has been available on the formation of interfacial films by proteins since Ascherson (1840) first observed protein "skins" surrounding oil droplets in protein solutions. More thorough experiments have subsequently been performed to confirm the presence of an interfacial protein network by Langmuir and Schaefer (1939) and Fourt (1939). Graham and Phillips (1979a; 1979b; 1979c; 1980a; 1980b) produced an

excellent series of papers looking at adsorption kinetics, interfacial tension, structure of the interfacial layer and interfacial rheology. However, despite these early pioneers, information regarding the thickness, structure and protein conformation after adsorption is still relatively sparse and a fundamental understanding of the processes involved in protein adsorption is still lacking (Middelberg *et al.*, 2000).

The formation of a protein film must include the following: diffusion to the interface, adsorption at the interface, followed by conformational changes and/or alteration of the orientation of the protein molecule. MacRitchie (1970) considered the adsorption of protein at the air-water interface. Upon adsorption at an interface, intramolecular stabilising bonds, present within the protein in aqueous solution, are broken. "These bonds may re-form intermolecularly and this is favoured by the relatively high concentrations possible in the monolayer" (MacRitchie, 1970). The result is an interfacial film with some degree of mechanical "strength" (Fourt, 1939; Dickinson *et al.*, 1985; Petkov *et al.*, 2000).

### *2.2.1. Native Protein Stabilisation Forces*

Proteins and peptides are polymers of amino acids. The properties of a protein are determined by the sequence of its constituent amino acids. The twenty common naturally occurring amino acids have different side chains and chemical properties. Aromatic and aliphatic side chains are described as hydrophobic, as it is energetically unfavourable for them to exist in an aqueous phase. Side chains that are charged or can form multiple hydrogen bonds tend to be hydrophilic. Hydrophobic interactions are thought to be the dominant mechanism for protein folding and stabilisation in the native state (Dill, 1990). Non-polar residues disrupt the structure of the surrounding water molecules, decreasing the entropy of the system. Such free energy considerations result in a degree of entropic stabilisation of a protein in aqueous solvents. This stabilisation mechanism can be thought of as a pseudo "anti-hydrogen" bond between hydrophobic residues in an aqueous phase (Kauzmann, 1959). In the native state, aromatic and aliphatic residues tend to be sequestered into the hydrophobic core of a protein in order to reach a free energy minima (Chothia, 1975). If the protein or peptide contains a significant proportion of hydrophobic residues,

then it will not be possible for the molecules to fold without leaving any exposed hydrophobic groups, due to the steric limitations imposed on the molecule by the carbon backbone.

### 2.2.2. *Protein-Interface Interactions*

The exposed surface hydrophobicity of a protein in its native state provides the driving force for adsorption at the air-water or oil-water interface (Graham and Phillips, 1979c; Lu *et al.*, 1999). If the protein molecule can locate at the interface with some exposed hydrophobic groups penetrating into the oily phase, the disruption of the hydrogen bonded water is reduced and hence so is the free energy of the system. Penetration of the interface by hydrophobic residues results in a lowering of the free energy of the interface or surface tension (Beverung *et al.*, 1999) and modification of the interfacial rheology. Once adsorbed, proteins can become denatured at the air-water and oil-water interfaces. The modelling work of Anderson *et al.* (2000) confirms that a protein-like heteropolymer, capable of folding to a unique structure in bulk solution, undergoes conformational changes after adsorption at an oil-water interface. Once adsorbed, the heteropolymer begins to unfold inwards from its external surface and ultimately adopts a loop and train structure, in agreement with the experimental results of Graham and Phillips (1979c). However, the work of Caessens *et al.* (1999) shows that secondary structure formation can be induced in β-casein fragments by adsorption to a hydrophobic polymer surface from aqueous solution. Therefore, higher order protein structure is modified, but not necessarily destroyed, after adsorption at an interface. The protein undergoes conformational changes to reach a new, lower, energy state (Zayas, 1997). The high affinity of proteins for the boundary between aqueous and oily phases is a result of the large free energy decrease of the molecule upon adsorption and denaturation. This explains the frequently observed phenomena that protein adsorption is irreversible and no equilibrium exists with the protein in bulk solution (Table 2-1). Consequently, desorption of the protein requires very high dilution ratios to achieve a protein concentration in the bulk solution lower than the plateau value of the adsorption isotherm. For this reason, the Gibbs adsorption equation, used extensively in small molecule surfactant theory, does not hold for many large molecules and proteins (Graham and Phillips, 1979b; Walstra, 1996).

**Table 2-1** **Generalised characteristics of interfacial properties of low molecular weight surfactants and proteins. Reproduced from Bos and van Vliet (2001). Typical average values are given, but exceptions do exist. A = Air, W = aqueous solution, I = ionic strength.**

| Interfacial properties | LMW surfactants | Proteins |
|---|---|---|
| Number of molecules | $10^{-5}$ mol $m^{-2}$ | $10^{-7}$ mol $m^{-2}$ |
| Adsorbed amount | 1.0–2.0 mg $m^{-2}$ | 2.0–3.0 mg $m^{-2}$ |
| Adsorption | Reversible | Practically irreversible |
| Affinity to an interface | Rather small | Rather high |
| Molecular shape and size | Cylindrical (1x1x2 nm) | Often globular (4–5 nm) |
| Conformational changes upon adsorption | No | Yes |
| Film thickness in equilibrium fluid A/W/A | 40 nm (charged, low I)<br>< 40 nm (charged, high I) | 4 nm |
| $\gamma_{equilibrium}$ at A/W interface | 42–22 mN $m^{-1}$ | 57–47 mN $m^{-1}$ |
| Interfacial tension decrease on adsorption A/W | 30–50 mN $m^{-1}$ | 15–25 mN $m^{-1}$ |

### *2.2.3. Interfacial Protein-Protein Interactions*

When proteins become denatured at the air-water or oil-water interface, functional groups usually buried in the core of the protein may form covalent and non-covalent intermolecular bonds, resulting in the formation of an interfacial layer with a mechanical strength. A strong interfacially adsorbed protein network may form as a result of intermolecular hydrogen bonding or hydrophobic interaction, entanglement of the denatured polymer chains or via intermolecular covalent bonding. For example,

Faergemand *et al.* (1997) found that the viscosity of β-lactoglobulin films continued to rise even after monolayer coverage due to the crosslinking of β-lactoglobulin molecules at the interface via disulfide linkages.

## 2.3. Protein Interfacial Rheology

In emulsion processing, the presence of a protein layer having mechanical strength affects both the ease of initial droplet disruption (Williams *et al.*, 1997) and the subsequent emulsion stability during storage (Dickinson *et al.*, 1988). Knowledge of interfacial rheology is also important for biomedical applications (Geiger *et al.*, 1999; Wustneck *et al.*, 2001) and in oil recovery (Mohammed *et al.*, 1993). The dynamic response of an interfacial protein network can indicate the level of inter- and intra-molecular bonding, extent of molecular conformational change on adsorption and the degree of competition for interfacial space. The film response may be isolated into the recoverable (elastic) component and a non-recoverable component or interfacial viscosity. Boussinesq (1913) proposed an analogy between the interfacial viscosity and Newton's law of viscosity, dividing the former into an interfacial dilatational viscosity and an interfacial shear viscosity. Many theoretical treatments of interfacial rheology characterise such adsorbed films by the use of a complex shear modulus and complex dilatational modulus. In practice, however, it can be difficult to isolate all of the parameters and many workers simply make the assumption of a viscous or elastic film depending upon the experimental technique or application.

### *2.3.1. Experimental Techniques*

The dilatational modulus is a result of the energy required to increase the area of the interface and the shear modulus represents the resistance of the interface to deformation at constant area. Both moduli may consist of an elastic component and a viscous component. Techniques exist to model interfacial rheology for clean interfaces and systems of small molecule surfactants. For a series of alcohols in aqueous solution, Ward and Tordai (1946) were able to relate the increase in surface coverage on expansion of the interfacial region to the kinetics of adsorption and desorption. However, for the case of an interfacially adsorbed protein network where use of models such as the Gibbs isotherm is no longer valid, such approaches are not

helpful. Mechanical testing of a structured protein network is difficult because any experimental technique will partly destroy the network, unless the degree of deformation is extremely small. In small deformation experiments, the material properties are often assumed to be in the initial linear elastic regime. This causes two major problems. Firstly, in most cases there is no way to check this assumption experimentally, and secondly the low strain material response is not necessarily representative of the material behaviour at large deformation. In addition experimental results are usually only available for a specific system from a single rheological method. Studies often report results for the shear modulus but the dilatational modulus is reported much more rarely. In practice the measured interfacial response is often assumed to be either perfectly viscous or perfectly elastic to avoid isolating the recoverable and non-recoverable components of the energy input. For these reasons interpretation of the results from some techniques is highly subjective.

Some of the earliest experiments to determine surface shear rheology were performed by measuring the damping of a torque pendulum located at the interface (Langmuir, 1936). For this type of test a disk or ring is suspended at the interface by a fine tungsten wire. The wire is rotated through a defined angle and the length of time required for the disk to rotate through the same angle is taken as a measure of the interfacial viscosity. The film is considered to be solid-like if the angle of disk rotation is much less than the forced rotation of the wire support.

Graham and Phillips (1980a; 1980b) considered both the dilatational and shear properties of protein films adsorbed from aqueous solution at the air-water and oil-water interfaces. Measurements of dilatational modulus essentially quantify the magnitude and phase angle of the interfacial pressure $(\pi)$ response to a change in interfacial area $(A)$. In the first paper (Graham and Phillips, 1980a), an oscillating barrier in a Langmuir trough was used to generate changes in area, and the interfacial tension response was measured by the Wilhelmy plate technique. The variation in mean trough area, $dA$, was 1%.

Boyd and Sherman (1970) designed and built a surface rheometer consisting of a disk rotating at low speed over a small angle and equipment to measure the resulting viscous drag on the disk. Briefly, the rheometer consisted of a disk or ring supported at the fluid interface by a "frictionless" air bearing. A constant force was exerted on the disk through the use of a magnet and coil, and the interface deformation observed by means of a lamp and scale arrangement. The same equipment was later used to measure the surface viscosity of α-casein, β-casein, κ-casein, α-lactalbumin, bovine serum albumin (BSA) and β-lactoglobulin (Boyd *et al.*, 1973). This design was modified by Graham and Phillips (1980b) and used to measure the rheological properties of BSA and lysozyme at both the air-water and oil-water interfaces.

Dickinson *et al.* (1985) have used a torsion wire viscometer with greater sensitivity than the equipment of Graham and Phillips (1980b) to measure the shear viscosity of mixed β-casein and gelatin films at the oil-water interface. The apparatus consisted of a biconical disk suspended at the oil-water interface by a torsion wire. The dish containing the liquids was rotated at low speed, and the effect of viscous drag on the disk was calculated from the steady state deflection. A stated advantage of this equipment over that of Boyd and Sherman (1970) is that the dish can be rotated continuously providing a more sensitive measure of surface viscosity. However, only a viscous component can be isolated in this manner and it seems probable that the interfacial layer will also exhibit an elastic component in the rheological response.

Benjamins and Vader (1992) have investigated the viscoelastic properties of an interface using a surface shear rheometer. This piece of apparatus consists of two concentric glass rings placed at the air-water interface. The outer ring is driven by an electric motor and oscillates about its axis with small amplitude (~0.05 rad). The inner ring is held stationary by a torque motor connected to an electrical supply in-phase with the supply driving the outer ring. The voltage required to hold the outer ring steady is measured. The equipment is calibrated with liquids of known viscosity and the results presented as a shear modulus and phase-shift angle. The elastic response is given by the in-phase signal and the viscous response by the out of phase component. This gives a measure of the complex shear modulus.

$$\mu_s = \mu_s^{'} + \mu_s^{''} = |\mu_s| \exp(i\phi) \qquad (2.4)$$

where $\mu_s$ = shear modulus, $\phi$ = viscous phase angle, superscript ' = elastic response, superscript " = viscous response.

Burgess and Sahin (1997) also use an item of equipment they named an interfacial shear rheometer. A du Nouy ring is placed at the interface and oscillated about small angles in the vertical direction. The amplitude of motion is measured at different frequencies to find the resonant frequency of the film, and this is used to calculate the film elasticity. The authors only report film elasticity for their experiments with BSA and human immunoglobulin G (HIgG) using the justification that such films have been shown, in previous work, to exhibit solid-like behaviour. The production of waves in the surrounding liquids is not considered explicitly although the equipment is calibrated against a clean interface. This technique may have problems due to the ring leaving the interfacial region. In the case of adsorbed films of β-casein and lysozyme the interfacial region may have a thickness of only 5 nm at an interfacial coverage of 2 mg/m$^2$ – 3 mg/m$^2$ (Graham and Phillips, 1979a, 1979b). Despite the fact that only small oscillations are permitted, it seems likely that the ring will move in and out of this thin interfacial region. Surprisingly, Dickinson *et al.* (1985) report that interfacial viscosity measurements from experiments using a rotating disk are not particularly sensitive to the disk position relative to the interface. No effect could be detected within the range ± 1 mm of the interface, provided that the edge of the disk remained in contact with the meniscus. The interpretation of these results must, therefore, be done with care.

The techniques and problems discussed above show that it is very important to obtain an independent measure of the material properties that can be tested against theories or assumptions rather than calculated from them. All experimental methods discussed previously either do not measure all the required properties or cannot resolve the different components.

Whilst, in theory, it is possible to obtain an elastic modulus for the interfacial material by straining it only a small amount so as not to disrupt the interfacial layer, the value of such an approach is called into question by the experiments of Costello *et al.* (1994). Their work considered the viscoelastic properties of confined polymer layers. The technique used was to apply an oscillatory motion to a confined polymer layer using a piezoelectric device. The motion transmitted through the polymer layer was measured using a second piezoelectric crystal. At high compression Hookean elastic behaviour was observed, at no compression the polymer showed Newtonian viscous behaviour, and at intermediate distances a complex viscoelasticity. This demonstrates experimentally that results obtained in one regime do not accurately and fully describe the complete material mechanical properties. The dependence of observed behaviour on the strain used to mechanically test the protein layer was dealt with by Benjamins and Vader (1992) by extrapolating the experimental results to provide an elastic or shear modulus at the theoretical limit of zero deformation. However, an interfacially adsorbed material surrounding a liquid droplet may experience a large total strain during the disruption event. If the type of behaviour observed is a function of strain, then measurements made at small strain may be not be the only information required for a generalised correlation between droplet breakup and mechanical properties of interfacially adsorbed material. Having determined that the adsorption of proteins at the oil-water interface may result in a film with some mechanical strength, and that this negates the applicability of the capillary number plot, it follows that an alternative approach is required to model the system. Such an approach must take into consideration the mechanical strength of the interfacial film.

Even if the adsorbed interfacial material shows true elastic behaviour, the response at large deformation may be viscoelastic or plastic due to the diffusion of additional protein molecules to the interface. When the interface is deformed the interfacial tension will deviate from its equilibrium value. "The magnitude of this deviation depends on the competition between the interfacial deformation and the mechanisms that tend to restore the adsorption equilibrium: interface-bulk emulsifier exchange and lateral emulsifier redistribution. The elastic restoring force thus becomes a

viscoelastic one" (Janssen *et al.*, 1994). Therefore, any experimental procedure would ideally be able to vary both the total strain and rate of strain if an accurate picture of the material behaviour is to be obtained. In essence, to enable overarching interpretation of the experimental results from protein interfacial rheology experiments a full constitutive equation is required for the interfacially adsorbed material, rather than an elastic or shear modulus determined at some arbitrarily selected strain. In summary, whilst it is necessary to give quantitative figures representing material elasticity and viscosity, interpretation should be performed with care and the knowledge that such results are strongly influenced by the strain and experimental method chosen.

### 2.3.2. *Experimental Results*

The experimental results of Graham and Phillips (1980a; 1980b) show that β-casein films adsorbed at the air-water interface have a dilatational modulus in the range 5 mN/m – 30 mN/m and molecular reorientation within the film during compression-expansion cycles results in a relaxation time of order $10^{-8}$ s. In contrast, the globular proteins BSA and lysozyme show dilatational moduli independent of frequency with values in the range 60 mN/m – 400 mN/m and 200 mN/m – 600 mN/m. The authors also investigated the shear properties of adsorbed films of the same proteins under similar experimental conditions. This provides one of the few examples where dilatational and shear properties can be meaningfully compared. The rheological properties under shear were measured by performing creep compliance tests at constant low shear stress. Shear viscosity of β-casein films adsorbed at the air-water or oil-water interface was so low as to be barely detectable. Lysozyme films exhibited the greatest resistance to shear with a maximum surface viscosity coefficient greater than $10^4$ mN.s/m, more than 25 times higher than BSA at similar interfacial concentrations. This work establishes interfacial shear rheology as a technique very sensitive to protein inter- and intra- molecular bonding.

Boyd *et al.* (1973) used a surface rheometer consisting of a disk rotating at low speed over a small angle to measure the interfacial viscosity of protein solutions. Films of α-casein and β-casein showed no detectable viscosity. κ-casein and α-lactalbumin

gave viscous films, whilst BSA and β-lactoglobulin produced viscoelastic films. The films were spread at the air-water interface and for kinetic reasons the protein molecules may adopt a different conformation from the same protein molecules adsorbed from aqueous solution. The results, however, are broadly comparable with those of Graham and Phillips (1980b) as β-casein films had no detectable viscosity and the highest surface viscosities were obtained with the globular proteins BSA and β-lactoglobulin. The results suggest that globular proteins adsorb at the interface to create films with a higher viscosity than those formed by random coil proteins.

Dickinson *et al.* (1985) used a torsion wire viscometer with greater sensitivity than the equipment of Graham and Phillips (1980b) to measure the shear viscosity of mixed β-casein and gelatin films at the oil-water interface. In these experiments the interfacial region was subjected to a constant rate of strain with unlimited total deformation. The apparent surface shear viscosity of a film adsorbed from a $0.75 \times 10^{-3}$ % w/v casein + $0.25 \times 10^{-3}$ % w/v gelatin solution was around 2 mN.s/m after a 2 h adsorption time.

Benjamins and Vader (1992) present a comparison of the shear and dilatational moduli for films of BSA and ovalbumin. The authors' shear rheometer consisted of two concentric rings placed at the air-water interface. The outer ring oscillated with small amplitude and the stationary inner ring measured the resulting forces. The authors found that the shear modulus depended linearly upon the magnitude of the deformation so extrapolated the data to the limit of zero deformation. Reproducibility of the shear data was poor with deviations of over 10% – 40% in parallel repeats where a new interface of the same protein solution was formed. The authors suggest that the phase angle difference may be even larger and point out that the error far exceeds the accuracy of the apparatus, so is probably due to non-reproducibility of initial interface formation. Comparison of the shear and dilatational moduli for ovalbumin, BSA and sodium caseinate, again suggest that shearing experiments are more sensitive to changes in the adsorbed protein layer than the dilatational modulus. The globular proteins ovalbumin and BSA exhibited greater resistance to interface dilation and shear than the caseinate films. The increase in area for the dilatational experiments was 6.6%. The proteins were adsorbed from 0.03% w/v solutions and aged at the interface for 2 h. The maximum values of shear and dilatational moduli

were obtained with ovalbumin, giving elastic components of 57 mN/m and 14.0 mN/m respectively. The main conclusions drawn from the work are that for both types of film the interfacial elasticity increases with time and protein concentration, but decreases with temperature, in line with the experimental results of other workers. The interfacial tension was found to decrease as the bulk protein concentration was increased, in contrast with the film elasticity which was greatest at the highest protein concentration considered.

Faergemand and Murray (1998) found that at the air-water interface native β-lactoglobulin had a maximum dilatational elastic modulus of ~6 mN/m at a straining frequency of $10^{-3}$ Hz. Adsorbed films of this protein showed viscoelastic behaviour with predominantly elastic behaviour at high frequency and viscous behaviour at the lower frequencies with a cross-over point at $3 \times 10^{-4}$ Hz. Spread protein monolayers were used in some experiments so that the contribution of $\gamma$ relaxation back to the "equilibrium" value, due to adsorption of further protein from the bulk, could be neglected.

Surface shear rheometry of α-casein, β-casein and β-lactoglobulin at the *n*-tetradecane-water interface was performed by Faergemand *et al.* (1997). The Couette type surface rheometer was operated at an intermittent steady shear rate of $1.3 \times 10^{-3}$ rad/s. The plane interface was sheared continuously for 10 min prior to each measurement. The authors state that this was to ensure steady state conditions, however, destructive testing in this manner may be inappropriate for measuring the intrinsic mechanical properties of a structured material. Burgess and Sahin (1997) used an oscillatory interfacial shear rheometer to determine resistance to interfacial shearing and a Wilhelmy plate to measure interfacial tension of BSA and HIgG films adsorbed at the air-water interface. All data are presented as interfacial elasticity because "it was shown previously that adsorbed films of BSA and HIgG exhibit elastic (solid-like) interfacial activity rather than viscous (liquid-like) activity". The shearing experiments consisted of placing a platinum du Nouy ring at the interface and imposing a forced oscillation of "a few degrees" at the resonant frequency. Values of interfacial elasticity as high as 1103 mN/m for HIgG at 1.5% w/v concentration were reported.

Although no unifying understanding has been developed, there is clear evidence in the literature that ensemble interfacial behaviour depends on a range of factors. The results reported in the literature often use different measuring techniques, degrees of deformation, methods of interfacial film formation and interfacial ages. Therefore, performing an accurate assessment of the relationship between protein structure, inter- or intra- molecular bonding and film strength is extremely difficult. There are many conflicting results in the reported behaviour of protein films adsorbed at both the air-water and oil-water interfaces. However, one of the few consistent patterns to emerge is that globular proteins give rise to interfacial films with greater shear and dilatational moduli than random coil proteins (Graham and Phillips, 1980a, 1980b; Williams and Prins, 1996; Faergemand *et al.*, 1997; Faergemand and Murray, 1998), confirming that properties depend on the structure of the adsorbing protein.

Graham and Phillips (1980b) observed that the resistance to shear of lysozyme was greater than BSA, and that lysozyme retained more residual tertiary structure after adsorption at the interface. The authors state that a greater degree of retained tertiary structure results in a greater degree of intra- and inter- molecular cohesion for the lysozyme films. β-casein has been shown to adopt a more extended configuration at the air-water interface (Graham and Phillips, 1979c) and adsorbed β-casein layers show little intermolecular cohesion, as measured by interfacial shear experiments. Williams and Prins (1996) have observed that the interfacial dilatational modulus of β-lactoglobulin adsorbed at the air-water interface rises sharply when the bulk protein concentration exceeds 0.01 mg/mL, suggesting the formation of a cohesive elastic network at some critical protein concentration.

The interfacial shear properties of adsorbed proteins have been shown to be highly sensitive to protein-protein interactions (Dickinson *et al.*, 1985), although inhomogeneities in local shear rates, caused by continuous shearing of the interfacial region, make quantitative interpretation of such data difficult. Techniques for measuring the resistance to shear of adsorbed protein layers generally show the greatest variation in experimental set-up. In addition, there is no standard deformation used to determine the shear modulus. Therefore, research groups often use different values or define the level of strain in a different way, and in some cases the strain is

not even quoted. Creep tests at constant shear stress provide a slightly different type of information and are particularly sensitive to the constant shear stress used.

## 2.4. Modification of Protein Network Mechanical Properties

The age of a protein network can have considerable impact upon the physical properties of a protein stabilised emulsion. For example, McClements *et al.* (1993) found that the viscosity and stability against coalescence of an emulsion stabilised with whey protein isolate increased with time. The authors ascribe these effects to the formation of intermolecular disulfide bonds between denatured proteins causing a long-term increase in the viscoelasticity of the interfacial film. The result is important both in terms of the mechanism for increased viscoelastic properties and because it provides additional evidence that a higher interfacial modulus of elasticity increases emulsion stability against coalescence. Unfolding and polymerisation of β-lactoglobulin after adsorption at the oil-water interface through disulfide bonding has been confirmed by Dickinson and Matsumura (1991). β-lactoglobulin was allowed to adsorb at the *n*-tetradecane-water interface and aged for periods up to 72 h. The adsorbed layer was then displaced with a surfactant (sodium dodecyl sulfate, SDS). The size of the desorbed species was analysed using SDS polyacrylamide gel electrophoresis (PAGE). The results clearly showed various sizes of polymer larger than a single monomer unit. In contrast, the control experiment of aged but non-adsorbed β-lactoglobulin showed monomeric protein at all times after emulsification. This result is consistent with the large time-dependent growth in surface viscoelasticity observed by Dickinson *et al.* (1990) for β-lactoglobulin adsorbed at the oil-water interface.

The use of a chemical or enzymatic method to crosslink or modify the adsorbed protein will have a large impact upon the interfacial properties. Dickinson *et al.* (1990) observed interesting experimental results by cleaving the disulfide bonds of β-lactoglobulin and blocking them through substitution of the sulfhydryl groups on the cysteine residues. The adsorbed and modified protein reached a steady value of surface viscosity after just 3 h – 4 h, yet no steady-state value was found for the native protein under the time-scale of the experiment. The result implies that blocking the

disulfide bonds produces a more disordered protein, which adsorbs more readily at the oil-water interface and that the ageing effects of films of unmodified β-lactoglobulin are due to slow disulfide bond formation.

Transglutaminase linkage has been successfully used by Faergemand *et al.* (1997) to crosslink sodium caseinate, α-casein, β-casein and β-lactoglobulin adsorbed at the *n*-tetradecane-water interface. All the systems showed an increase in surface viscoelasticity due to the enzymatic crosslinking of glutamine residues and primary amines located within the proteins. Casein systems showed rapid increases in surface viscoelasticity upon enzymatic crosslinking, β-lactoglobulin gave initial viscoelasticity two orders of magnitude higher than the caseins but showed less relative increase. This is probably due to the cysteine residues in β-lactoglobulin allowing the formation of some disulfide crosslinks before the addition of the transglutaminase. With adsorbed sodium caseinate at high degrees of crosslinking, the surface shear viscosity showed an initial peak and then fell to around half this value after longer shearing times. This can be attributed to the rapid formation and subsequent brittle failure of the protein network. Faergemand and Murray (1998) also report increased interfacial dilatational moduli of β-lactoglobulin and sodium caseinate films upon crosslinking with the same enzyme. They found crosslinked films generally had higher dilatational moduli than non-crosslinked films at both the air-water and oil-water interfaces. For spread β-lactoglobulin films aged at the interface for 2 h it was found that crosslinking had a more pronounced effect at the oil-water interface than at the air-water interface. The authors attribute the greater effect of crosslinking at the oil-water interface to a higher degree of protein unfolding at this interface as shown by $\pi$-$A$ isotherms for β-lactoglobulin. Faergemand and Qvist (1999) have showed the importance of using a $Ca^{2+}$ ion independent transglutaminase for crosslinking β-lactoglobulin. Calcium ions allow the formation of non-covalent aggregates of the protein. This retards the formation of crosslinks, presumably by obscuring possible binding sites.

Enzymatic crosslinking has potential for use in the food industry where the possible side effects and toxicity of chemical modification may be unacceptable. However, for this work chemical crosslinking is favoured due to the lower cost and difficulties

associated with maintaining and measuring enzyme activity. Marquie *et al.* (1997) used the chemicals agents glutaraldehyde, formaldehyde and glyoxal to crosslink cottonseed proteins. All the substances can react with the side chains of the basic amino acids, particularly those of the lysine residues. In alkaline conditions, formaldehyde led to the formation of methylene crosslinks between just over 40% of the lysine side chains. The authors reported an increase of around a factor of four in the force required to puncture a cottonseed protein film after it had been crosslinked using formaldehyde. Formaldehyde reacted with fewer residues that the alternative chemicals tested, yet resulted in stronger films. This is because the crosslink formed by formaldehyde is much shorter and more rigid than the corresponding crosslinks formed by glutaraldehyde and glyoxal. The result is a more compact film demonstrating higher strength, but without reaction of every lysine residue.

Ultimately, it is hoped that it will be possible to design a film to meet given requirements for elasticity, viscosity, deformability and thickness. Selection of different natural proteins allows interfacial networks with differing mechanical properties to be created. The use of crosslinking agents and ageing of the protein film provides an additional level of control. Even greater choice of material properties can be achieved by the use of short chain peptides rather than proteins. The ability to control the individual amino acid sequence allows potential for the covalent bonding, electrostatic interaction and hydrogen bonding characteristics of the peptide to be varied independently. This leads to the wider issues of designing new peptides for the selective control of film mechanical properties and the creation of new biomaterials. Literature related to peptide molecular design is discussed in Chapter 7.

# 3. Materials and Methods

## 3.1. Overview of the Cambridge Interfacial Tensiometer (CIT)

The CIT uniaxially strains a protein layer immobilised at the air-water or oil-water interface, in the plane of the interface. This is achieved by binding the protein film between two parallel T-bars, as shown schematically in Figures 3-1 and 3-2. One T-bar is connected to a solid state motor capable of providing a linear displacement over a wide range of operating speeds at high resolution. The other T-bar is connected to a sensitive force transducer that measures the force transmitted laterally through the interfacial film (Figures 3-3 and 3-4). The motor incorporates an internal position encoder capable of indicating the T-bar position with an accuracy of 50 nm. The fluid-fluid interface in the CIT has no curvature and, therefore, the instrument is insensitive to interfacial tension. The CIT gives a direct measure of the mechanical properties of the adsorbed interfacial material, and the results presented in the following chapters provide the first results of such a direct examination of interfacial protein films.

A system highly resistant to chemical attack or leaching of contaminants into the protein solution is created by the use of a stainless steel dish to contain the protein solution, and T-bars constructed from silica fibres joined with melted polypropylene. All items contacting the protein solution are acid washed before use. The only exception is the silica T-bars that have been derivatised with an alkyl silane to promote protein adhesion. Fibre selection, derivatisation and washing procedures are described subsequently in this chapter in greater detail. The surface chemistry of the T-bars is altered (e.g. by silanisation or gold deposition) to promote attachment of the interfacial protein.

At the start of each test the fibres are level with the edge of the stainless steel dish. The dish is slowly filled with 90 mL of the required protein solution, resulting in an air-water interface that is slightly higher than the dish edge (Figure 3-1). The T-bars "float" at the liquid interface as the dish is filled, providing a consistent mechanism of self-location at the air-water interface. The CIT is unique in attempting to create a full stress-strain curve to much higher degrees of deformation than those previously

reported. As force measurements are made over the whole displacement range, no initial assumptions about the material behaviour are required (e.g. linear response to a pre-defined percent strain). The approach is also one of the few to attempt "self-location" of force transmitting or measuring structures at the interface and to explicitly test the influence of the solid surface chemistry.

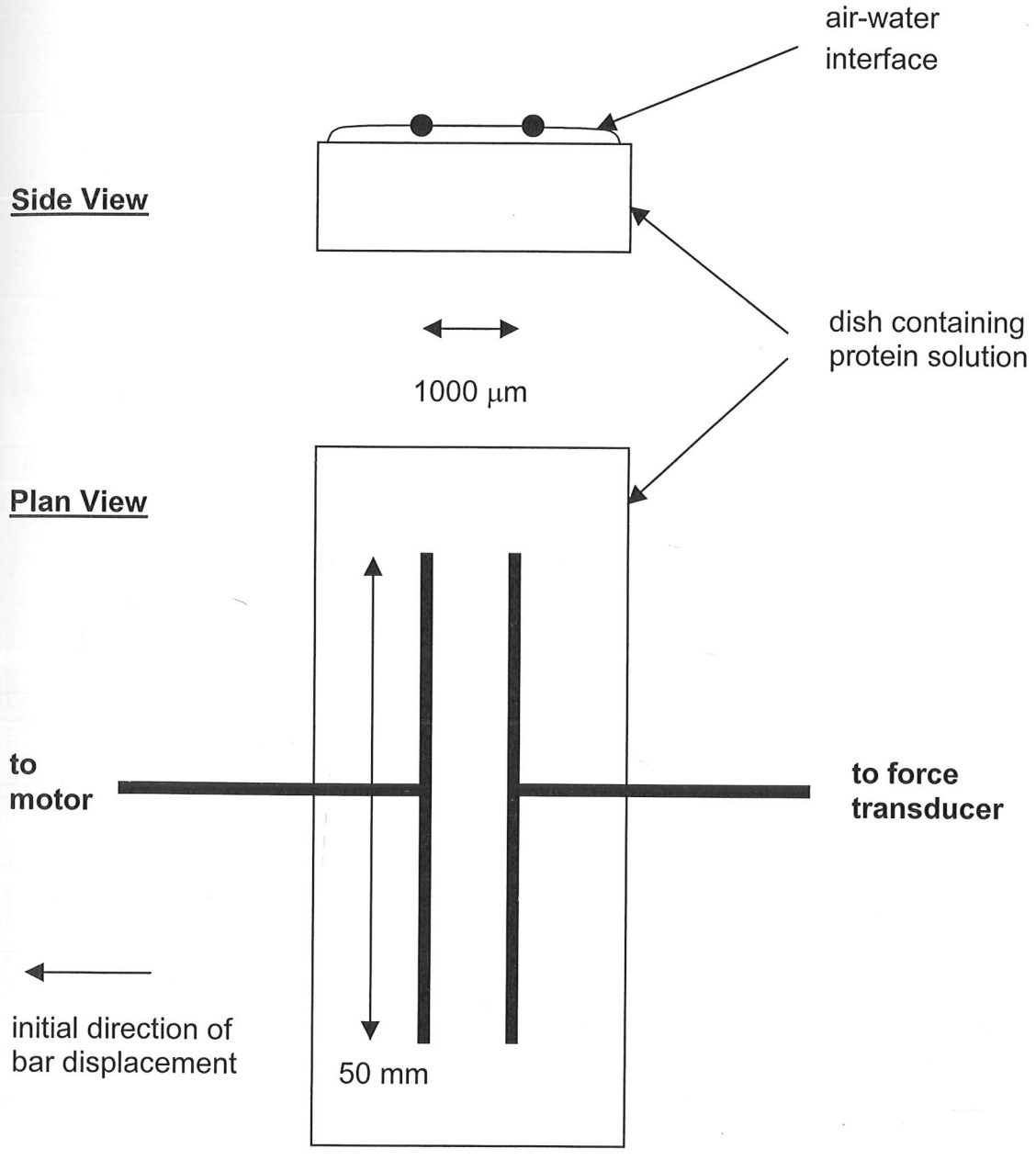


**Figure 3-1** **Overview of the CIT design.**

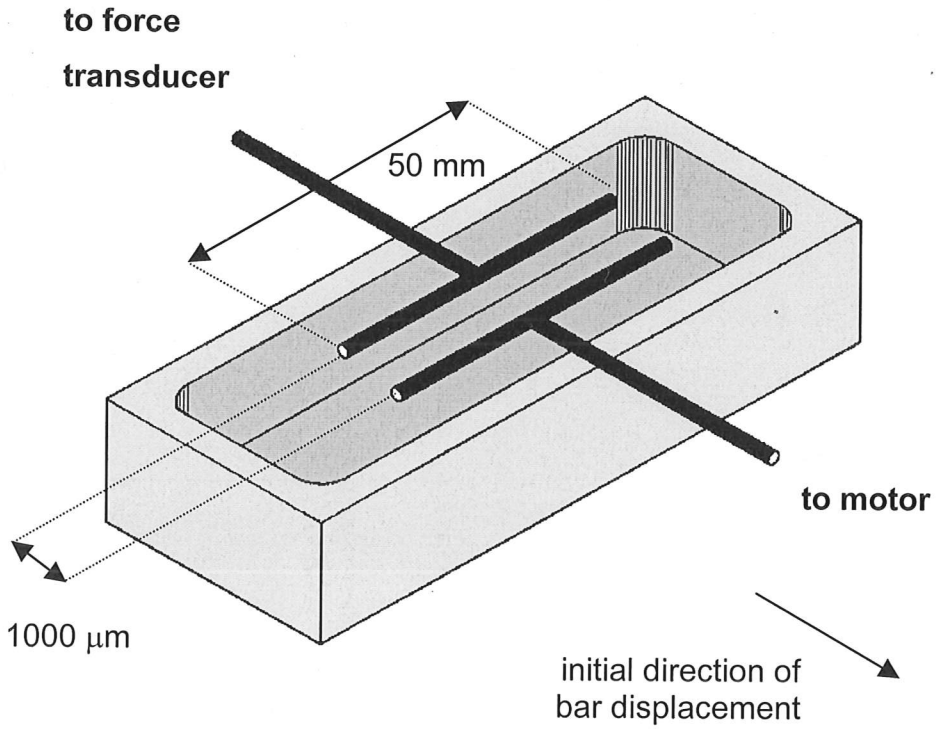


**Figure 3-2** **Schematic diagram of the CIT.**

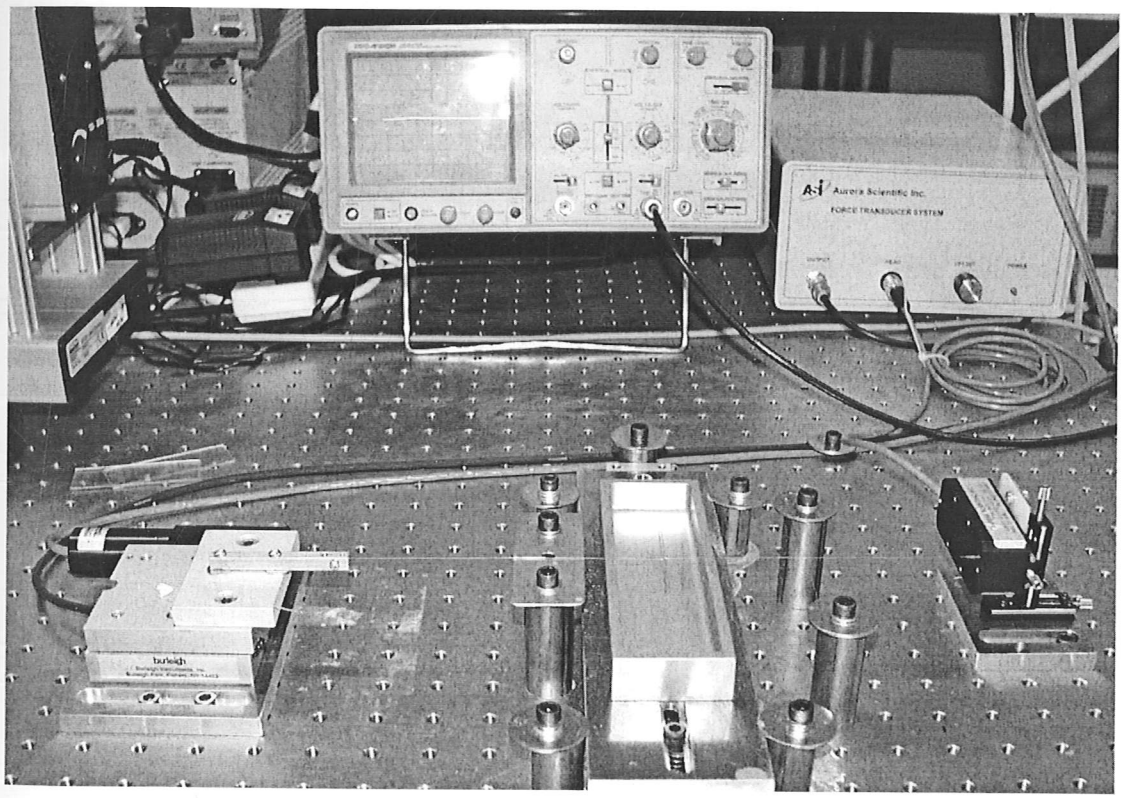


**Figure 3-3** **Photograph of the CIT setup.**

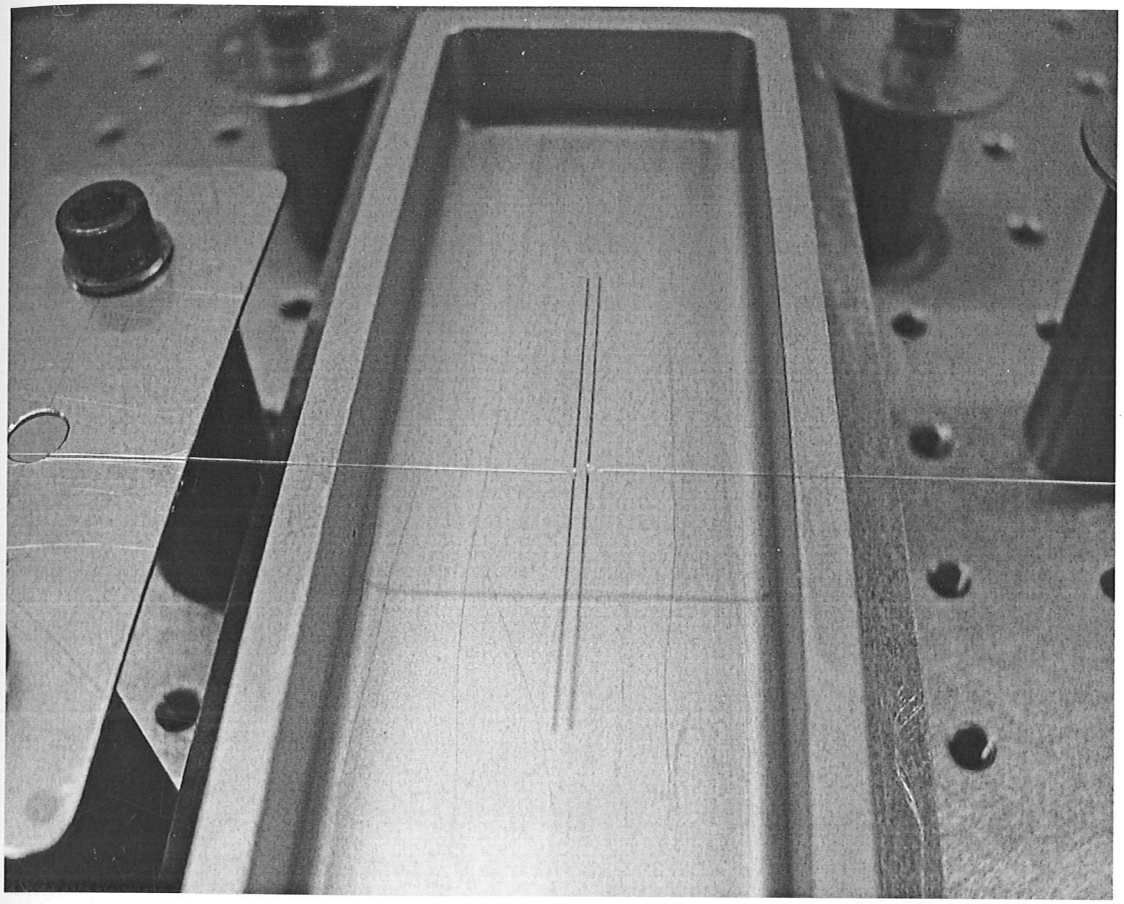

**Figure 3-4** **Close-up photograph of the CIT dish and silica T-bars.**

## 3.2. Modes of CIT Operation

Two types of test were performed using the CIT. The first type continuously measured the transmitted force to high deformation (typically 1000%). These data were used to generate a full stress-strain curve for the adsorbed network. In all tests of this type, the initial T-bar separation was 1000 μm, the bar length was 50 mm, and the T-bar was initially moved with a linear speed of 200 μm/s to a total separation of 11 000 μm. Following this tensile test, the direction of travel was reversed and the T-bar returned to its starting position causing a compressive (negative) force. The procedure therefore has two stages, the first being a tensile testing phase and the second a compressive test. The interface was always aged for a period of 1 h prior to this type of test to allow sufficient time for adsorption and some degree of protein conformational change.

Force measurements were normalised by dividing by the T-bar length (usually 50 mm) to give an interfacial stress, and displacement was converted into engineering strain using the initial separation. This allowed the creation of a complete stress-strain plot for the interfacially adsorbed protein network. Interfacial elasticity modulus (*Et*) was calculated by dividing the interfacial stress (mN/m) by material strain. A total strain of 1% was selected for this calculation. The calculated interfacial elasticity modulus is, therefore, essentially a two-dimensional analogue of Young's Modulus of Elasticity.

Production of a full stress-strain plot results in a loss of structural integrity of the interfacially adsorbed material. The CIT, however, can be operated in a low strain (5%) non-destructive cyclic mode leaving the network largely intact. This allows lateral force transmission through a single protein network to be recorded as a function of time. In these tests the separation of the T-bars is increased to 1050 μm from 1000 μm. The direction of travel is then reversed and the moving T-bar returned to the original position at a speed of 200 μm/s. For tests with a total duration less than 90 min the cyclic test was performed with a frequency of 10 cycles per min but this was reduced to one cycle per min for longer testing periods. This mode of CIT operation, therefore, enables micro-mechanical characterisation of the interfacial protein network as a function of time.

A strain of 5% was chosen for the cyclic tests as this is the threshold below which the experimental error in the force measurements became significant as the signal to noise ratio is reduced by the lower levels of lateral force transmission. The force transmission at 5% strain is fundamentally a very similar measure to the interfacial elasticity modulus *(Et)* or the initial gradient of the stress-strain plots. The 5% strain cyclic tests essentially convey the same information as constructing the chord between 0% and 5% strain on the full stress-strain plots. However, the two will only be equivalent in the case of a perfectly linear material response at low strain. The methods of data analysis and the relationship between the results obtained by operating the CIT in different modes are discussed in greater detail in Chapter 4. An advantage of the CIT is that full stress-strain plots are created, so no initial

assumptions are required for data capture. If simplifications are required during data analysis the validity of any assumptions can be confirmed from the experimental data.

### 3.3. Protein and Buffer Solutions

All reagents were purchased from Sigma-Aldrich unless otherwise stated.

β-lactoglobulin (3x crystallised and lyophilised) or β-casein (lyophilised) was dissolved in phosphate-buffered saline (PBS, 137 mM NaCl, 2.7 mM KCl, 12 mM $Na_2HPO_4$, 1.8 mM $KH_2PO_4$, adjusted to pH 7.4 with HCl). Ultrapure water was produced by a MilliQ Gradient System (Millipore, UK) and had a resistivity of > 18.2 MΩ.cm. For the detection of fluorescence wavelength shift, buffers with a different pH value were required. PBS buffer at pH 4.8 was made by mixing 100 mM solutions of $Na_2HPO_4$ and $NaH_2PO_4$ in the appropriate proportion. Carbonate buffer (40 mM $Na_2CO_3$, 60 mM $NaHCO_3$) was adjusted to pH 10.8 using NaOH.

### 3.4. Injected Solutions

The equipment is used to measure the mechanical properties of adsorbed protein films rather than spread monolayers, so protein molecules must be contained in the bulk aqueous phase. The simplest method, used in all experiments generating full stress-strain plots, is to add protein solution directly to the CIT at the required concentration. The second method is to run the CIT initially with clean buffer solution only. Concentrated protein solution, dissolved in the same buffer, is then injected into the bulk aqueous phase. The bulk protein concentration required in the CIT is used to calculate the volume and concentration of the injected protein solution. The corresponding volume of buffer is always removed from the CIT dish prior to solution injection and the same buffer is used to create the protein solution for injection and to initially fill the CIT dish.

Solutions of dithiothreitol (DTT, Melford Laboratories Ltd., Chelsworth, Suffolk, UK) and Tween 20 were added to the CIT using a clean hypodermic needle and syringe. The needle (0.6 x 30 mm, Terumo Europe N. V., Leuven, Belgium) was initially filled with air and, to avoid interfacial contamination, the solution for

injection was not allowed to reach the end of the needle until it had penetrated the interfacial region. Both reagents were dissolved at the concentration required to give a 400 μL injection volume into the CIT, and two equal volumes of solution were injected into the bulk protein solution at a position 15 mm from each end of the T-bars. Formaldehyde solution was injected at 37% concentration and the injection volume was calculated to give a concentration equivalent to 1% in the CIT.

## 3.5. Oil Phase

Figure 3-5 shows a cross-section of the CIT instrument and the T-bar location at the oil-water interface. The oil phase in these experiments was octane. Before use, the octane was passed 10 times through a 25 cm column of silica gel (35–70 mesh ASTM, Fluka, UK), that had been roasted for 14 h at 290 °C, to remove any surface-active contaminants.

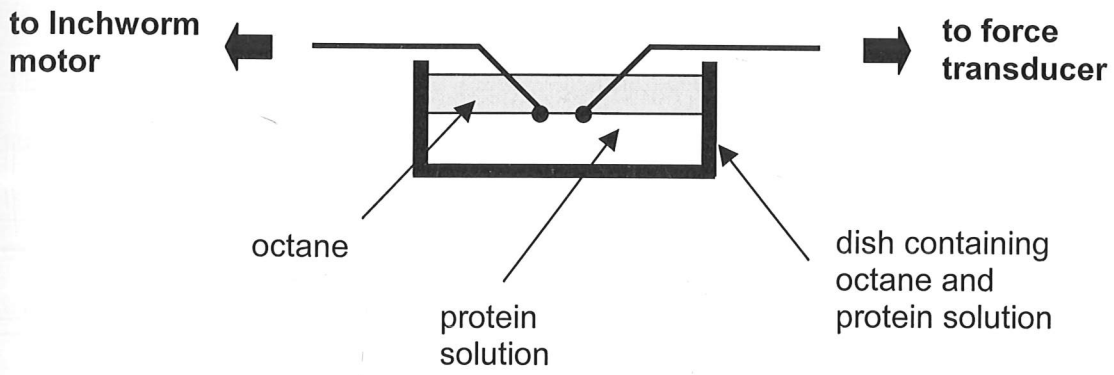


**Figure 3-5** **Schematic diagram of the CIT. Operation at the oil-water interface.**

## 3.6. T-Bar Construction

The T-bars were all formed from fibre optic cables supplied by Thorlabs Inc., NJ, USA. A small section of a 10 μL polypropylene pipette tip (Fisher, UK) was melted to join two individual fibres forming a T-shaped structure (Figure 3-4). Other joints required in the system, which do not directly contact the protein solution, were

secured using a UV cured glue ("GlassBond", Loctite, UK). Experiments to determine the effect of surface chemistry (silica, gold, particulate, amine and thiol data sets) were performed using T-bars constructed from the silica cladding and core of silica-silica fibre optic cable (Type FG-200-UAT) giving an external bar diameter of 250 μm. Investigations into the effect of bar diameter were performed with 240 μm, 300 μm and 400 μm diameter bars and used fibre types FG-200-UCR, FT-300-UMT and FT-400-UMT respectively. All remaining tests used the FT-400-UMT fibres. The FT-300-UMT and FT-400-UMT fibre optic cables have a polymer cladding material. This was removed by soaking and wiping the fibres with acetone, followed by heating in a butane flame to remove any remaining polymer. All fibres were cleaned by soaking in "piranha solution" (70% $H_2SO_4$, 30% $H_2O_2$) for 30 min, followed by washing to pH neutrality with ultrapure water, before use in the CIT or further surface treatment, as described subsequently.

## 3.7. Fibre Surface Coating

### *3.7.1. Gold Fibre*

The fibre was coated with gold by evaporation under vacuum to give a 55 nm Au film supported by a 20 nm thick NiCr adhesion layer. The fibre orientation was then reversed and the evaporation repeated to give a fibre coated over its entire surface, except for the ends and a narrow, longitudinal strip. This un-coated strip is caused by the difficulty in performing two consecutive evaporations with perfect fibre orientation, but its effect was minimised by orientating this section to face the central support of the "T-bar" section.

### *3.7.2. Amine Fibre*

The fibre was coated with (3-aminopropyl)triethoxysilane (APTS) to give an amine alkyl silane functionalised surface. This was performed by immersion in a solution consisting of 50 mL of toluene, 50 μL of APTS, 50 μL of ultrapure water, 5 μL of Tween 20 and shaking for 20 min. The fibre was then washed extensively in ultrapure water.

### 3.7.3. Thiolated Fibre

The thiolated fibres were created by first performing the amine alkyl silane derivatisation described above. The surface-bound amine groups were then reacted with the heterobifunctional cross-linking agent 3-(2-pyridyldithio)propionic acid N-hydroxysuccinimide ester (SPDP) to give the thiolated surface. 6.0 mg of SPDP was dissolved in a minimum volume of absolute ethanol and added slowly to 2.0 mL of PBS buffer, whilst periodically agitating the mixture. The fibre was immersed in the cross-linking solution for 1 h and then quenched in Tris-EDTA (TE) buffer (10 mM Tris, 1 mM EDTA, pH 7.5) for 15 min before washing with ultrapure water. EDTA = ethylenediaminetetraacetic acid.

### 3.7.4. Particulate Coating

To increase the bar surface area available for protein binding, 20 μm beads were bound to the smooth silica fibres. The particles were removed from a pre-packed C4 High Performance Liquid Chromatography (HPLC) column (Whatman International Ltd, Maidstone, Kent, UK). The column packing is spherical, with an average diameter of 20 μm and is derivatised by the manufacturer with a four carbon alkane chain to increase the packing hydrophobicity and promote protein binding. The particles were bound to the silica bars using "Glassbond" UV cured glue (Loctite, UK) diluted 1:2 with acetone. The fibres were dipped in the glue solution, the acetone was allowed to evaporate for 2 min, and the fibres were then brushed with the particulate material.

## 3.8. Fibre and Dish Cleaning

Before each test the silica fibres were rinsed *in situ* with 100 mL of ultrapure water. For the bare silica and gold surfaces only, the fibres were then immersed in piranha solution for 10 min followed by rinsing with 100 mL of 2 M NaOH. The thiolated fibres were washed with DTT solution (50 mM Tris, 30 mM DTT, 138 mM NaCl, 2.7 mM KCl, pH 8.0) and left to soak for 30 min to reduce any protein-solid disulfide bonds. All fibres and the stainless steel dish were then washed three times with ultrapure water, then with acetone followed by ethanol and finally rinsed a further three times with ultrapure water. For each step using ultrapure water the items were

allowed to soak for 2 min. This soaking period was increased to 5 min for the acetone and ethanol cleaning steps.

### 3.9. Force Measurement

The force transmitted through the interfacial layer was measured with a type 403A force transducer system (Aurora Scientific Inc., Ontario, Canada), based upon a variable displacement capacitor. This system has a full-scale deflection equivalent to the weight of 0.5 g, giving an output between +10V and –10V linearly dependent upon the applied force with the sign indicating tension or compression, respectively. This type of force transducer was selected for its low compliance, high frequency response, and sensitivity. A low compliance reduces the effect of any interfacial material behind the force measuring fibre, whilst a high frequency response and resolution allow accurate measurement of viscoelastic materials. To maximise the signal to noise ratio of the force transducer output, the CIT instrument was mounted on a vibration isolation table (RS2000, Newport, CA, USA).

### 3.10. Strain Application

Movement of the straining fibre is achieved with an "Inchworm Motor" solid state linear positioning device (Burleigh Instruments Inc., NY, USA). The motor consists of three cylindrical piezoelectric actuators around a central drive shaft. Application of high voltage sequentially to the piezoelectric actuators provides a clamping and expansion mechanism, causing a linear displacement of the central shaft. This equipment offers several advantages over a conventional stepper-motor. The lack of any gearing in the Inchworm device eliminates backlash and provides greater resolution (~4 nm step size). The maximum speed (1200 μm/s) and range of linear motion of the device are also much higher than for an equivalent stepper-motor, providing a wide range of operating conditions to the CIT instrument. The Inchworm motor is incorporated into the Burleigh TSE-150 positioning system with integral linear encoder giving a position resolution of 50 nm. Displacement of the straining fibre was usually performed at 200 μm/s until a total separation of 11 000 μm had been achieved. The direction of travel was then reversed and the fibre returned to its original position at the same speed.

### 3.11. Data Logging

The wires carrying the force transducer system output signal were connected to a shielded connector block (SCB-68, National Instruments, TX, USA) where the signal was routed both to an oscilloscope and PC for data capture. LabVIEW software (National Instruments) and an analogue to digital conversion card (PCI-6024E, National Instruments) were used to record the force transducer output. Commands to control the Inchworm motor were generated using LabVIEW software. Information was sent to the control circuitry, and received from the linear displacement encoder, via a motion control card (Model 671 Interface, Burleigh Instruments Inc.).

### 3.12. Interfacial Visualisation

Carbon spheres (Graphpac GC, Alltech, IL, USA) with an 80/100 mesh-size (150 μm – 180 μm) were spread over the liquid interface to allow interfacial visualisation.

### 3.13. Detection of Fluorescence Wavelength Shift

1.0 mg/mL β-lactoglobulin solutions were made using buffer solution at the required pH. Four wells of a black 96 well assay plate (Becton Dickinson Labware Europe, Le Pont De Claix, France) were filled with 200 μL of protein solution for each pH value. The solutions were excited at 295 nm and the fluorescence signal scanned between 320 nm and 380 nm using a luminescence spectrometer (Perkin Elmer Ltd., Bucks, UK). The scan speed was 200 nm/min and slit widths were 2.5 nm and 4 nm, for excitation and emission respectively. Each scan was repeated three times. Therefore, the results for each sample type represent the average of twelve scans in total. A least squares fit to a Gaussian peak was performed on the each result using four fit parameters. The reported fluorescence peaks are therefore the average calculated from twelve curve fits to a Gaussian peak.

### 3.14. Droplet Disruption and Sizing

Droplets were disrupted using custom-built Couette shear apparatus shown schematically in Figures 3-6 and 3-7. The component parts of the device were

manufactured by Dave Pittock (Engineering Department, University of Cambridge). The equipment consists of a rotating cylindrical bob surrounded by a stationary outer cylinder, creating approximate simple shear in the annulus due to the small separation (1 mm) relative to the cylinder diameter (40 mm). The inner cylindrical bob was rotated using an electric motor (Type R50, Phillip Harris Scientific, Ashby de la Zouche, UK) at around 800 r.p.m. depending on the exact shear rate required. Bob rotation speed was determined using a reflective strip glued to the drive shaft and an optical tachometer (Type TM-2011, RS Component Ltd., Corby, UK). The disrupted droplet size was between 1 and 2 orders of magnitude less than the annulus width (target droplet radius ~ 40 μm).

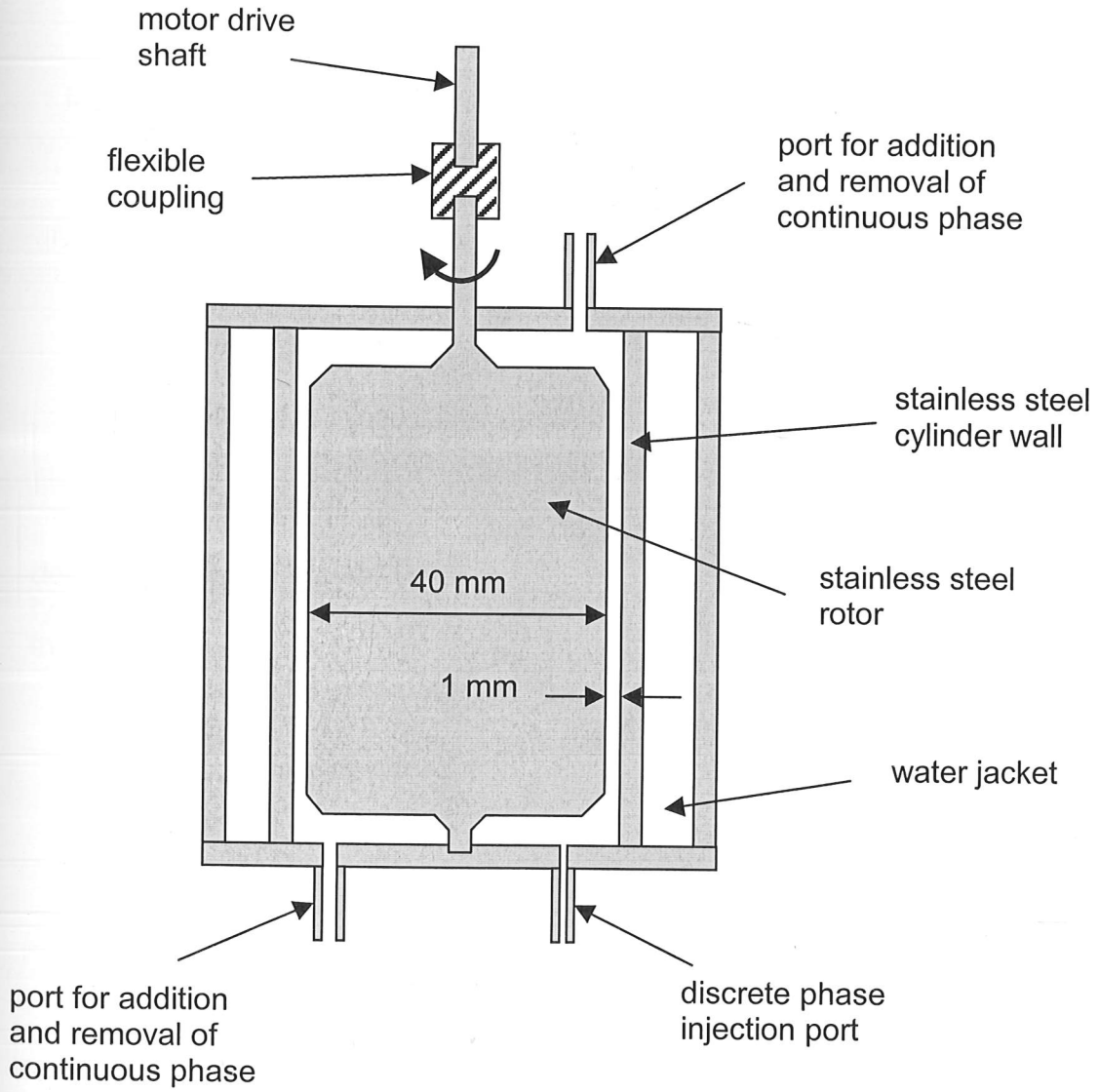


**Figure 3-6** **Schematic diagram of the Couette shear apparatus.**

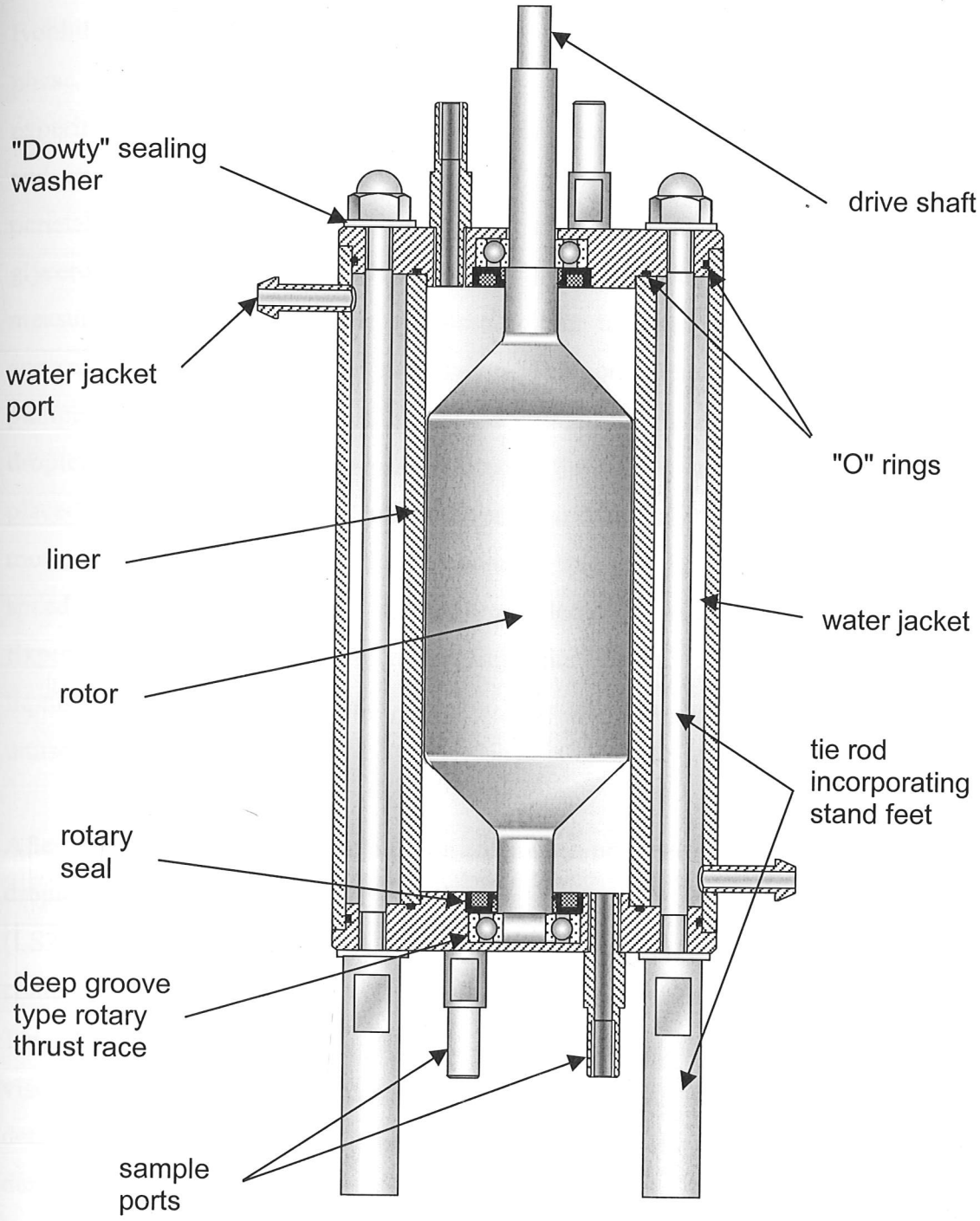


**Figure 3-7** **Detailed diagram of the Couette shear apparatus. Drawn by Dave Pittock (Engineering Department, University of Cambridge).**

The continuous phase was 80% glycerol (BDH Laboratory Supplies, UK) solution in ultrapure water, with varying concentrations of β-lactoglobulin (3x crystallised and lyophilised). Silicone oil (AS4, $\eta$ = 6 mPa.s, Fluka, UK) was used as the dispersed phase. Both the continuous and discrete phases are Newtonian at the chosen experimental conditions. The two larger ports shown in Figure 3-6 were used to fill and empty the device using PVC tubing (Tygon-Food, Cole Parmer, UK) and a peristaltic pump. The oil phase was injected after the apparatus had been filled with glycerol solution and was withdrawn with the continuous phase for droplet size measurements. The ratio of the oil phase volume to continuous phase volume was approximately 1:100 in all the experiments. The continuous phase was very slowly pumped backwards and forward during a 5 min shearing phase during which the oil droplets experienced multiple passes through the narrow annulus. The pump was placed such that the dispersed phase never passed through the pump itself. Vertical motion of the oil droplets through the annulus was very low relative to the rotation speed of the inner cylinder and is therefore neglected in the calculation of shear rate. Experiments were conducted at room temperature (20 °C – 22 °C). Heating of the liquids in the apparatus was not found to be significant and the water jacket was unused.

After 5 min of shearing a sample of the continuous phase containing the disrupted oil droplets was removed for particle sizing using a laser diffraction particle sizer (LS230, Beckman Coulter, UK). The emulsion sample required dilution as the continuous phase viscosity far exceeded the 5 mPa.s limit of the laser particle sizer. This dilution was performed with 0.25 mg/mL β-lactoglobulin solution to reduce viscosity whilst retarding coalescence of the oil droplets. Coalescence times were determined experimentally and found to be greater than the measurement time scale due to the lean nature of the diluted emulsion and the high protein concentration. The droplet radius occurring with the maximum frequency was used in all further calculations.

### 3.15. Calculation of the Capillary Ratio

The capillary number is defined as:

$$\Omega = \frac{\eta_C . G . r}{\gamma} \qquad (3.1)$$

where $G$ = shear rate ($s^{-1}$), $\eta_C$ = continuous phase viscosity (Pa.s), $r$ = droplet radius (m) and $\gamma$ = the interfacial tension (N/m).

Interfacial tension for a droplet of silicone oil in 80% glycerol solution was determined using pendant drop apparatus (DSA10, Kruss, Germany). The interfacial tension was measured at all the protein concentrations used for droplet disruption at the same interface age (5 min) because a true equilibrium value of interfacial tension for protein solutions is rarely reached (Beverung *et al.*, 1999).

The capillary ratio is defined as the critical capillary number for the experimental conditions divided by the critical capillary number predicted from a plot of critical capillary number versus viscosity ratio (de Bruijn, 1989). In effect, the observed value divided by the expected value for a clean system with the same interfacial tension. In this study droplets are generated at the maximum stable droplet size so the capillary number under these conditions is taken as the experimental critical capillary number.

# 4. CIT Testing and Validation

## 4.1. Introduction

The problems outlined in Chapter 2 clearly establish the need for a new technique capable of operating over a wide range of total deformation and strain rate to enable a more insightful interpretation and unification of the existing literature. It is also clear that such a technique should not be limited to small deformation studies and must not require any assumptions about the behaviour of the interfacial material under test, thus enabling a truly objective analysis of the experimental results.

Chapter 3 described the design and operation of new equipment, the Cambridge Interfacial Tensiometer (CIT). The CIT design was inspired by conventional materials methodology and subjects an interfacially adsorbed film to uniaxial extension, providing full material constitutive behaviour enabling the generation of a complete stress-strain plot. The technique provides a direct measure of the force transmitted laterally through a protein film, in the plane of the interface, and therefore differs from approaches producing a $\pi$-$A$ phase diagram analogous to a $P$-$V$ isotherm. The test performed by the CIT bears more similarity to the "Instron" test used for conventional solid materials, except that the interfacially bound material renews by transport of additional protein molecules from the bulk. A section of the adsorbed protein layer is bound between two T-bars and "stretched". One T-bar undergoes a linear displacement in the plane of the interface and an identical, but stationary, T-bar measures the force transmitted in the plane of the interface through the network of bound material.

The CIT is the first instrument capable of establishing the mechanical properties of an adsorbed protein network using conventional stress-strain approaches to high material deformation. Therefore, no existing data sets were available that could be reproduced to quickly confirm the accuracy of results generated by the CIT. The objective of this chapter is to validate the CIT data. This is performed to provide confidence in the results and allow interpretation of the information from more complicated systems presented in later chapters. Specifically the objective is to show that the results are not a function of CIT design or operating parameters. β-lactoglobulin was chosen as a

model protein for interfacial adsorption, since its structure is well documented, its surface-activity has been extensively studied, and it contains cysteine residues having a reactive sulfhydryl group. Sulfhydryl groups enable the formation of intermolecular disulfide bonds, which has been proposed as a mechanism for strengthening the interfacial layer (Dickinson *et al.*, 1990).

The effects of equipment dimensions are investigated by changing the T-bar length and diameter. Five different T-bar surface coatings are tested and checked to ensure attachment of the interfacial film to the bar surface. The influence of equipment operating parameters is also investigated. This is performed by altering the material strain rate through changes in linear bar displacement speed and initial separation.

In summary, this chapter confirms that the CIT provides useful data that can be meaningfully interpreted. The optimum T-bar size and surface coating is selected and standard equipment operating parameters are finalised. These conditions are used in all subsequent chapters. Data analysis is also discussed and improvements are made to allow more accurate extraction of material properties from the CIT results. The CIT provides a generic alternative to existing interfacial rheology tests, which are limited by the need for assumptions during data interpretation and by inhomogeneities in the local shear rate for viscoelastic test materials such as protein networks.

## 4.2. Interpretation and Validation of CIT Data

The data in Figure 4-1 demonstrate that it is the interfacial adsorption of protein molecules that confers the ability to transmit force laterally in the plane of the interface during CIT tests. The solid line shows a full force-displacement curve for 1.0 mg/mL β-lactoglobulin adsorbed at the air-water interface from PBS buffer, and aged for a period of 1 h. The dashed line shows the equivalent control using PBS buffer without protein. The CIT was operated both in tensile and compressive modes to generate the data shown in this figure. The T-bars had an initial separation of 1.0 mm, shown on the $x$-axis as 0.0 mm displacement. One bar was driven at a constant speed of 200 μm/s until a displacement of 10.0 mm had been reached. The direction of travel was then reversed, and the moving T-bar returned to its starting position (0.0 mm displacement). In the first section, the network was subjected to

uniaxial tension resulting in a tensile (positive) force. The second stage compressed the protein network generating compressive (negative) forces. The T-bar motion causes a straining of the interfacially bound material and an identical, but stationary T-bar, connected to a force transducer measures the force transmitted through the film. The CIT therefore provides a direct measure of the mechanical properties of an adsorbed protein film both under tension and compression. The ability to transmit force between two unconnected T-bars is consistent with reports in the literature of the formation of an interfacial protein network (Fourt, 1939; Dickinson *et al.*, 1985; Petkov *et al.*, 2000).

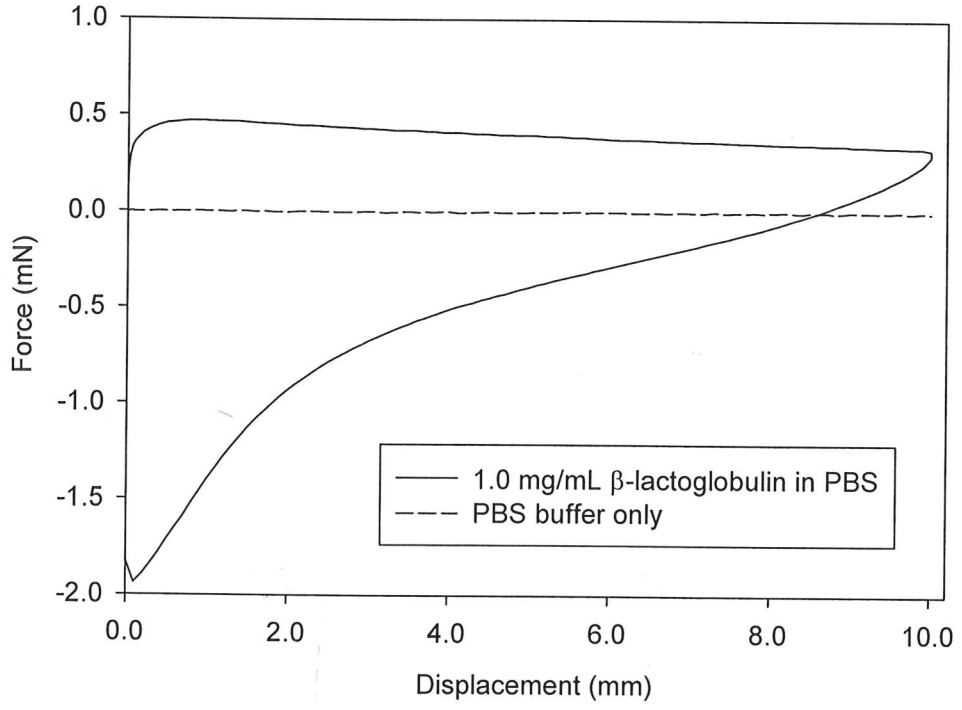


**Figure 4-1** **Complete force versus displacement curve for an interfacial protein network created by adsorption at the air-water interface from PBS buffer (pH 7.4) containing 1.0 mg/mL β-lactoglobulin. Initial T-bar separation = 1.0 mm, length = 50 mm, displacement speed = 200 μm/s.**

The direction of travel is reversed after a total displacement of 10.0 mm. The slight time delay (~1 s) in changing direction causes the small vertical drop visible on the plot of force versus displacement shown in Figure 4-1. This indicates the viscous time-dependent component of the observed stress-strain response for the interfacial

protein film. The transmitted force becomes negative very early in the compressive section of the test (~8.0 mm), indicating transport of new material to the interfacial area between the T-bars during the course of the experiment. The compressive modulus begins to increase, at approximately 5.0 mm displacement. Very high compressive forces are measured before the T-bar returns to its original position (Figure 4-1), strongly suggesting the compression of multiple protein layers at this stage of the experiment.

### *4.2.1. Location of Material Failure Point*

Confirmation of protein binding to the bars is critical for data interpretation to ensure that failure occurs at the fluid-fluid interface between the bars, rather than at the solid surface. Figure 4-2 shows a β-lactoglobulin film adsorbed from 0.01 mg/mL solution where 150 μm – 180 μm carbon spheres have been spread over the liquid interface to allow interfacial visualisation, and a buffer only control. Selected images from the tensile testing of the β-lactoglobulin film were enlarged and enhanced and are shown in Figure 4-3. One T-bar was displaced to increase the bar separation from 1.0 mm to 11.0 mm (1000% strain). The direction of travel was then reversed and the T-bar returned to its starting position. Essentially the same test as that used to generate the force-displacement plot shown in Figure 4-1. However, force data were not collected during these experiments due to the possible influence of the carbon particles. The figure shows a complete change in behaviour upon the addition of a low concentration (0.01 mg/mL) of β-lactoglobulin to the PBS buffer. The comparable pictures at maximum displacement (10.0 mm) show this change very clearly. There are no particles present along the centreline between the two T-bars when the buffer does not contain any protein molecules, due to the hydrophobic nature of the carbon spheres and derivatised T-bars. This hydrophobicity causes aggregation of the carbon spheres at the interface that cannot be resisted in the case of a truly fluid-like interfacial region. The interfacially aggregated carbon particles then stick to the hydrophobic surface of the amine-derivatised T-bars causing the high degree of segregation observed for the case of PBS buffer only. In contrast to the clean air-buffer interface, the film of adsorbed β-lactoglobulin shows considerable "necking" but is still intact at 10.0 mm displacement. There is also relatively little particle aggregation as the carbon

spheres are unable to move freely in the viscoelastic protein film. These results are in full agreement with the data shown previously in Figure 4-1 where no force transmission in the plane of an air-buffer interface is observed when protein is not present. Note that for the protein system, an individual particle starting close to the bar in the first photograph remains at that point throughout the whole experiment, indicating that network failure by detachment from the solid surface does not occur.

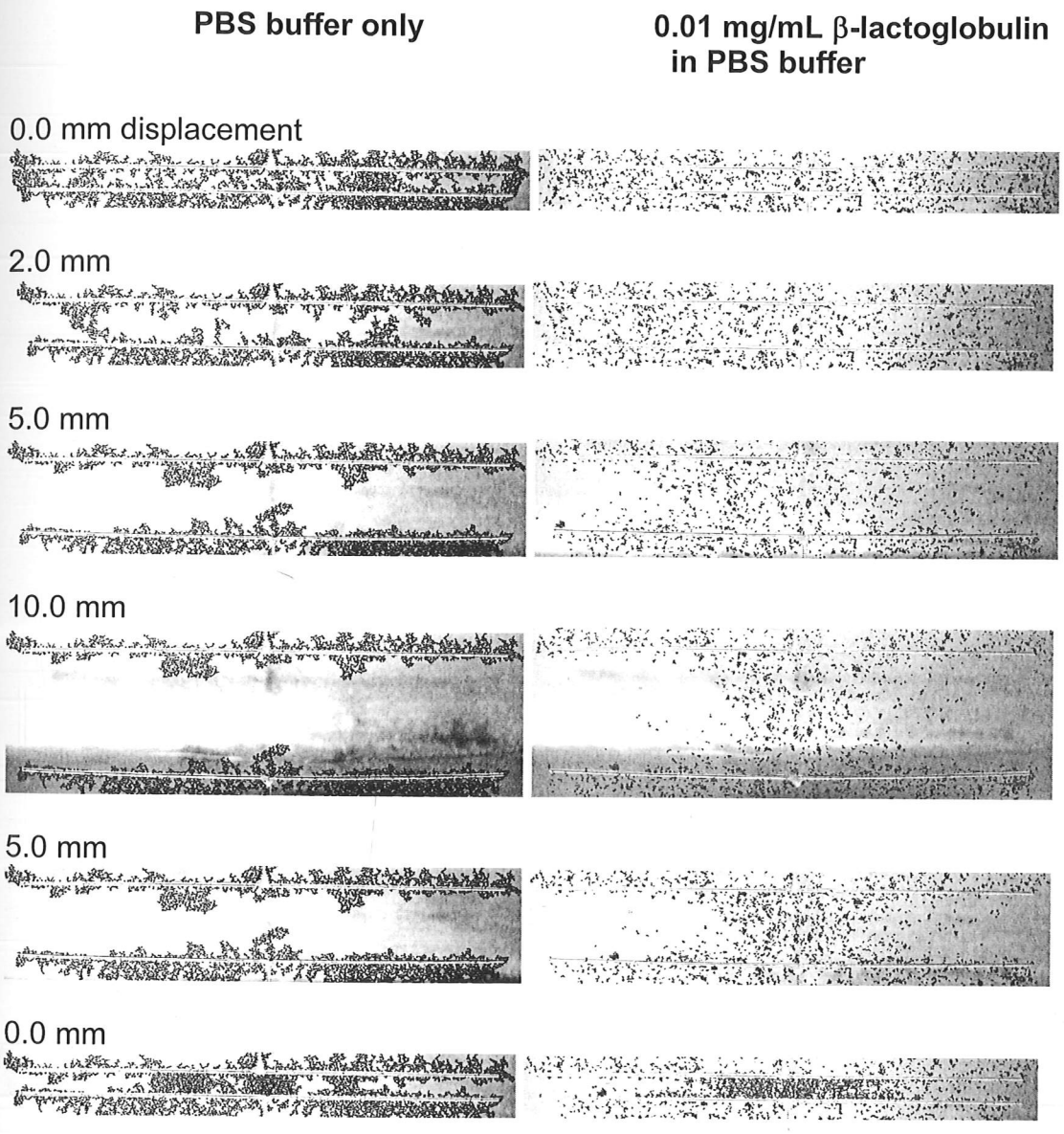


**Figure 4-2** **Visualisation of the interfacial region between the T-bars with and without protein present during the test procedure. 150 μm – 180 μm carbon spheres were spread over the interface. Conditions are identical to those used to generate data shown in Figure 4-1. Initial T-bar separation is 1.0 mm (0.0 mm displacement).**

The lack of a localised failure point up to such high strain gives confidence that the technique creates approximately uniform shear in the inter-bar region. This observation suggests that the CIT avoids the detrimental effect of inhomogeneous localised shear rate that affects many other techniques for measuring the interfacial rheology of viscoelastic films. At very high strain, a necking phenomenon consistent with that observed in conventional materials testing can be seen. The test visually behaves as one would expect for tensile testing of a networked polymer.

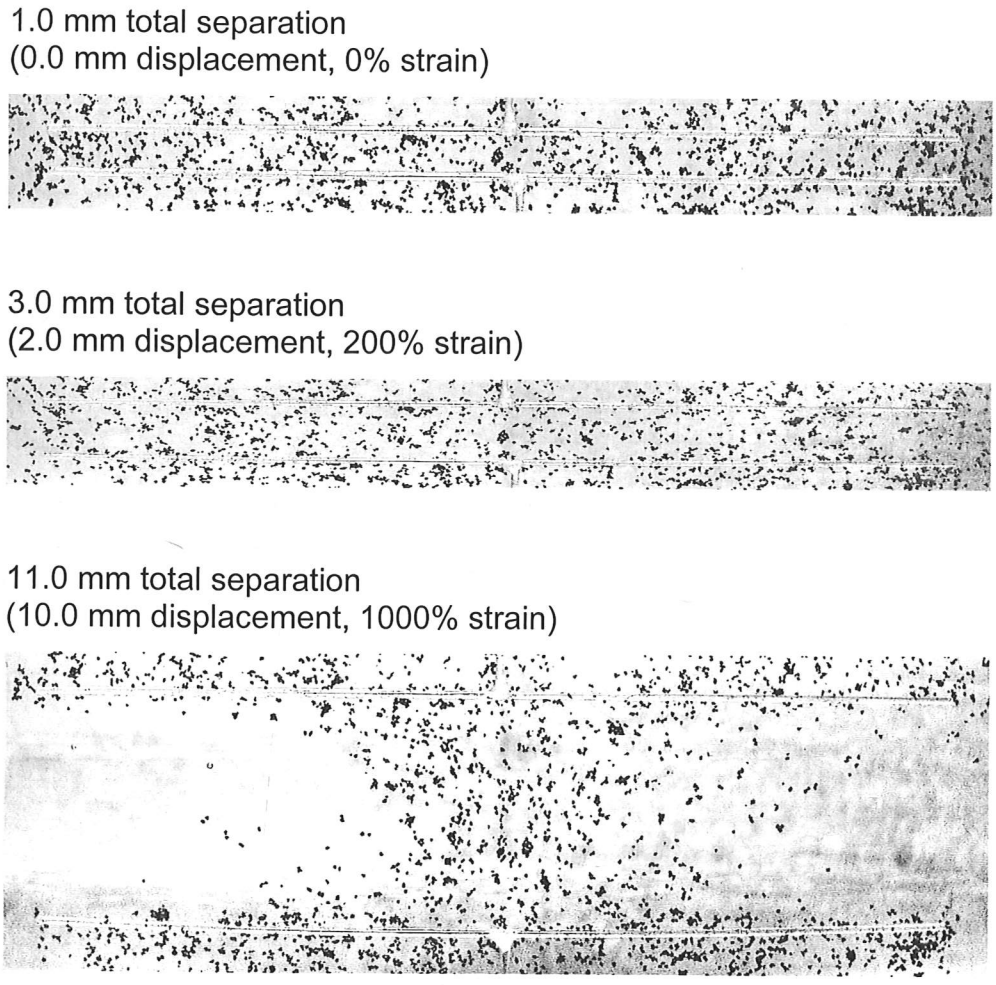


**Figure 4-3** **Enhanced interfacial visualisation of a β-lactoglobulin network adsorbed from PBS buffer (pH 7.4) with a 0.01 mg/mL bulk protein concentration. 150 μm - 180 μm diameter carbon spheres were spread over the interface.**

### 4.2.2. Protein Network Rigidity

Interfacial shear rheology has been shown to be highly sensitive to the interactions between proteins adsorbed at a fluid-fluid interface (Dickinson *et al.*, 1985), but steady state shear data can only be obtained after any interfacial network has been partially destroyed. An initial modulus of rigidity may be a more valuable parameter for a structured material, but data interpretation requires the implicit assumption that there is no loss of structure during the test. The advantage of testing the material to failure with the CIT instrument is that such an assumption is not initially required because a departure from linearity on the stress-strain plot is clearly visible.

The response of an adsorbed β-lactoglobulin network is initially rigid with high interfacial elasticity modulus *(Et)*, as shown in Figure 4-4 and the low strain region of Figure 4-1. Using a Langmuir trough and Wilhelmy plate, Graham and Phillips (1980a) have shown that the measured interfacial elasticity modulus at low strain is greater for more structured proteins. It is likely that the behaviour in this regime is dominated by strain induced conformational changes in the protein molecules, so the stiff network response observed at low strain would, therefore, be expected. Supporting evidence is also found in the work of Benjamins and Vader (1992), although a different experimental technique was used. They found the elasticity modulus for the globular protein, bovine serum albumin (BSA), to be around five times greater that the corresponding measurement for the more flexible sodium caseinate molecule.

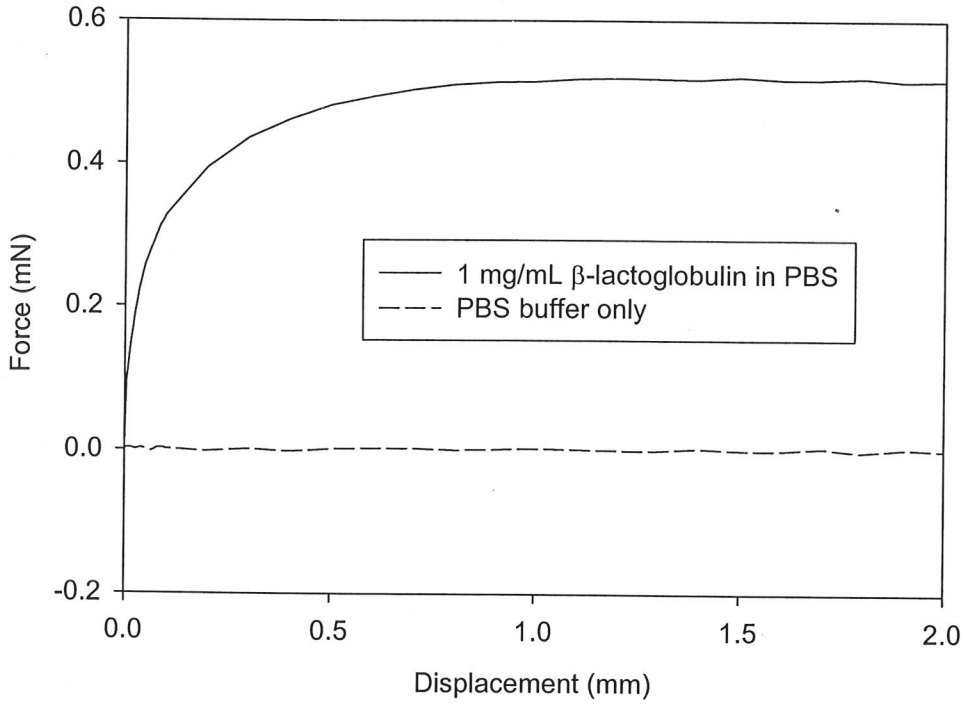


**Figure 4-4** **Low strain regime of force versus displacement curve for 1.0 mg/mL β-lactoglobulin adsorbed from PBS (pH 7.4) to the air-water interface. Data are the same as for Figure 4-1.**

Calculation of interfacial elasticity modulus *(Et)* was explained in the Materials and Methods section. Briefly, the interfacial stress is divided by the material strain in a two-dimensional analogue of Young's Modulus of Elasticity. Figure 4-5 shows data from the low strain region in Figure 4-1, with two additional tests confirming technique reproducibility. Numerical values of *Et* are defined using the force registered at 1% strain, giving a quantitative measure of network rigidity derived from the largely linear region of the stress-strain curve.

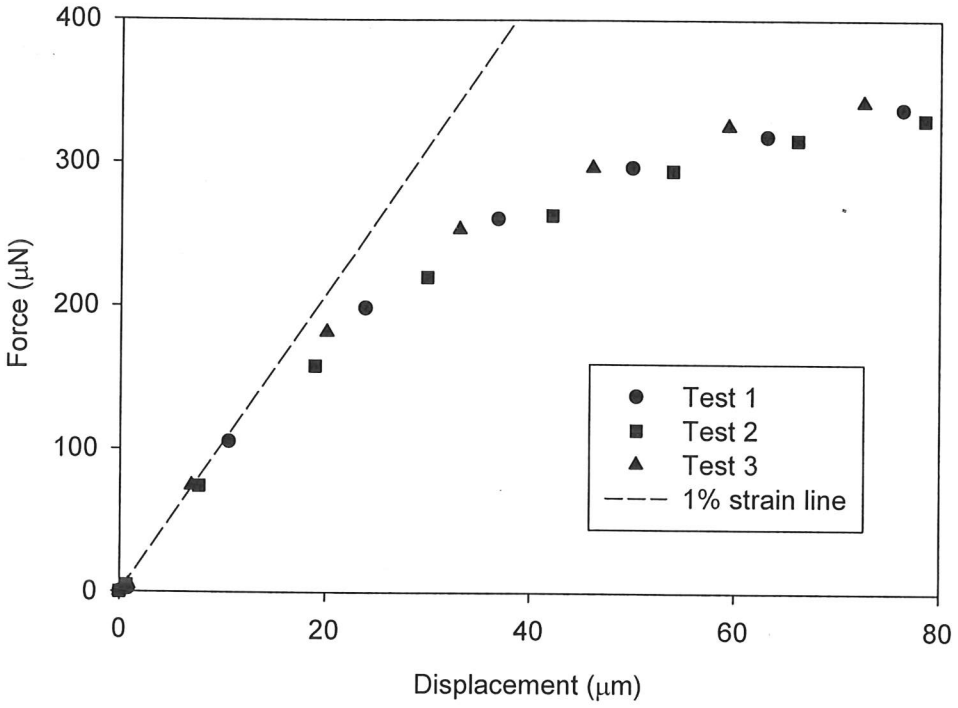


**Figure 4-5** **Stress-strain data at low strain showing technique reproducibility during independent tests, and estimation of the interfacial elastic modulus. Tests performed using 1.0 mg/mL β-lactoglobulin in PBS buffer.**

Interfacial elasticity modulus at 1% strain is used to characterise interfacial networks in all subsequent chapters. The measurement is technically difficult as it requires the capture of the rate of change of micro-Newton forces on a 50 ms timescale. This chapter describes equipment development and testing. At this stage of development the CIT could not reliably capture such data, so the decision was taken to use 5% strain to calculate the initial network rigidity, as this is a common value in the literature and the data were available for all tests performed. Such a decision is valid for two reasons. Firstly, in this chapter, no conclusions are drawn regarding the absolute values determined for the network rigidity beyond the observation than they lie within the range of values reported by other workers. Secondly, the CIT has the unique ability to generate a complete stress-strain plot for the adsorbed material, so any departure from linearity is clearly visible and the accuracy of the approximation can be determined. To distinguish between the two measurements, the term "Low-

strain rigidity parameter" is used in this chapter to describe the network rigidity calculated at 5% strain. This will obviously lead to a numerical value below that of the "Interfacial elasticity modulus" calculated from the linear region of the stress-strain curve at 1% strain.

Substantial yielding of the interfacial material occurs between 10% and 50% strain (0.1 mm - 0.5 mm displacement, Figure 4-4). This may be caused by dis-entanglement and slippage of the protein domains on adjacent molecules. In nearly all cases the maximum level of tensile stress is reached at approximately 100% strain. A long plateau region where the film shows considerable ability for "self-repair" follows this, and a true material failure point is not observed (Figure 4-1). The high bulk protein concentration (1.0 mg/mL) is probably responsible for conferring this "self-healing" property on the protein film, as high bulk concentration results in a rapid rate of protein adsorption at freshly exposed sites on the interface. The effect of bulk protein concentration is investigated further in Chapter 5.

## 4.3. Equipment Design and Operating Parameters

The CIT can be operated in a different, minimally-invasive, cyclic mode in the 0% to 5% strain regime. Five percent strain is used for all cyclic tests as this provides the optimum compromise between interfacial disturbance and signal to noise ratio. The technique is similar to the low deformation shear rheology tests of other workers in the field (Benjamins and Vader, 1992; Burgess and Sahin, 1997) and typical results are shown in Figure 4-6. Such a method of operation allows changes in the behaviour of the adsorbed material to be tracked with respect to time, and may show additional effects resulting from the kinetic limitations of protein adsorption and rearrangement. In this test the bars are initially at 1.0 mm separation, they are then moved to a total separation of 1.05 mm at 200 μm/s. The difference in the measured force, before and after the tensile 50 μm displacement, is taken as a measure of film strength and represented by the solid line in Figure 4-6. The T-bar is then returned to the starting position (1.0 mm separation) and the cycle is repeated once per min. Initially the equipment operates using PBS buffer and no force difference is registered. After 30 min, 1.0 mg/mL β-lactoglobulin solution is injected, and the corresponding amount of buffer removed, to give an equivalent protein concentration in the CIT of

0.01 mg/mL. A difference in the measured force at 0 μm and 50 μm displacement is immediately detected and the difference continues to increase for the next 60 min. This clearly demonstrates that the ability to transmit a tensile force in the plane of the interface is conferred solely by the presence of protein molecules at the interface adsorbed from the aqueous phase.

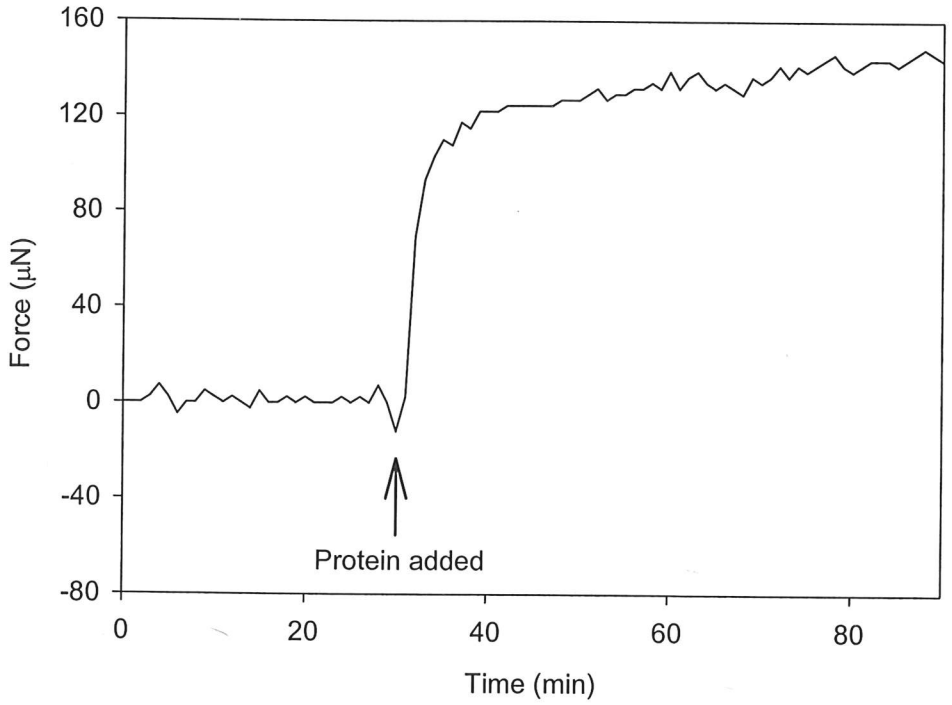


**Figure 4-6** **Non-destructive cyclic operation of the CIT in the 0% - 5% strain region. The solid line shows the increase in tensile force on applying a 50 μm tensile displacement. Initial T-bar separation = 1.0 mm, length = 50 mm, displacement speed = 200 μm/s. An interfacial film is formed after protein injection at 30 min (0.01 mg/mL equivalent bulk protein concentration).**

### *4.3.1. T-Bar Surface Chemistry*

As indicated previously, binding of protein to the solid surface of the T-bars is an extremely important requirement in interpretation of data from the CIT. To ensure that the results obtained are truly representative of the mechanical properties of the adsorbed protein film, five different T-bar surface chemistries were investigated. Figure 4-7 shows the average of five parallel repeats for four of the coatings. The

fibre surfaces tested were bare silica, gold, an amine alkyl silane, a thiolated alkyl silane and a hydrophobic particulate coating. A protein concentration of 1.0 mg/mL was used in all tests. The gold and thiolated surfaces provide the possibility of binding the protein molecules to the solid surface via the sulfhydryl group of the cysteine residues in β-lactoglobulin. Due to the high variance of the data for the gold surface (Table 4-1), a *t*-test does not show a statistically significant difference on changing the surface chemistry from silica to gold ($Pr = 0.734$). The greater variation for the gold data may be to due to greater surface roughness after the coating procedure.

**Table 4-1** **Variation in interfacial stress transmission with equipment design parameters.**

| | Interfacial low-strain rigidity parameter (mN/m) | Standard deviation | Max interfacial stress (mN/m) | Standard deviation | Min interfacial stress (mN/m) | Standard deviation |
|---|---|---|---|---|---|---|
| Silica | 67.4 | 11.3 | 9.9 | 0.5 | -25.7 | 6.1 |
| Gold | 73.2 | 34.0 | 10.1 | 1.1 | -26.2 | 7.4 |
| Amine | 102.2 | 14.1 | 10.7 | 0.4 | -32.1 | 4.2 |
| Thiol | 108.8 | 20.4 | 10.4 | 0.4 | -32.4 | 3.8 |
| C4 Particles | 17.4 | 2.2 | 9.9 | 0.6 | -11.1 | 4.2 |
| 50 mm long, 240 μm dia | 104.9 | 8.4 | 9.9 | 0.4 | -33.6 | 2.4 |
| 50 mm long, 300 μm dia | 119.7 | 15.0 | 10.0 | 0.4 | -33.4 | 3.0 |
| 50 mm long, 400 μm dia | 134.9 | 20.6 | 10.4 | 0.4 | -30.2 | 3.8 |
| 25 mm long, 400 μm dia | 130.4 | 8.9 | 10.0 | 0.3 | -33.8 | 4.7 |
| 100 mm long, 400 μm dia | 76.6 | 11.8 | 10.0 | 0.5 | -26.4 | 5.5 |

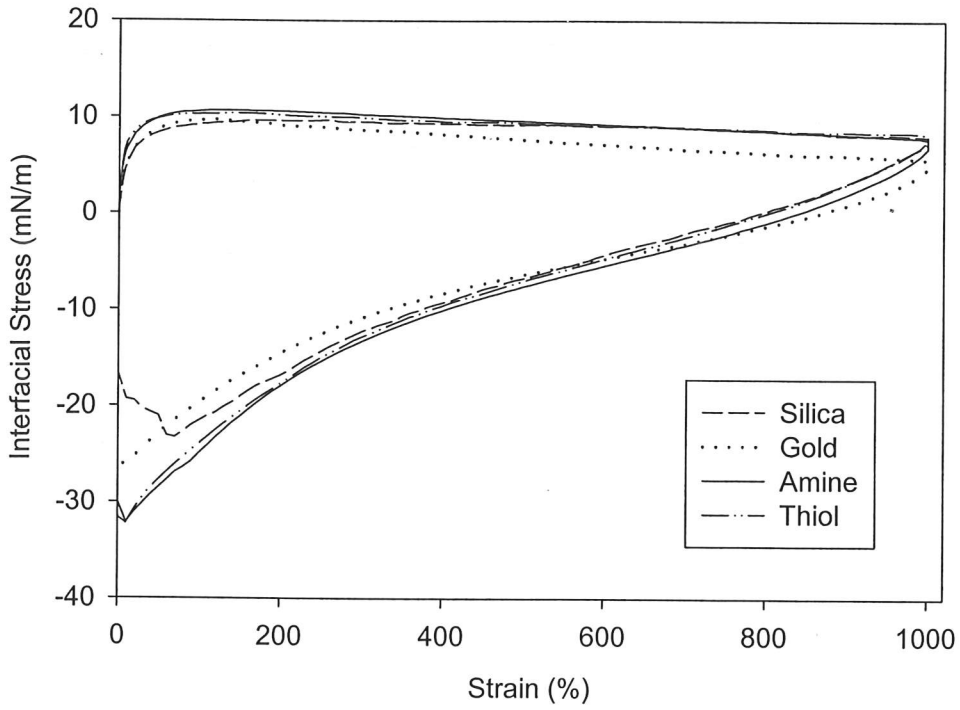


**Figure 4-7** **Stress versus strain curves for various T-bar surface chemistries. Initial T-bar separation = 1.0 mm, length = 50 mm, displacement speed = 200 μm/s, protein concentration = 1.0 mg/mL.**

A deliberate attempt to increase T-bar roughness and the surface area available for protein binding was made by sticking hydrophobic particles (C4 HPLC column packing, 20 μm diameter) to the silica T-bars. The results are shown in Figure 4-8 and Table 4-1. The four other T-bar surface coatings generated stress-strain plots of very similar shape and only the average is shown in Figure 4-7. However, the particulate coating resulted in erratic force measurements and the three separate tests plotted in Figure 4-8 show this effect. Table 4-1 indicates that the low-strain rigidity parameter is greatly reduced after coating the T-bars with the hydrophobic particles. The reduced value of the measured film rigidity and erratic force signal are caused by the detachment of the particles from the T-bars, which was clearly visible during the test procedure. Therefore, the low standard deviation of the low-strain rigidity parameter for the C4 particle coated T-bars should be interpreted with caution, as it probably indicates particle detachment at a consistent level of stress. Although the particulate coating technique is not used again, the results are highly significant as the method

effectively introduces a weak point into the protein network at the three-phase boundary. The dramatic impact on the experimentally determined film rigidity clearly demonstrates that the CIT measures the force transmitted through the interfacial protein network and not localised changes of interfacial tension.

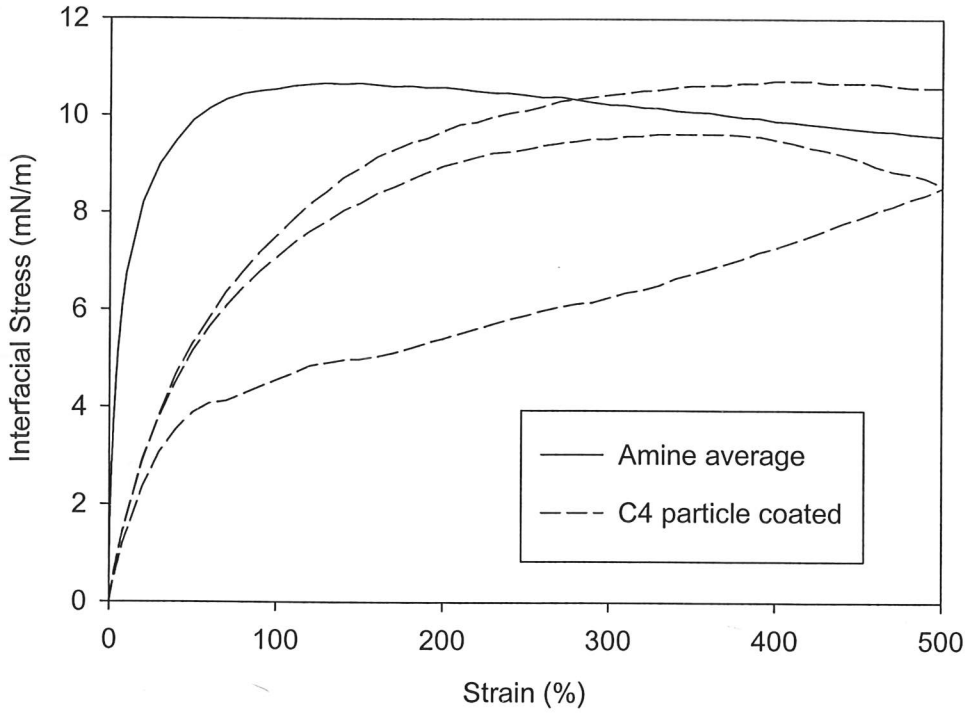


**Figure 4-8** **Stress versus strain curves for T-bars derivatised with hydrophobic silica particles (20 μm average diameter). Initial T-bar separation = 1.0 mm, length = 50 mm, displacement speed = 200 μm/s, protein concentration = 1.0 mg/mL.**

Data in Table 4-1 produced using the four non-particulate surface coatings show division of the data into two distinct groups: the silane derivatised and non-silane derivatised surfaces. The data sets for the amine and thiol functionalised surfaces match closely. Both the interfacial low-strain rigidity parameter and the maximum transmitted stress are greater for the silanised surfaces than for the silica and gold surfaces. A *t*-test, looking for a statistically significant difference between the data sets for the interfacial low-strain rigidity parameter, only achieves a confidence level > 95% when comparing data from the two silanised fibres with the data obtained using the bare silica T-bars. This suggests that fibre hydrophobicity is the dominant factor in determining the strength of protein bonding to the solid surface, rather than

the ability of the fibre to covalently bind with the protein molecules. The importance of fibre hydrophobicity is also shown by the lower magnitude of the compressive force measured for the bare silica and gold coated fibres at the end of the compressive section of the tests (shown in Figure 4-7 and Table 4-1). During the equipment testing with hydrophilic silica T-bars, it was observed that the bars tended to sit lower in the interface and the ends became submerged after the compressive phase of the experiments, reducing the available length for force transmission (see Figure 4-7, silica curve). The data in Table 4-1 show that the amine derivatised surface resulted in the maximum level of stress transmission through the protein film, a high modulus of elasticity, and the lowest variation between tests. Therefore, the amine alkyl-silane derivatised fibres were taken as the standard in all subsequent experiments with the CIT. The most common protein concentration used for the tests in this chapter was 1.0 mg/mL and together with the amine surface coating, initial bar separation of 1.0 mm and displacement speed of 200 μm/s, is referred to as "normal conditions" in all subsequent tests.

Care was taken to ensure that protein bound to the T-bars was consistently removed between tests as this had been seen to affect the reproducibility of earlier experiments. This is consistent with the data from the particulate coating experiments where the presence of loosely bound material resulted in the measurement of an erratic force signal. The silica and gold-coated fibres were cleaned in piranha solution as this has been shown to regenerate a gold surface after thiol immobilisation (Georgiadis *et al.*, 2000) and can hydrolyse the protein molecules. The T-bars were then washed in acetone, ethanol and water to remove any remaining material. For the thiolated T-bar, where cleaning with piranha solution was not possible, washing with dithiothreitol (DTT) solution was performed to reduce any protein-solid disulfide bonds.

### *4.3.2. T-Bar Dimensions*

The physical dimensions of the T-bars were systematically varied to ensure that the results are representative of the material properties and not a function of equipment size. Graphs showing the testing of equipment design parameters are presented as plots of stress versus strain rather than force versus displacement. Force is normalised with bar length, and displacement converted to engineering strain using the initial

separation. Figure 4-9 shows that the behaviour is very similar for all bar diameters tested. The measured interfacial low-strain rigidity parameter increases slightly with bar diameter as the T-bars become stiffer (Table 4-1), but the variance of the data also rises.

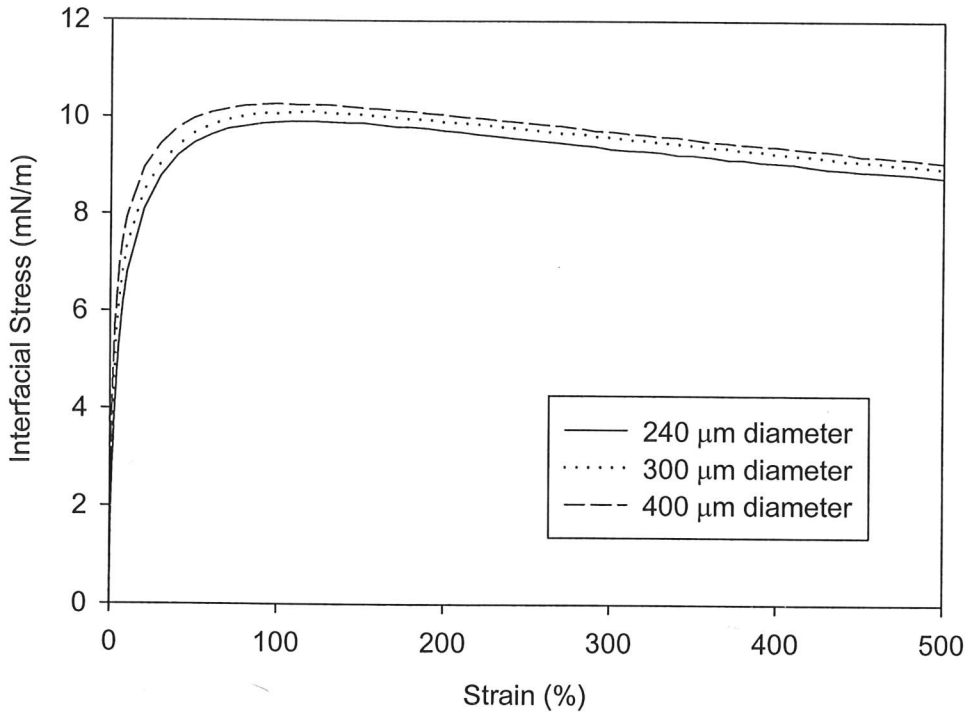


**Figure 4-9** **Variation in stress-strain behaviour with T-bar diameter. Initial T-bar separation = 1.0 mm, length = 50 mm, displacement speed = 200 μm/s, protein concentration = 1.0 mg/mL.**

Shortening the T-bars from 50 mm neither increases the maximum measured interfacial stress nor the interfacial low-strain rigidity parameter (Figure 4-10, Table 4-1). The data for the 100 mm long bars show reduction in the measured low-strain rigidity parameter and changed curve shape in Figure 4-10 due to the greater compliance of the bar under load, but no significant reduction in maximum transmitted interfacial stress. If the T-bars are not sufficiently stiff, then the measured elasticity will be reduced. This is because the average displacement of the T-bar will be lower than that registered by the position encoder in the Inchworm motor due to the fibre flexing towards the other T-bar. The recorded data will overstate the actual value of strain and hence the calculated interfacial low-strain rigidity parameter will

be reduced. Maximum interfacial stress remains unaffected by T-bar stiffness as the maxima do not occur at a predefined displacement. A compromise must be reached between shortening the T-bars to reduce bending, and the negative influence of the bar ends on transmitted stress. The effect can be seen in Figure 4-10 where the rate of stress decrease, after the maxima, occurs in reverse order of bar length. This negative effect of the bar ends is discussed again in the next paragraph. Table 4-1 shows that the maximum values of interfacial low-strain rigidity parameter (135 mN/m) and transmitted interfacial stress (10.4 mN/m) are obtained with 50 mm long, 400 μm diameter T-bars. These results for β-lactoglobulin, lie within the 60 mN/m – 400 mN/m range reported by Graham and Phillips (1980a) for the dilatational elasticity modulus of the globular protein BSA and are in reasonable agreement with the figure of 57 mN/m reported by Benjamins and Vader (1992) for ovalbumin. The data suggest that a 400 μm diameter, 50 mm long T-bars gives the optimal compromise between stiffness, disturbance of the aqueous phase whilst the bar is moving, influence of the bar ends and equipment signal to noise ratio.

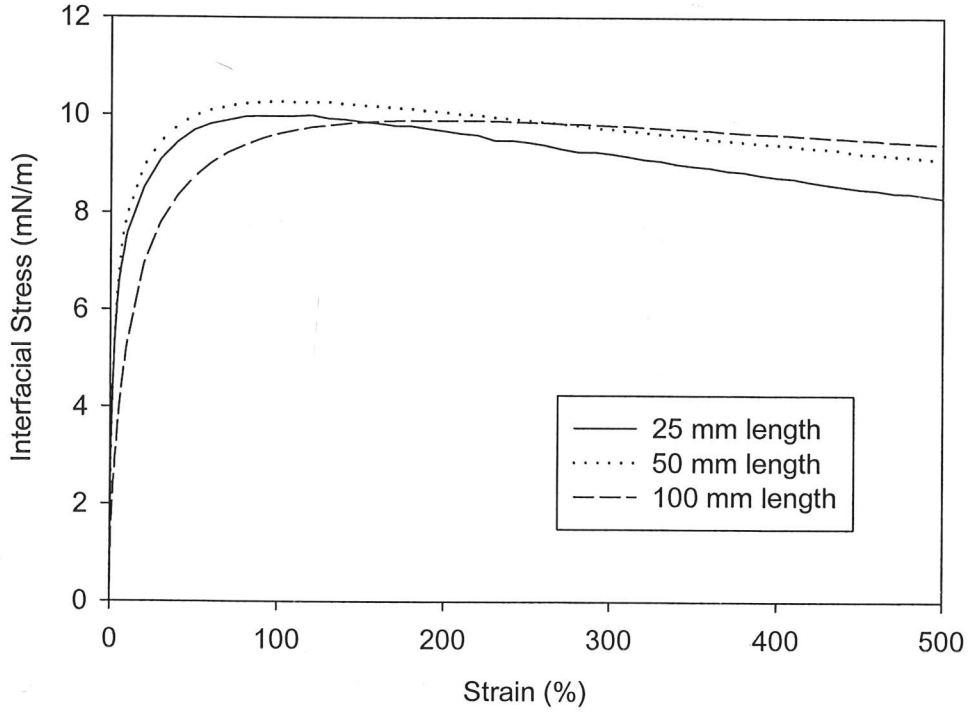


**Figure 4-10** **Variation in stress-strain behaviour with T-bar length. Initial T-bar separation = 1.0 mm, displacement speed = 200 μm/s, protein concentration = 1.0 mg/mL.**

### 4.3.3. Material Strain Rate

Figure 4-11 and Table 4-2 show the strain-rate dependence of the interfacially-bound material. The strain-rate is doubled or halved by changing the bar displacement speed or initial separation. When the results are plotted as normalised stress versus strain, the data at the corresponding strain-rates collapse almost onto a common curve. The two curves higher than that for "normal conditions" show the data where the strain-rate was doubled, either by halving the initial separation or by doubling the bar speed, and the two lower curves indicate the effects of halving the rate of strain. The force data are normalised with respect to T-bar length and displacement converted to engineering strain by dividing by the initial separation. At a given strain-rate, the CIT provides a very similar stress-strain curve regardless of bar separation or displacement speed, within the limited parameter range tested. This gives further confidence in the measurement, as the dominant effect observed with these tests is a strain-rate dependent behaviour of the interfacial layer. This would be expected for a thin film of a polymeric material. However, it is important to note that the changes are more extreme when the strain-rate is altered by changing the initial bar separation rather than the speed of motion. When the initial separation is altered, the ratio of bar length to open path between the bars is also changed, altering the shape of the test section and possibly introducing regions of greater localised stress build-up with the film.

**Table 4-2** **Changes in material mechanical properties with strain-rate.**

| | Interfacial low-strain rigidity parameter (mN/m) | % change | Max interfacial stress (mN/m) | % change | Min interfacial stress (mN/m) | % change |
|---|---|---|---|---|---|---|
| Normal conditions | 126.2 | 0.0 | 9.4 | 0.0 | -37.8 | 0.0 |
| 400 μm/s | 125.8 | -0.3 | 10.0 | 6.4 | -37.6 | -0.5 |
| 100 μm/s | 114.5 | -9.3 | 8.6 | -8.2 | -33.9 | -10.3 |
| 2000 μm separation | 91.3 | -27.6 | 8.4 | -10.2 | -27.6 | -26.9 |
| 500 μm separation | 147.4 | 16.8 | 10.3 | 9.7 | -41.9 | 10.9 |

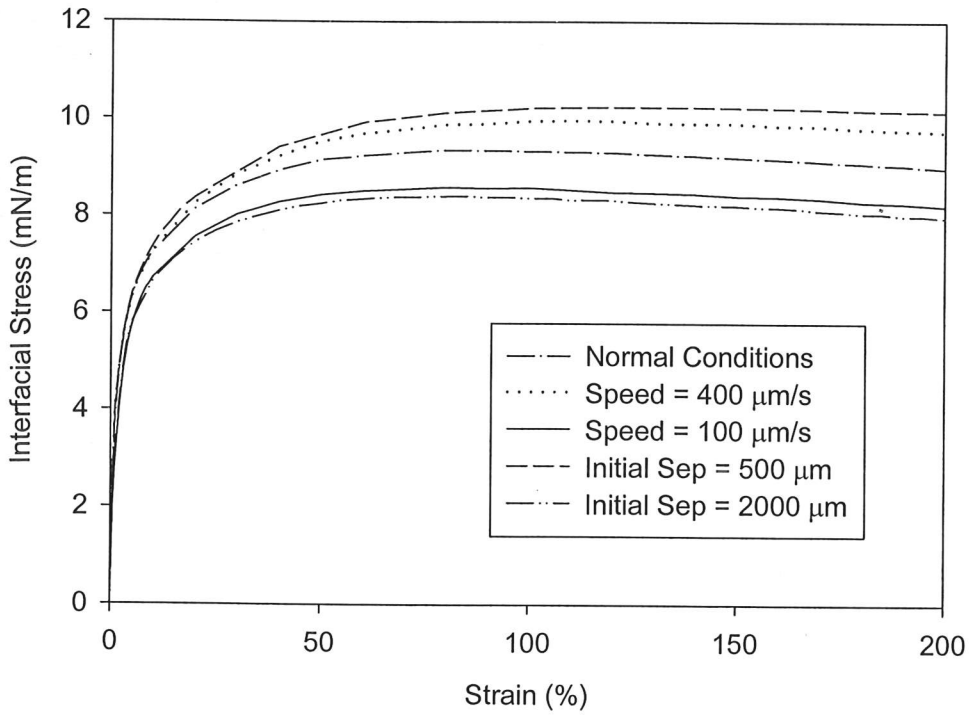


**Figure 4-11** **Strain-rate dependent stress-strain response of an interfacially adsorbed β-lactoglobulin film. "Normal Conditions" : initial T-bar separation = 1.0 mm, length = 50 mm, displacement speed = 200 μm/s, protein concentration = 1.0 mg/mL.**

## 4.4. Conclusions

The CIT has been shown to be capable of providing a direct measure of the mechanical properties of an adsorbed protein layer at the air-water interface. The instrument is able to determine the stress-strain response of an interfacially adsorbed protein network to high strain or to the material failure point. The results obtained have been validated by systematic changes in equipment dimensions and operating parameters. Effects caused by equipment size and geometry are minimal and the interfacial protein layer exhibits a strain-rate dependent response, as expected for a polymer-like material. The results are essentially independent of the method used to vary the strain rate (e.g. by altering the initial separation or bar speed).

Films of β-lactoglobulin adsorbed at the air-water interface and aged for a period of 1 h show highly rigid behaviour to 5% - 7% strain. Values of interfacial low-strain rigidity parameter are in the region of 100 mN/m for all experiments performed. This is in broad agreement with the results of Graham and Phillips (1980a) and Benjamins and Vader (1992) for the dilatational elasticity moduli of the globular proteins BSA (60 mN/m – 400 mN/m) and ovalbumin (57 mN/m). Substantial yielding of the network begins to occur between 10% and 50% strain and the peak interfacial stress is usually reached at around 100% strain.

The protein films showed considerable "self-healing" ability at large strains due to protein transport into the interfacial region, probably as a result of the relatively high bulk protein concentration (1.0 mg/mL). β-lactoglobulin films do not show a true failure point and significant detachment from the solid T-bars does not occur. Binding of the protein to the solid surface depends upon the hydrophobicity of the fibre surface to a greater extent that any ability to covalently crosslink using the thiols present in β-lactoglobulin.

The CIT is able to generate full constitutive data on the test material in the form of complete stress-strain curves for adsorbed protein films up to a high degree of deformation. This is this first time such data have been reported.

# 5. Molecular Structure and Network Mechanical Properties

## 5.1. Introduction

Chapter 4 demonstrated the ability of the Cambridge Interfacial Tensiometer (CIT) to characterise the micro-mechanical response of β-lactoglobulin networks adsorbed at the air-water interface. The technique is an interfacial two-dimensional analogy of conventional materials testing methodology, but is conducted with high spatial resolution and requires the measurement of micro-Newton forces. The previous chapter verified data reproducibility and demonstrated that the results reflect the constitutive properties of the test material rather than equipment design or operating parameters. Data analysis was discussed and supporting evidence provided to confirm the validity of the methods used.

The key figure in Chapter 4 (Figure 4-1) clearly demonstrated that it is the presence of adsorbed protein molecules that confers the ability to transmit force laterally in the plane of the interface, as negligible force transmission was observed for the case of buffer only. It is believed that after adsorption at the interface, conformational changes occur resulting in the formation of an interfacial network of finite thickness. The CIT probes the dominant inter- and intra- molecular interactions through the dynamic response of this interfacial layer to an external straining force. The CIT technique was shown to complement existing surface rheology approaches for the characterisation of interfacial protein networks, and advantageously does not require *a priori* assumptions about network properties and behaviour.

The aim of this chapter is to continue following ideas originating from the analogy with conventional material testing mentioned above. In Chapter 2 several authors were shown to have observed the formation of rigid (solid-like) interfacial films of adsorbed protein. The body of literature generated by previous workers also indicates that globular proteins give rise to films with greater dilatational and shear moduli than random coil proteins. This result strongly suggests that fundamental insight into the properties of interfacial protein networks may be gained by regarding them as nanostructured biomaterials. In summary, the aim is to use the newly tested and

validated CIT to address the complex interplay between the material mechanical properties and the structure at a molecular level.

## 5.2. Networks as Nanostructured Biomaterials

The high initial gradient of the stress-strain curves in Figure 5-1 indicates a high interfacial elasticity modulus *(Et)* of the β-lactoglobulin network at low strain. Numerical values of *Et* are defined using the force registered at 1% strain, giving a quantitative measure of network rigidity derived from the largely linear region of the stress-strain curve. The accuracy of this approximation and the reproducibility of the experimental technique were discussed in the previous chapter and displayed graphically in Figure 4-5. The average interfacial elasticity modulus *(Et)* for the data shown in Figure 5-1 corresponding to 1.0 mg/mL β-lactoglobulin concentration is 193 mN/m (Table 5-1). Carrion-Vazquez *et al.* (1999) have carried out Atomic Force Microscopy (AFM) unfolding studies on the protein I27 from human cardiac muscle. Unfolding forces of approximately 200 pN were detected in a polymer of eight repeating units, with the peaks spaced by 24.1 nm. Similar tests performed by Best *et al.* (2001) on a protein having no physiological requirement for mechanical strength (barnase), gave unfolding forces of approximately 70 pN. Using a guide to protein diameter of 1.5 nm for I27 (Improta *et al.*, 1996) and 6.6 nm for barnase (Mauguen *et al.*, 1982), the elasticity moduli obtained are 44 MPa and 3.5 MPa, respectively. In the CIT tests, these moduli correspond to *Et* values of 222 mN/m for I27 and 18 mN/m for barnase, assuming 100% molecular packing density at the air-water interface and a 5 nm film thickness (Graham and Phillips, 1979b). This shows that the stresses generated during mechanical testing of interfacial protein networks with the CIT are comparable to the forces required to unfold protein tertiary structure. Stress-induced conformational changes in the interfacially adsorbed protein molecules appear to determine the magnitude of *Et* measured by the CIT at low strain.

**Table 5-1** **Effect of bulk β-lactoglobulin concentration on the mechanical properties of protein films adsorbed at the air-water interface. Percent change values are relative to the data at 0.01 mg/mL.**

| | Interfacial elasticity modulus (mN/m) | Maximum interfacial stress (mN/m) | Minimum interfacial stress (mN/m) |
|---|---|---|---|
| 0.01 mg/mL β-lactoglobulin | 124.3 | 12.3 | - 28.1 |
| (% change) | (0.0) | (0.0) | (0.0) |
| 0.1 mg/mL β-lactoglobulin | 156.5 | 12.9 | - 31.3 |
| (% change) | (+ 25.9) | (+ 4.7) | (+ 11.2) |
| 1.0 mg/mL β-lactoglobulin | 192.9 | 9.4 | - 37.9 |
| (% change) | (+ 55.2) | (- 23.1) | (+ 34.8) |

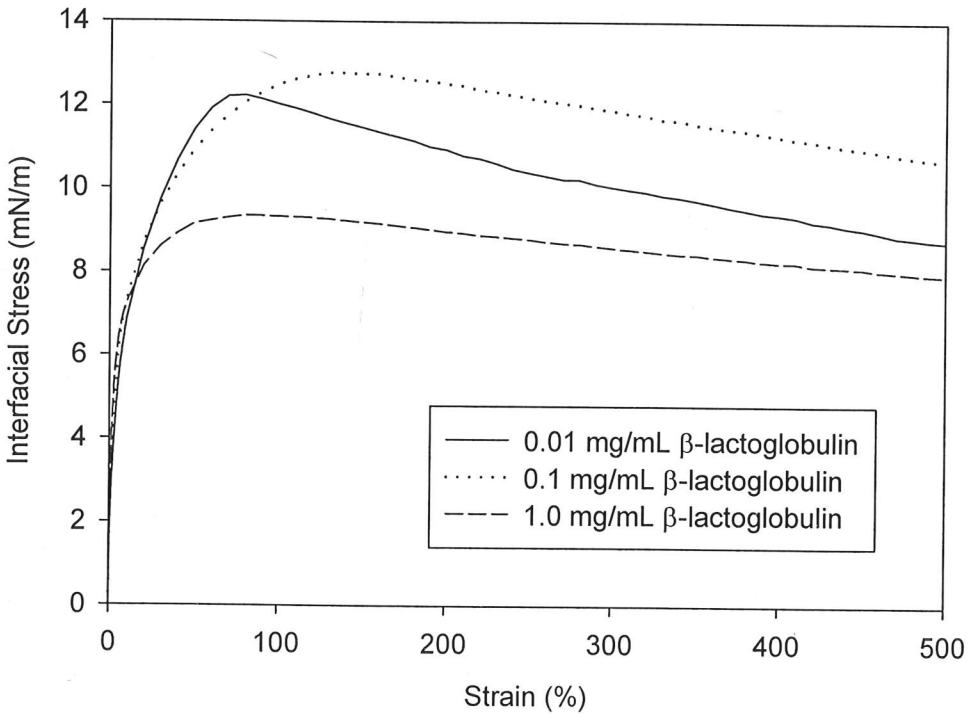


**Figure 5-1** **Stress versus strain response of β-lactoglobulin networks adsorbed from PBS buffer (pH 7.4) at different bulk protein concentrations.**

AFM was used by Idiris *et al.* (2000) to investigate the spring mechanics of an α-helical polypeptide. Young's Modulus of Elasticity was found to be of order 3 GPa giving an interfacial elasticity modulus of 15 N/m, assuming a 5 nm thick β-lactoglobulin layer. *Et* values of approximately 15 N/m are far higher than those determined experimentally on real β-lactoglobulin films with the CIT (order 200 mN/m). Therefore, it seems reasonable to assume that, in the context of CIT tests, any protein secondary structure present at the interface can be considered mechanically stiff.

### 5.2.1. Concentration Dependence

Figure 5-1 shows the average stress-strain plots (up to 500% strain) for β-lactoglobulin films adsorbed from different bulk protein concentrations and aged for 1 h at the air-water interface. Each curve shows the average of three parallel repeats performed in random sequence on different days. Reduction of the bulk β-lactoglobulin concentration from 1.0 mg/mL to 0.01 mg/mL increased by 31% the maximum force transmitted through the protein network (Table 5-1). Lowering the bulk protein concentration results in a lower rate of transport to the interface, and consequently proteins will experience less initial competition for space at the clean interface. It is therefore probable that a reduction in bulk protein concentration results in a greater degree of protein conformational change after adsorption, and hence the likelihood of more extensive molecular entanglement. The resulting increase in maximum force transmitted through the network reflects a greater extent of intermolecular protein interactions, and a resulting enhancement of network integrity. Such a hypothesis is supported by the modelling work of Dickinson and Euston (1992) who suggested that protein molecules may unfold upon reaching a bare interface, but will remain folded if the interface is already covered with adsorbed molecules. This is also supported by the studies of Middelberg *et al.* (2000), which showed that removal of a single helical peptide from a bulk tetramer into the interfacial region is inhibited when the fractional interfacial coverage exceeds some critical value. The tetrameric peptide assembly is not unlike a simple protein – it cannot unfold in the subinterfacial region when the interface is already covered. The highest interfacial stress is observed with 0.1 mg/mL β-lactoglobulin solution

(Figure 5-1 and Table 5-1). Under these conditions, and after a 1 h ageing period, the adsorbed protein network shows the optimal compromise between intermolecular bonding and film packing density. Intermolecular bonding is enhanced by protein conformational changes, but such changes may be retarded at high protein concentration due to high interfacial packing density caused by the rapid transport of protein molecules to the interface.

Table 5-1 shows the numerical data extracted from Figure 5-1. Although the maximum tensile stress is highest at the intermediate protein concentration, interfacial elasticity modulus rises as bulk protein concentration is increased. At higher protein concentrations, each protein molecule experiences only a short time at the clean air-water interface before becoming crowded by its nearest neighbour. If the protein molecule is unable to denature and spread significantly after adsorption, the packing density of secondary structure at the interface will be high, resulting in a rigid film. Therefore, although the stress generated in the CIT is unlikely to unfold an α-helical structure, stress-induced conformational changes in the protein molecule probably dominate the low strain behaviour of the β-lactoglobulin network.

### *5.2.2. Secondary Structure Packing Density*

It may be useful to view proteins that are correctly folded in the bulk solution as "islands of cooperatively-ordered hydrogen-bonded structure, floating in an aqueous network of less-well ordered H-bonds" (Cooper, 2000). The same idea could be extended to partially denatured proteins adsorbed at the air-water interface, except for the phase boundary between the weakly H-bonded water structure and the air. The important properties of a protein molecule then become the amount of secondary structure present, rigidity of this structure, and the mobility of these rigid structural elements within the molecule (a form of tertiary structure). Such an analysis makes the implicit assumption that protein or peptide secondary structure is preserved after adsorption from aqueous solution. Infrared spectra of polymethyl glutamate monolayers spread at the air-water interface indicate the presence of secondary structure (Loeb and Baier, 1968) and Caessens *et al.* (1999) have demonstrated that the helical content of peptides derived from β-casein increases upon adsorption to a hydrophobic solid surface. Evidence to support the hypothesis of rigid units of

secondary structure within a more flexible protein molecule can be found in the work of Boyd *et al.* (1973). Experimental values of interfacial shear viscosity are compared with the theory of Moore and Eyring (1938). The model envisages an energy barrier to viscous flow equal to the energy required to create a "hole" in the interfacial layer sufficient to accommodate one flow element. Boyd *et al.* (1973) report that the area required for molecular flow in the interface is less than the area of one whole protein. The authors interpret this to mean that part of the energy barrier to molecular flow in the interface must result from the strength of the protein intramolecular bonds. This outcome is in agreement with the hypothesis of one unit of secondary structure as the flow element. One of the few consistent trends to emerge in the study of interfacial rheology of protein films is that globular proteins (such as β-lactoglobulin) give rise to films with greater shear and interfacial dilatational moduli than more flexible random coil proteins such as caseins (Graham and Phillips, 1980a, 1980b; Williams and Prins, 1996; Faergemand *et al.*, 1997; Faergemand and Murray, 1998). This provides further evidence that the packing density of secondary structure at the interface is the dominant factor in determining the interfacial elasticity modulus of the adsorbed protein film.

### 5.3. Network Repair

The β-lactoglobulin films show considerable ability for "repair", defined as the ability to establish a stress plateau at high strain. Such materials do not exhibit the usual yield point that characterise conventional materials. A repair capability is probably conferred by the transport of additional protein to the interfacial region between the T-bars during the experiment. The hypothesis that "self-healing" of the protein film occurs by adsorption of protein molecules to freshly exposed interfacial area is supported by the data shown in Figure 5-1. The magnitude of the negative gradient at high strain (> 200%) is greatest for the lowest protein concentration studied, where the transport rate of protein molecules to the liquid interface will be slowest.

The characteristic time of the CIT experiments is 5.0 s for 100% marginal strain (speed = 200 μm/s, initial bar separation = 1.0 mm). Using the Polson equation (1950) to estimate protein diffusivity, and assuming a diffusion-controlled linear isotherm (Makievski *et al.*, 1997), time constants for protein adsorption can be approximated.

$$D = 2.85 \times 10^{-9} M^{-1/3} \qquad (5.1)$$

where $D$ is the diffusion coefficient in the bulk ($m^2/s$) and $M$ is the protein molecular weight (g/mol). β-lactoglobulin molecular mass is taken as 18 300 g/mol (Pace *et al.*, 1995; ProtParam, 2000).

$$t_d = \frac{1}{D}\left(\frac{\Gamma_{max}}{C_\infty}\right)^2 \qquad (5.2)$$

where $t_d$ is the characteristic time (s), $C_\infty$ is the bulk protein concentration ($mol/m^3$) and $\Gamma_{max}$ is the maximum interfacial coverage ($mol/m^2$). This gives a diffusion coefficient of $1.1 \times 10^{-10}$ $m^2/s$. Time constants for protein adsorption are approximately 0.04 s, 4 s and 400 s for bulk β-lactoglobulin concentrations of 1.0 mg/mL, 0.1 mg/mL and 0.01 mg/mL, respectively, if a value of 2 $mg/m^2$ is used for the maximum interfacial coverage (Graham and Phillips, 1979b). Clearly, at protein concentrations greater than 0.1 mg/mL the time constant of protein adsorption is much less than the characteristic experimental time, so significant protein adsorption would be expected during a test. The effects of adsorption time constants much greater and much smaller than the characteristic experiment time are shown in Figure 5-1. The maximum level of force transmission through the film has been reached by 100% strain (1.0 mm displacement), and this is true for almost all the β-lactoglobulin networks tested. The network repair ability, after the peak interfacial stress, is reduced as the bulk protein concentration falls. The stress plateau becomes less pronounced as the characteristic time for transport falls below that of the experiment.

Additional evidence for the transport of protein molecules to the interfacial region between the T-bars is found in Table 5-1 and was shown previously in Figure 4-1. In the full stress-strain curve plotted in Figure 4-1 the detected force became negative very early (at ~8.2 mm) in the compressive section of the test procedure. The magnitude of the negative gradient also began to increase rapidly after around 5.0 mm displacement, suggesting the compression of multiple protein layers at this point in the test. Parameters extracted from the stress-strain plots shown in Figure 5-1 are

provided in Table 5-1. The data show that the magnitude of the maximum compressive force increases at higher protein concentrations, indicating that the rate of protein transport to the inter-bar region is enhanced as the bulk protein concentration rises.

## 5.4. The Nature of Network Intermolecular Interactions.

### *5.4.1. Hydrophobic Interactions*

The CIT is also capable of operating in a cyclic, minimally invasive, mode in the low strain regime. This mode of operation provides a similar test to the oscillatory shear rheometers of other workers in the field (Benjamins and Vader, 1992; Burgess and Sahin, 1997). The increase in the registered force provides a semi-quantitative indication of film rigidity or interfacial elasticity modulus. An additional advantage of operating the CIT in cyclic mode, resulting from the minimally invasive nature of the test, is that a protein film can be formed, tested and then subjected to some change in local environment. In this way variations due to the formation of a fresh interface for each test are eliminated as the same film is tested over the whole time period. Figure 5-2 shows the results from cyclic testing of a film formed from PBS buffer containing 1.0 mg/mL (55 μM) β-lactoglobulin. The protein molecules were allowed to adsorb at the air-water interface for a period of 30 min prior to injection of a concentrated solution of Tween 20 or dithiothreitol (DTT) to give bulk concentrations of 55 μM and 100 mM, respectively. The experiment was continued for a further 60 min to show any changes in film rigidity resulting from the addition of these chemicals.

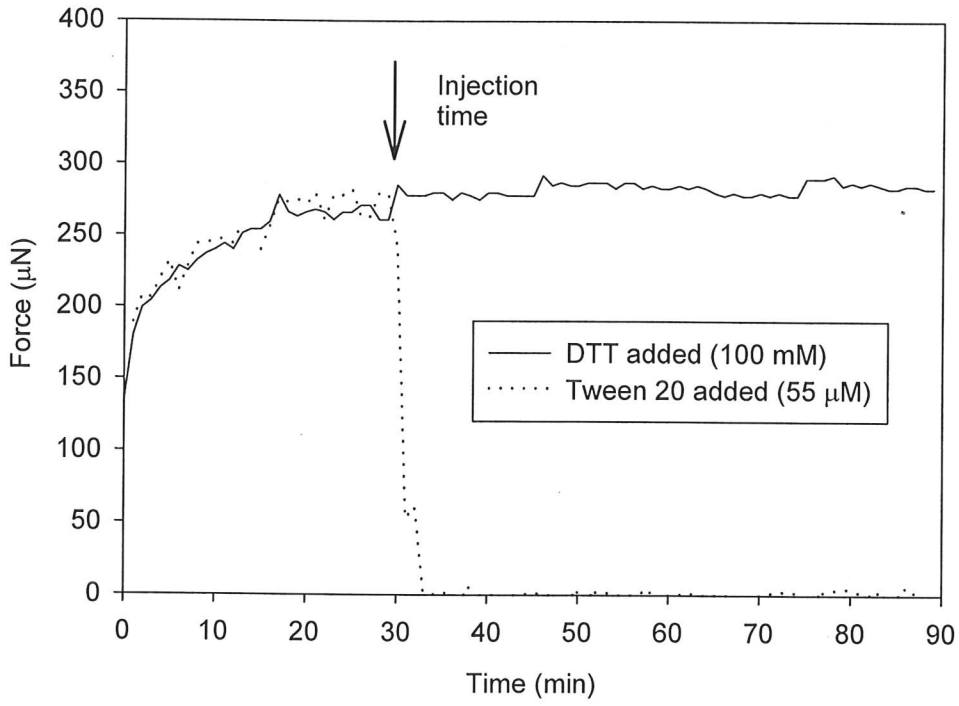


**Figure 5-2** **Non-destructive cyclic operation of the CIT to 5% strain. The data represent the increase in tensile force after the application of a 50 μm tensile displacement from a 1.0 mm initial T-bar separation. The interfacial network was formed for 30 min from a 55 μM (1.0 mg/mL) β-lactoglobulin solution in PBS buffer (pH 7.4). Dithiothreitol (DTT) or Tween 20 was injected after 30 min to give bulk concentrations of 100 mM and 55 μM, respectively.**

Figure 5-3 also shows data from the CIT operating in cyclic mode after addition of the same surfactant (Tween 20). The plot shows an extension of the data reproduced in Figure 4-6, from a total interface age of 90 min to 150 min. At 94 min a small amount of the non-ionic surfactant, Tween 20, was added giving a bulk concentration of $10^{-5}$ M. In this experiment, however, the lower protein concentration (0.01 mg/mL, 0.55 μM) means that the surfactant and protein are no longer in an equi-molar ratio.

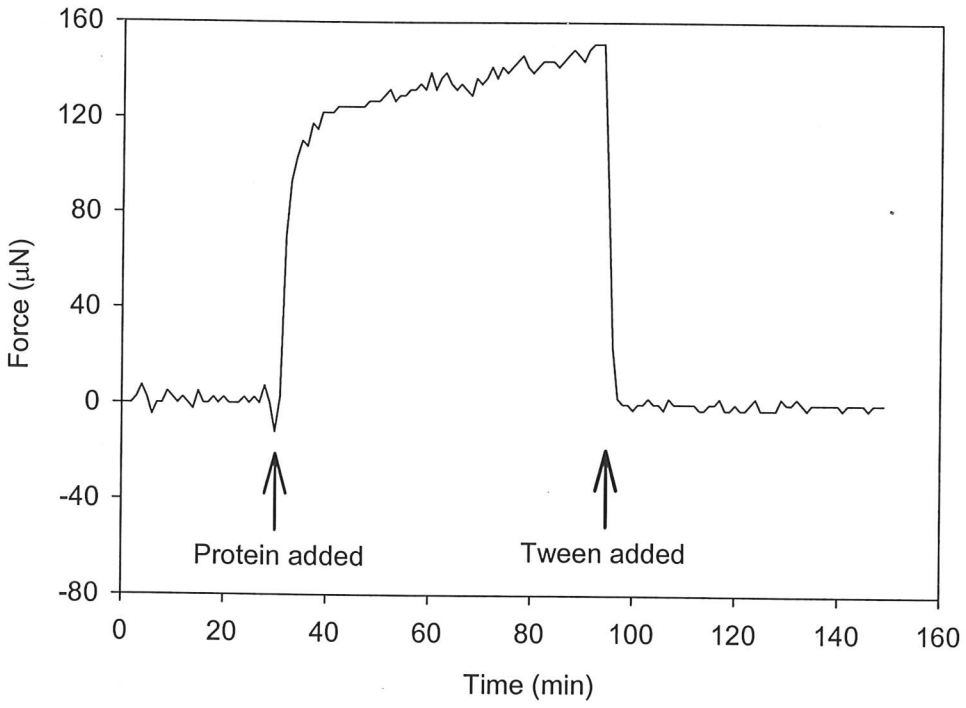


**Figure 5-3** **Cyclic CIT operation showing rigid film formation after addition of β-lactoglobulin to give 0.01 mg/mL bulk concentration, and subsequent loss of lateral force transmission with injection of Tween 20 after 94 min to give $10^{-5}$ M bulk concentration.**

Disruption of the hydrophobic bonding ability of the protein molecules with the low molecular weight, non-ionic, surfactant Tween 20 (55 μM) is shown by the dotted line in Figure 5-2. The result is immediate and complete fluidisation of the interfacial region and the loss of ability to transmit force laterally between the parallel T-bars of the CIT. A similar response to Tween addition has been observed for the gold and bare silica T-bar surface chemistries. This finding is confirmed by the work of Petkov *et al.* (2000) and Courthaudon *et al.* (1991) who have shown that addition of Tween 20 to the bulk aqueous phase below an interface covered with adsorbed protein causes fluidisation of the interfacial region. The amount of protein present at the interface during the competitive adsorption of β-lactoglobulin and Tween 20 has been characterised as a function of the molar ratio of surfactant to protein *(R)* by Clark *et al.* (1994) and Courthaudon *et al.* (1991). By measuring fluorescence recovery after

photobleaching of thin protein films, Clark *et al.* (1994) have shown that at certain Tween 20 concentrations ($0.1 < R < 0.8$) the film thickness actually increases. However, when $R > 1$ the equilibrium film thickness rapidly reduces to a value typical of Tween 20 films. The authors note that "there is still significant protein present in the adsorbed layers of the thin films up to $R = 5$". This result is in keeping with the findings of Courthaudon *et al.* (1991) who demonstrated that a surfactant-to-protein ratio of eight was required before complete displacement of β-lactoglobulin from the *n*-tetradecane-water interface occurred.

A more recent study by Mackie *et al.* (1999) has, for the first time, achieved visualisation of protein films undergoing competitive displacement by Tween 20. The results indicate an "orogenic" mechanism where the surfactant first adsorbs at defects in the network structure of protein molecules adsorbed at the interface. The surfactant patches then grow and compress the protein layer, initially without any accompanying protein desorption. This explains the increase in film thickness at intermediate values of $R$ observed by Clark *et al.* (1994) and the prolonged presence of protein at the interface at much higher values of $R$. Interestingly, a simulation performed by Wijmans and Dickinson (1999), considering the protein layers as a network of bonded spherical particles, predicted both the formation of an interfacial gel-like structure and the experimentally observed "orogenic" displacement mechanism.

In light of these previously observed effects it is expected that once the interfacial protein network has been partially destroyed by the surfactant, the interfacial region will behave in a fluid-like manner and no lateral force transmission will be observed. This assertion matches the experimental observations with $R = 1$ (Figure 5-2), providing evidence that hydrophobic bonding is an important mechanism in the formation of solid-like interfacial networks. The Tween 20 molecules themselves have a well-defined separation of the hydrophilic and hydrophobic sections of the molecule. When such molecules partition at the air-water interface there is no lateral hydrophobic interaction between the molecules, explaining the molecular mobility and fluid-like nature of the interfacial region. In contrast, proteins such as β-lactoglobulin have an amphiphilic nature but the exposed hydrophobic patches are "randomly" distributed across the protein surface. Therefore, the free energy of the

system can be reduced both by interfacial adsorption of the protein molecules and through protein-protein hydrophobic interactions. Hence lateral force transmission through the adsorbed network is possible.

### *5.4.2. Disulfide Bonding*

It has been previously suggested that intermolecular disulfide bond formation is an important mechanism in the formation of β-lactoglobulin films with a high dilatational or shear modulus (Dickinson and Matsumura, 1991; Dickinson, 1997). β-lactoglobulin contains two disulfide bonds and one free cysteine residue (McKenzie, 1972). Intermolecular disulfide bonding could occur via the free cysteine residue or by rearrangement of the existing disulfide bonds. If such a hypothesis is true, molecules capable of destroying disulfide bonds (such as DTT) should change the mechanical properties of a β-lactoglobulin network measured with the CIT. Figure 5-2 shows an interfacially adsorbed β-lactoglobulin film aged for 30 min and then subjected to a highly reducing environment through the addition of DTT. Freshly made DTT solution was injected to give a bulk concentration of 100 mM. No detectable change in network strength was observed, strongly suggesting that disulfide bonding is not the dominant mechanism of protein-protein interaction for molecules adsorbed at the air-water interface. This finding presents an independent verification of the work of Petkov *et al.* (2000), using an entirely different technique. The reason that addition of DTT has no effect is probably because the packing density is already determined by the initial protein adsorption rate. This explains why the method of initial interface formation is so important and the large variation in the results of Benjamins and Vader (1992) when a new interface was formed between experiments. The results in Figure 5-2 suggest that conformational changes occur in other weaker sections of the β-lactoglobulin molecule, and that significant strain is not generated in regions of the protein containing the disulfide bonds. It is possible to hypothesise alternative scenarios such as non-reduction of the disulfide bonds through air oxidation of the DTT or projection of all disulfide bridges out of the aqueous phase. However, it seems unlikely that the adsorbed β-lactoglobulin molecule has sufficient mobility to project all sulfur containing residues into the air phase and there are other amino acids present in β-lactoglobulin with greater hydrophobicity than

cysteine. In addition, the highly reducing environment of 100 mM DTT will continue to break disulfide bonds even if some reactive DTT is lost through oxidation.

## 5.5. Dependence of Network Nanostructure on Protein Structure

Figure 5-4 shows cyclic test results for networks formed from proteins having different structure in bulk solution. The dotted lines indicate data for β-lactoglobulin pre-reduced for 30 min in 100 mM DTT and then added to the CIT in the same DTT containing buffer. Comparison of these data with those for native β-lactoglobulin (solid lines) indicates that disruption of protein tertiary structure in the bulk results in a protein network of lower rigidity. This is in contrast with the results shown in Figure 5-2, where no change in force transmission was detected when DTT was added after the network had formed. This observation emphasises that interfacial nanostructure depends on the tertiary structure and stability of the monomeric protein units in the bulk solution. Pre-reducing the disulfide bonds of the β-lactoglobulin molecules before adsorption allows more rapid conformational changes in the protein molecules after adsorption, and hence a greater degree of molecular spreading. Interestingly, the differences between the dotted lines (pre-reduced β-lactoglobulin) and the solid lines (native β-lactoglobulin) increase with time. This indicates a more rapid approach to a "steady-state" network rigidity for pre-reduced β-lactoglobulin, in agreement with the surface shear viscometry data of Dickinson (1990). The previously discussed data shown in Table 5-1 and Figure 5-1, strongly suggest that a greater degree of molecular spreading results in reduced packing density of secondary structure at the interface and the formation of a protein network with decreased rigidity.

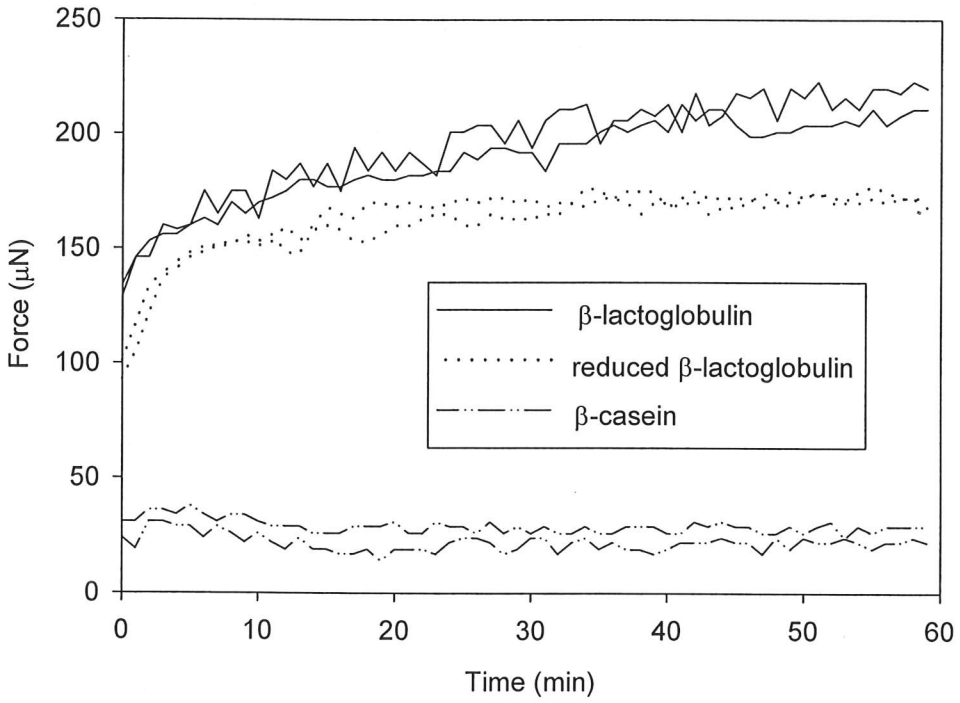


**Figure 5-4** **Cyclic operation of the CIT to 5% strain for β-lactoglobulin, reduced β-lactoglobulin and β-casein protein networks (data shown for two parallel repeats). Bulk protein solution 0.55 μM (0.01 mg/mL) in PBS buffer (pH 7.4). For the "reduced" tests, β-lactoglobulin was incubated for 30 min in 100 mM DTT prior to addition to buffer, also containing 100 mM DTT, in the CIT.**

Table 5-2 shows selected parameters extracted from full stress-strain tests of β-lactoglobulin and β-casein protein networks aged at the air-water interface for 1 h. The results show β-casein films have a much lower rigidity than β-lactoglobulin films, as determined by the magnitude of the interfacial elasticity modulus. *Et* values for β-casein were found to be only 11% of those obtained with β-lactoglobulin under the same experimental conditions. This is in agreement with the work of Williams and Prins (1996) who report interfacial dilatational moduli of approximately 62 mN/m and 13 mN/m for β-lactoglobulin and β-casein, respectively, at bulk protein concentrations greater than 0.03 mg/mL. However, the results obtained from the CIT show that that the maximum stress that can be transmitted through the β-casein film is 47% of that for a β-lactoglobulin film under the same conditions. This information

cannot be obtained using conventional surface rheology methods. It provides further evidence that conventional techniques measuring the low strain response of adsorbed protein films largely detect the structural rigidity of the adsorbed protein molecules, as the degree of intermolecular cohesion does not appear to be reduced to the extent that has been previously suggested (Williams and Prins, 1996).

**Table 5-2** **Effect of protein structure on the mechanical properties of protein films adsorbed at the air-water interface. Percent change values are relative to the data in row 1.**

| | Interfacial elasticity modulus (mN/m) | Maximum interfacial stress (mN/m) | Minimum interfacial stress (mN/m) |
|---|---|---|---|
| 0.01 mg/mL β-lactoglobulin | 124.3 | 12.3 | - 28.1 |
| (% change) | (0.0) | (0.0) | (0.0) |
| 0.01 mg/mL β-lactoglobulin | 132.0 | 12.2 | - 27.1 |
| (% change) repeat | (+ 6.2) | (- 0.5) | (- 3.8) |
| 0.01 mg/mL β-casein | 13.8 | 5.7 | - 13.2 |
| (% change) | (- 88.9) | (- 53.2) | (- 53.1) |

An unsuccessful attempt was made to increase the rigidity of an adsorbed β-lactoglobulin film by the introduction of inter- or intra- molecular covalent bonds between amine residues contained in the protein molecules. To produce a chemically crosslinked film, formaldehyde was added to the buffer solution to give a 1% formaldehyde solution capable of crosslinking the amine residues (particularly lysine) of the protein via the methylene crosslink (Marquie *et al.*, 1997). Attempting to crosslink the amine residues with formaldehyde did not greatly enhance the maximum stress that could be transmitted through the protein network as the peak interfacial

stress transmitted through the film was not changed significantly for any of the experiments performed. The implications of such a result are that network integrity was not enhanced and that the degree of intermolecular crosslinking was limited. This could indicate that further conformational changes in the protein molecules are required for a large number of intermolecular bonds to be formed, suggesting some degree of steric limitation to formaldehyde crosslinking under the conditions tested. Further experiments were performed using 1% formaldehyde solutions at various pH values as the solution pH can affect protein conformational stability (Dill, 1990) and may alter the rate of any crosslinking reactions (Marquie *et al.*, 1997).

During a 2 h ageing period, the β-lactoglobulin network rigidity was much more sensitive to the pH of the buffer solution than the degree of crosslinking possible with 1% formaldehyde solution. A significant effect of pH can be seen in the data shown in Figure 5-5, again obtained by cyclic operation of the CIT. The force difference detected before and after a 5% displacement varied by over 100% when the pH was changed between pH 4.8 and pH 10.8 at the same bulk β-lactoglobulin concentration. The network rigidity was highest at the lowest pH and decreased as the pH was increased. This demonstrates that the closer the solution pH to the isoelectric pH value of β-lactoglobulin, the greater the rigidity of the interfacial film. The theoretical isoelectric pH value for β-lactoglobulin is pH 4.8 (ProtParam, 2000). The solid line shows β-lactoglobulin dissolved in water. The data are similar to, but slightly higher than, those for PBS at pH 7.4. This would be expected for ultrapure water with no buffering capacity, as the pH will fall over time due to adsorption of $CO_2$ from the atmosphere creating low levels of carbonic acid. The greater network rigidity observed when the protein is close to its isoelectric point may be a function of a more compact molecular structure when the protein does not carry any net charge (Burgess and Sahin, 1997), or may be indicative of a greater density of adsorbed molecules at the interface. If the protein molecules carry a high net charge then repulsive forces between protein molecules adsorbed at the air-water interface may reduce the molecular packing density and degree of intermolecular bonding.

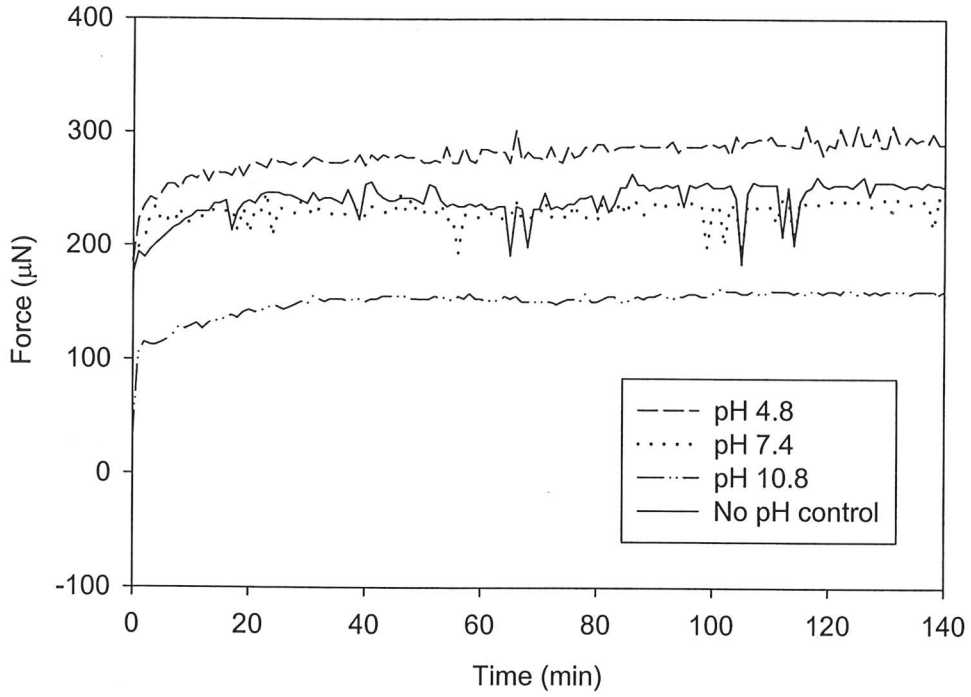


**Figure 5-5** **Cyclic CIT operation showing the effect of pH on the force transmitted (at 5% strain) through a β-lactoglobulin film adsorbed from 1.0 mg/mL aqueous solution containing 1% v/v formaldehyde. PBS buffer used at pH 7.4 and pH 4.8. Sodium carbonate buffer (100 mM) used at pH 10.8. The solid line shows data obtained with protein dissolved in ultrapure water with no pH buffering capacity.**

A hypothesis based upon packing density of secondary structure at the interface is supported by the data in Table 5-3 and Figure 5-6. β-lactoglobulin adopts a significantly more unfolded structure in bulk solution as the pH is increased. The wavelength shift of tryptophan fluorescence was used as an indication of the local environment of the hydrophobic tryptophan residues present in β-lactoglobulin. A shift to longer wavelengths indicates increased exposure of tryptophan to a polar environment (Lakowicz, 1999). Therefore any shift in fluorescence wavelength represents greater unfolding of the protein molecule, as the bulk of the hydrophobic amino acids would normally be sequestered into the hydrophobic core of the protein molecule. A least squares fit to a four parameter Gaussian peak was performed between 320 nm and 380 nm to accurately determine the wavelength of the

fluorescence maxima (see Figure 5-6). The large wavelength shift at high pH shows that some unfolding of the β-lactoglobulin molecules occurs. Therefore, the packing density of protein secondary structure at the air-water interface after adsorption is reduced and the force transmitted through the protein film is lowest at high pH values.

**Table 5-3** **Wavelength shift of tryptophan fluorescence for β-lactoglobulin solutions at different pH.**

| Buffer pH | Fluorescence peak wavelength (nm) | Peak shift from buffer at pH 4.8 (nm) |
|---|---|---|
| 4.8 | 341.5 | 0.0 |
| 7.4 | 342.0 | 0.5 |
| 10.8 | 350.3 | 8.8 |

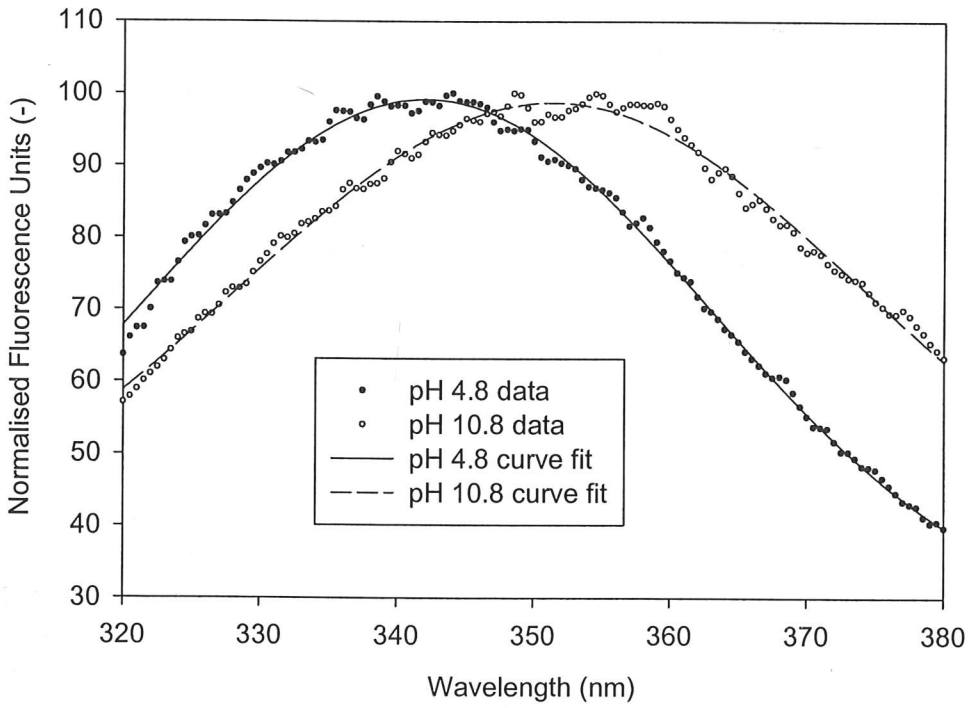


**Figure 5-6** **Tryptophan fluorescence shift for 0.01 mg/mL β-lactoglobulin in buffer at pH 4.8 and pH 10.8. Circles represent normalised data and the lines show the fit of a Gaussian peak to the experimental data.**

## 5.6. Conclusions

The CIT enables direct characterisation of the micro-mechanical properties of protein networks adsorbed at an interface. The instrument measures the resistance of a protein network to uniaxial extension in the plane of the interface, and is insensitive to interfacial tension. The interfacially adsorbed networks were characterised using an elasticity modulus *(Et)* derived from the gradient of the stress-strain plot at low strain (1%). Measured *Et* values were of order 200 mN/m at the air-water interface, consistent with a calculated ensemble average estimated using Atomic Force Microscopy (AFM) derived data on the unfolding of individual protein molecules.* The low strain interfacial elasticity modulus therefore measures an ensemble average unfolding force for protein molecules adsorbed at the air-water interface.

Interfacial elasticity modulus increased with protein concentration, although a 31% enhancement in the maximum stress transmitted through the protein film resulted when sub-interfacial β-lactoglobulin concentration was reduced from 1.0 mg/mL to 0.01 mg/mL. Reduced competition for interfacial space at lower protein concentrations is believed to result in greater conformational change in the protein molecules. Hence more extensive polymer chain entanglement is possible on adsorption at the clean interface. The lack of a direct correlation between elastic moduli obtained at small deformation and the maximum shear force that can be resisted by a β-lactoglobulin film, clearly demonstrates the additional insight provided by this new technique.

Hydrophobic intermolecular interactions were identified as a possible dominant mechanism by which networks transmit force laterally in the interfacial plane. Disruption of the protein hydrophobic bonding ability with Tween 20 resulted in the complete loss of ability to transmit force laterally through the layer of interfacially bound material. An interfacially adsorbed layer with no crosslinking capacity is unable to resist the tensile stress created in the CIT, and no direct force transmission is possible. Covalent disulfide linkages did not significantly contribute to network rigidity in these tests, as the addition of the reducing agent dithiothreitol (DTT) did not affect force transmission. Interfacial networks of the random coil protein β-casein exhibited both lower interfacial elasticity modulus and reduced interfacial stress

* Data from Carrion-Vazquez *et al.* (1999) and Best *et al.* (2001).

transmission compared with networks created by adsorption of β-lactoglobulin (globular protein). The interfacial elasticity modulus of β-lactoglobulin was shown to decrease as the solution pH was increased beyond the protein isoelectic point and the protein molecules adopted a less compact configuration.

Importantly, this study suggests that network mechanical response is determined by residual protein tertiary structure, and that adsorbed networks should therefore be analysed as nanostructured biomaterials. The interfacial protein networks demonstrated a clear ability for "repair" that is dependent on bulk protein concentration and hence the rate of transport into the interfacial region during tensile testing. There is a complex dependence of ensemble behaviour on protein structure in the bulk phase, the extent and nature of intermolecular bonding in the interfacial phase, and the unfolding characteristics of individual molecules. The multitude of experimental parameters yielded by the CIT, and lack of simplifying assumptions in the analysis, make it an ideal instrument to resolve the complex interplay between these factors.

# 6. Predicting Droplet Breakup

## 6.1. Introduction

Conventional theories for predicting droplet disruption are based upon a dimensionless capillary number and fail when a protein emulsifier is present at moderate concentration. The work of Williams *et al.* (1997) has shown that the widely used approach of calculating a capillary number, and comparing with a plot of critical capillary number, fails when a moderate concentration (> 0.01 mg/mL) of the globular protein β-lactoglobulin is present in the aqueous phase. The result is a droplet that is smaller than that predicted from the equilibrium interfacial tension using conventional theories. This indicates a droplet destabilising mechanism that results in disruption at a lower shear rate than expected from interfacial energy correlations.

In this chapter improvement in the prediction of droplet disruption is tackled through two specific objectives. Firstly, investigation of the destabilising effect caused by moderate to high concentrations of β-lactoglobulin and conclusive demonstration that an interfacial network capable of lateral stress transmission can be formed at the oil-water interface. Secondly, determination of the full stress-strain constitutive behaviour for interfacial protein networks to high deformation at the oil-water interface. Such data are required to provide the basis for a full material constitutive equation that would enable computational modelling of droplet deformation and breakup.

Previous chapters have described development of the Cambridge Interfacial Tensiometer (CIT) at the air-water interface and use of the instrument to provide detailed information about the mechanical properties of interfacial protein networks. In this chapter the CIT design is refined to allow operation at the oil-water interface to generate data for use in the prediction of emulsion droplet disruption. A custom designed and built Couette shearing device is employed to disrupt oil droplets in a well-characterised flow regime. The detailed design and operation of the shearing device was discussed in Chapter 3. Briefly, an approximation to simple shear flow is created in the annulus between a rotating and stationary cylinder. The shear rate can be calculated from the cylinder rotation speed. Oil droplets are disrupted under shear

and removed from the apparatus with the continuous phase. The particle size distribution is then measured with a laser particle sizer.

## 6.2. Droplet Breakup

The results shown in Figure 6-1 demonstrate that the capillary ratio is reduced below unity when the β-lactoglobulin concentration in the aqueous phase is greater than 0.01 mg/mL. This clearly shows that the droplet destabilising mechanism observed by Williams *et al.* (1997) can be reproduced in a new system with very different physical properties. The capillary ratio indicates the ratio of the experimentally determined critical capillary number divided by that predicted from a plot of critical capillary number versus the viscosity ratio of the dispersed and continuous phases. This is effectively the observed value of the capillary number divided by the expected value. Actual droplet size obtained is reduced below that predicted by the interfacial tension (capillary ratio <1) when the bulk β-lactoglobulin concentration exceeds 0.01 mg/mL.

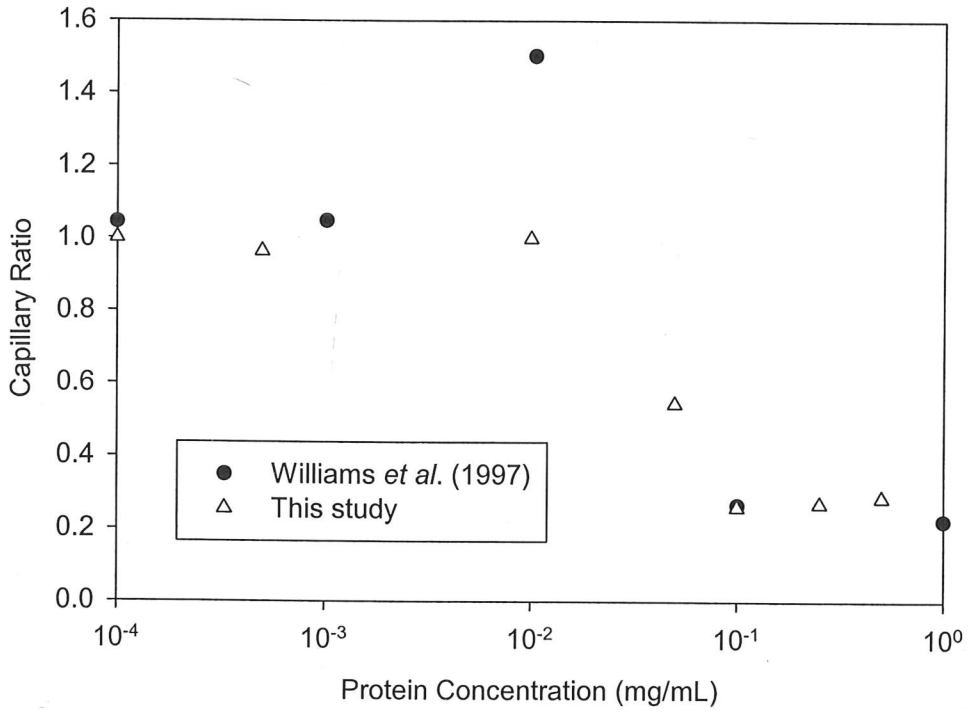


**Figure 6-1** **Capillary ratio as a function of β-lactoglobulin concentration. Filled circles show data of Williams *et al.* (1997), triangles show data presented previously elsewhere (Lomax, 2001).**

In this study, the dispersed phase was silicone oil and the continuous phase was 80% glycerol solution. The viscosity of the continuous phase was increased to provide sufficient shear force to disrupt the oil droplets. Glycerol was used to thicken the aqueous phase and silicone oil was chosen as the dispersed phase, as both show Newtonian behaviour under the experimental conditions. Droplet radius in this work was in the range 15 μm – 65 μm. Williams *et al.* (1997) inverted the phases, using silicone oil as the continuous phase and an aqueous droplet. Corn syrup was used to increase the viscosity of the aqueous phase and the droplets were around 1 mm in diameter. The same destabilising effect was observed despite such differences in experimental procedure, indicating the generic effect of high concentrations of β-lactoglobulin in modifying droplet disruption. Williams *et al.* (1997) also investigated the effect of β-casein and found that no such modification of the droplet disruption mechanism could be observed, beyond the changes expected due to reduced interfacial tension. Therefore, mechanical testing of protein networks adsorbed at an oil-water interface was performed, seeking to relate the protein network properties to droplet disruption characteristics. Two protein concentrations were chosen, one above and one below the β-lactoglobulin concentration shown to modify droplet disruption in a way that cannot be accounted for by the interfacial tension alone. The data presented in Figure 6-1 were collected with the help of Chris Lomax as part of an undergraduate research project under my supervision.

## 6.3. CIT Tests at the Oil-Water Interface

Figure 6-2 shows full stress-strain plots for β-lactoglobulin and β-casein adsorbed at the octane-water interface. Octane was used as the oil phase rather than silicone oil because silicone oil was found to be extremely difficult to clean from exposed areas of the CIT. The use of a volatile oil solved this problem and is justified because the results shown in Figure 6-1 indicate that modification of droplet disruption behaviour by β-lactoglobulin is not a system specific effect. The stresses transmitted through the protein film, in both tension and compression, are greatest when the bulk aqueous phase contains 0.1 mg/mL β-lactoglobulin. In this case the curve shows a very steep initial response where the network shows a high degree of rigidity or high interfacial elasticity modulus. This is then followed by a long plateau region where the network

shows considerable ability for "repair", probably as a result of adsorption of further protein molecules at the oil-water interface. When the direction of travel is reversed, the tensile stress is immediately reduced. This stress becomes negative (compressive) very early in this compressive section of the test, providing further evidence of protein adsorption during the tensile procedure. The very high compressive forces registered probably indicate the compression of multiple protein layers at this point.

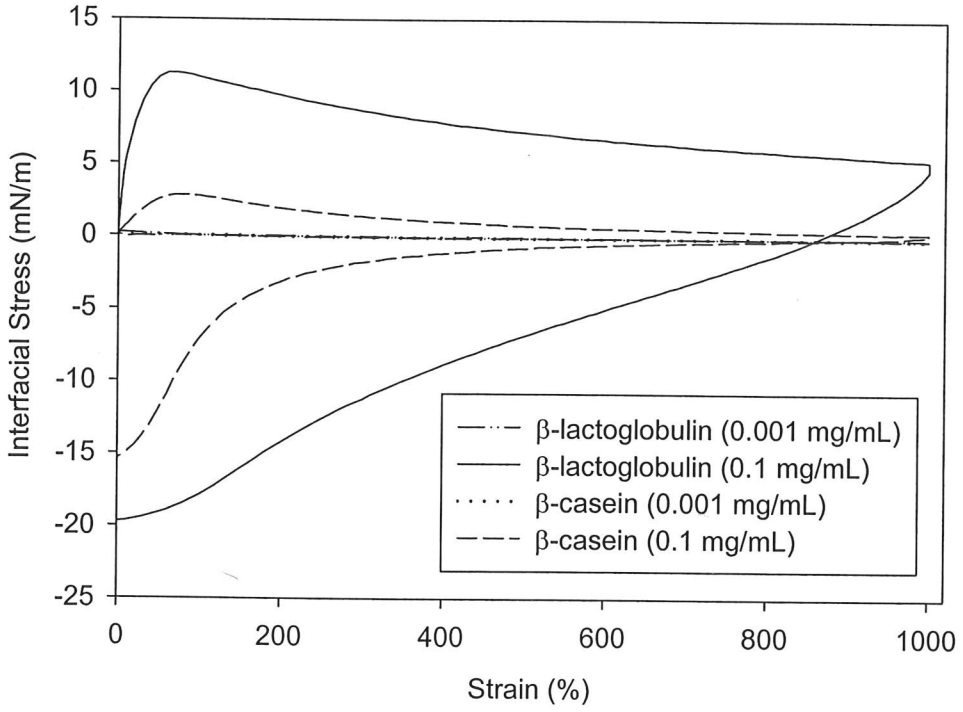


**Figure 6-2** **Average stress-strain plots for protein films adsorbed at the octane-water interface from solution in PBS buffer (pH 7.4).**

The results for 0.1 mg/mL β-casein show a much lower initial elasticity modulus and peak interfacial stress than obtained for 0.1 mg/mL β-lactoglobulin. The peak interfacial stress for β-casein is not reduced by the same margin as the initial elasticity modulus. This demonstrates that the degree of intermolecular cohesion of β-casein molecules adsorbed at the interface is not as low as has been previously suggested (Williams and Prins, 1996) and that a protein network structure is still formed, albeit a weaker structure than for globular β-lactoglobulin. At a protein concentration of

0.001 mg/mL, neither β-casein nor β-lactoglobulin form a cohesive network structure capable of transmitting a significant force laterally through the adsorbed protein layer. The curves on Figure 6-2 represent the average of two tests at each set of experimental conditions. For a protein concentration of 0.1 mg/mL, where force transmission is significant, both runs have been plotted in the low strain regime in Figure 6-3. This shows the reproducibility of the technique and highlights the differences in initial elasticity modulus (initial gradient of stress-strain plot) between the two types of protein network.

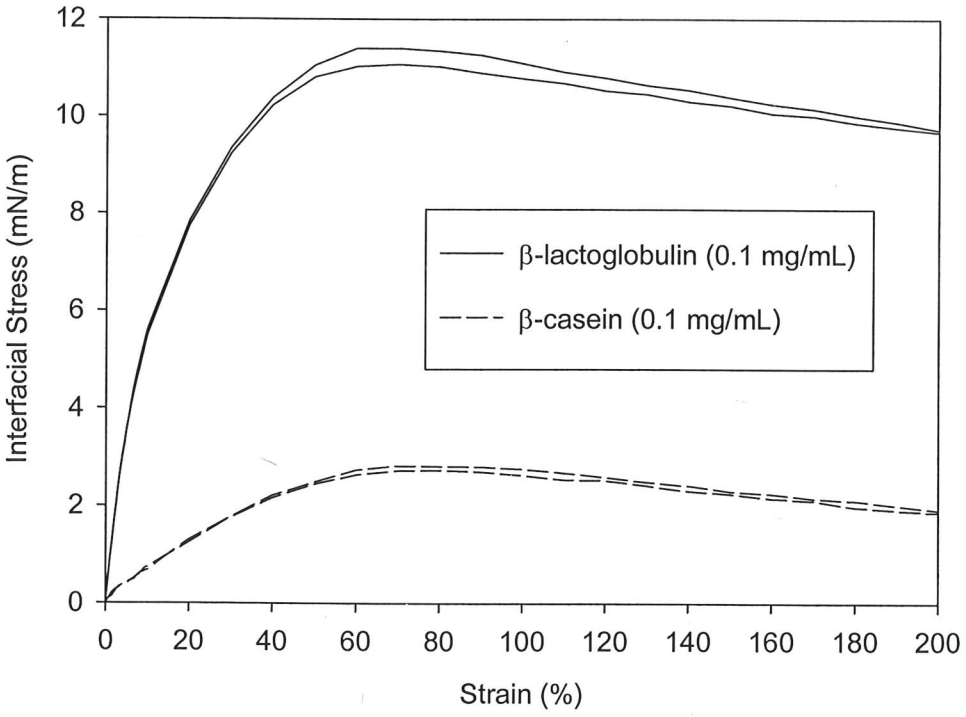


**Figure 6-3** **Stress-strain plots for β-lactoglobulin and β-casein films adsorbed at the octane-water interface from a 0.1 mg/mL protein solution in PBS buffer (pH 7.4).**

### *6.3.1. Dynamic Aspects*

The stress-strain plots shown in Figures 6-2 and 6-3 were all performed after a 5 min ageing time and, therefore, can provide little insight into the dynamics of the formation of interfacially adsorbed protein networks. To solve this problem the CIT

was operated in the cyclic mode, allowing lateral force transmission through the protein network to be probed in a minimally invasive manner. The T-bar separation was increased by 5% at a speed of 200 μm/s. The direction of travel was then reversed to return the T-bar to its original position and the cycle repeated 10 times per min. The results for duplicate runs of such tests are provided in Figure 6-4. The inset shows relevant data for β-lactoglobulin from the capillary ratio plot. The results show a striking difference between data for 0.1 mg/mL β-lactoglobulin and the other data. The protein network formed from a high bulk concentration of β-lactoglobulin shows a much higher level of force transmission at low strain than that obtained for the low protein concentrations or for 0.1 mg/mL β-casein.

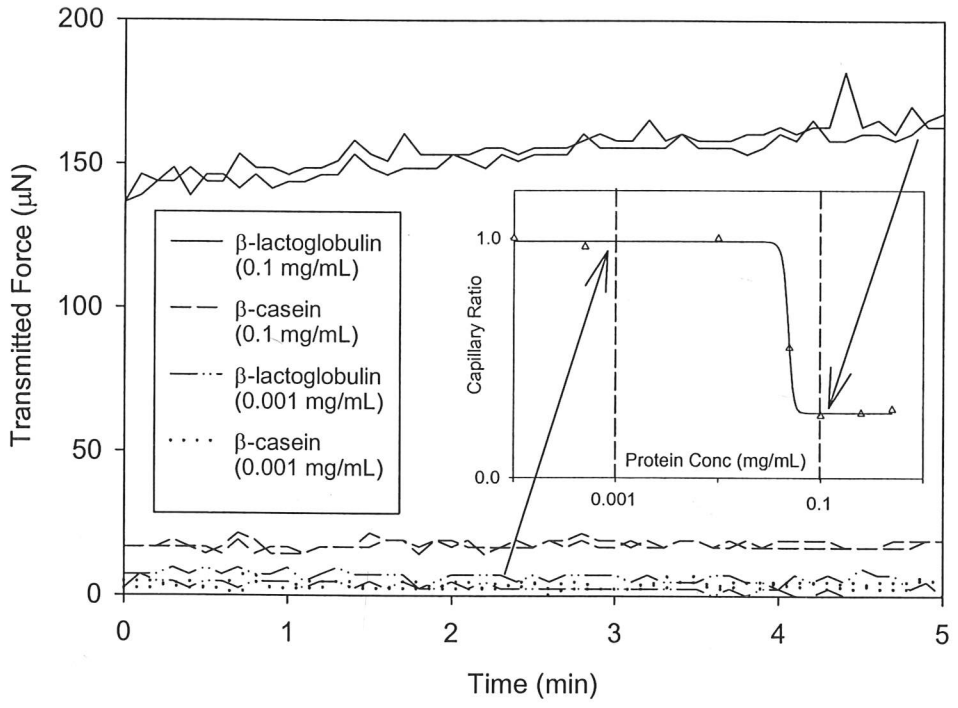


**Figure 6-4** **Lateral force transmission through protein films at low strain (5%). Proteins adsorbed at the octane-water interface from solution in PBS buffer (pH 7.4). Inset shows capillary ratio transition for β-lactoglobulin from Figure 6-1, with data points shown as Δ and the solid line drawn as a guide only.**

Figure 6-4 clearly shows that whilst there is some degree of enhancement in force transmission as the film ages over the 5 min period, a rigid protein network is formed

immediately as the aqueous and oil phases meet. This raises a very important point of experimental procedure, as it appears that protein network properties are determined, in the main part, by the initial adsorption of protein molecules at the clean fluid-fluid interface (discussed in greater detail in Chapter 4). In these tests, the octane is placed in the dish before the protein solution is added. The aqueous phase sinks below the octane as it is slowly poured into the dish, and the protein molecules adsorb at a clean octane-water interface. This contrasts with interfacial rheology experiments of other workers who have poured an oil phase over the top of an aqueous protein solution (Dickinson *et al.*, 1985; Williams and Prins, 1996), thereby modifying the behaviour of protein molecules that originally adsorbed at the air-water interface.

The fact that network rigidity is relatively constant over a 5 min period explains the observation made in this study that shearing times longer than 5 min have no significant effect upon the size distribution of the resulting emulsion. This is in agreement with Williams *et al.* (1997) who report that variation in the time taken to reach the critical capillary number (within the range 1 min – 20 min) had no effect on the results. If the dynamics of the formation of a protein network with high elasticity modulus are not important, then both modes of CIT operation can be used to predict whether the capillary number approach is a suitable tool to analyse droplet disruption.

## 6.4. Droplet Destabilisation

Data extracted from full stress-strain plots are presented in Table 6-1. This table also contains the elasticity modulus obtained from an analysis at 1% strain where the response of adsorbed β-lactoglobulin networks has been shown to be approximately linear (Figure 4-5). The network rigidity to 1% strain shows the same "on/off" behaviour as the destabilising mechanism occurring during droplet shearing. The initial elasticity moduli for β-casein and the lower β-lactoglobulin concentration are very small relative to that obtained for 0.1 mg/mL β-lactoglobulin, following exactly the same pattern as the droplet disruption experiments summarised in Figure 6-1. These results strongly suggest that the formation of a protein film with a high initial elasticity modulus causes the destabilisation of an emulsion droplet undergoing shear. This partially explains the widespread use of β-lactoglobulin as an emulsification

agent in foodstuffs and suggests that droplet disruption will be enhanced in the presence of emulsifiers capable of forming a rigid interfacial network. The CIT has a unique ability to detect the formation of a rigid protein network, unobscured by interfacial tension effects, and is therefore a valuable tool to predict whether droplet disruption is dominated by interfacial tension effects or by interfacial network formation. The instrument may be used to rapidly test new molecules for their likely efficacy in facilitating emulsification.

**Table 6-1** **Comparison of the mechanical properties determined by the CIT for β-lactoglobulin and β-casein protein networks adsorbed at the octane-water interface.**

| | β-lactoglobulin | | β-casein | |
|---|---|---|---|---|
| Protein concentration (mg/mL) | 0.001 | 0.1 | 0.001 | 0.1 |
| Maximum interfacial stress (mN/m) | 0.2 | 11.2 | 0.2 | 2.8 |
| Minimum interfacial stress (mN/m) | -0.2 | -19.7 | -0.2 | -15.4 |
| Interfacial elasticity modulus (1% strain, mN/m) | 9.2 | 88.6 | 5.9 | 12.4 |
| Force transmission (5% cyclic strain, μN) | 0.0 | 165.3 | 2.4 | 19.2 |

## 6.5. Alternative Droplet Models

Most attempts to model droplet disruption neglect all effects of emulsifiers other than their direct effect of modifying the equilibrium interfacial tension. Such approaches make two implicit assumptions. The first is that stresses are transmitted without loss between the internal and external fluid phases and secondly that the local interfacial tension is equal to the equilibrium interfacial tension. Breakup has been predicted to

occur when the droplet capillary number exceeds some critical value. This situation occurs when the stabilising Laplace (interfacial tension) forces can no longer balance the viscous forces, particularly near the waist of an elongated liquid droplet (Barthes-Biesel, 1991). Janssen *et al.* (1994) have show that, in the presence of small molecule surfactants, droplet breakup can be more difficult than predicted from the equilibrium interfacial tension (i.e. capillary ratios > 1). The authors characterise this effect by using an effective interfacial tension that is greater than the equilibrium interfacial tension, to account for the imbalance created by non-uniform surfactant distribution at the interface caused by droplet deformation. Regions of interface dilation (e.g. waist of elongated droplet) have a lower interfacial concentration of adsorbed surfactant. This results in a higher localised value of interfacial tension, generating a force that resists further deformation and makes droplet disruption more difficult. The results shown in Figure 6-1 indicate a qualitatively different effect, resulting in a droplet destabilising mechanism that cannot be explained by the presence of a non-zero dilatational elasticity modulus (change in interfacial tension with area).

Fisher *et al.* (1978) have compared the deformation and motion of liquid drops with that of red blood cells. The results obtained indicate that the mean interface rotation rate is independent of the viscosity ratio of the dispersed and continuous phases for red blood cells, due to the presence of the cellular membrane. These results are similar to those obtained by Williams *et al.* (1997) for high concentrations of β-lactoglobulin where solid-body rotation was observed and circulation rate was found to be independent of the viscosity ratio. The results for 0.1 mg/mL β-lactoglobulin shown in Figure 6-2 strongly suggest that under these conditions, a suspended fluid droplet is bounded by a rigid interfacial network capable of transmitting a force in the plane of the interface. Lateral interactions between interfacially adsorbed protein molecules result in the formation of a rigid interfacial network. As the number of adsorbed protein molecules rises, a critical interfacial concentration is reached where the individual adsorbed protein molecules are no longer able to move freely in the plane of the interface. This changes the droplet disruption regime from one dominated by dynamic interfacial energy considerations to a network-controlled regime. Thin membrane analysis performed by Barthes-Biesel (1991) predicts that under such network forming conditions the internal liquid undergoes bulk solid-body rotation and

is not sheared. "As a consequence, the externally applied tangential stresses are absorbed by the membrane deformation process." Effectively, departure from an interfacial energy dominated regime, where stresses are transmitted undiminished across the fluid-fluid interface, changes the boundary conditions of the problem description. The results of this study suggest that the formation of a rigid network allows forces to be transmitted laterally in the plane of the interface, increasing localised network stress and causing droplet destabilisation. This mechanism explains the ability of the globular protein β-lactoglobulin to destabilise liquid droplets by forming a rigid protein film when adsorbed at the interface in high concentrations.

Evidence of inhomogenous stress propagation through adsorbed protein films can be found in the results of some elegant experiments performed by Langmuir and Schaefer (1939) to investigate the degree of protein intermolecular cohesion. The experiments involved spreading a protein monolayer on the air-water interface and expanding the central region with a spreading oil. Two distinct pattern types were formed by different proteins, a star-like pattern and a smooth circular pattern. These results are reproduced in Figure 6-5.

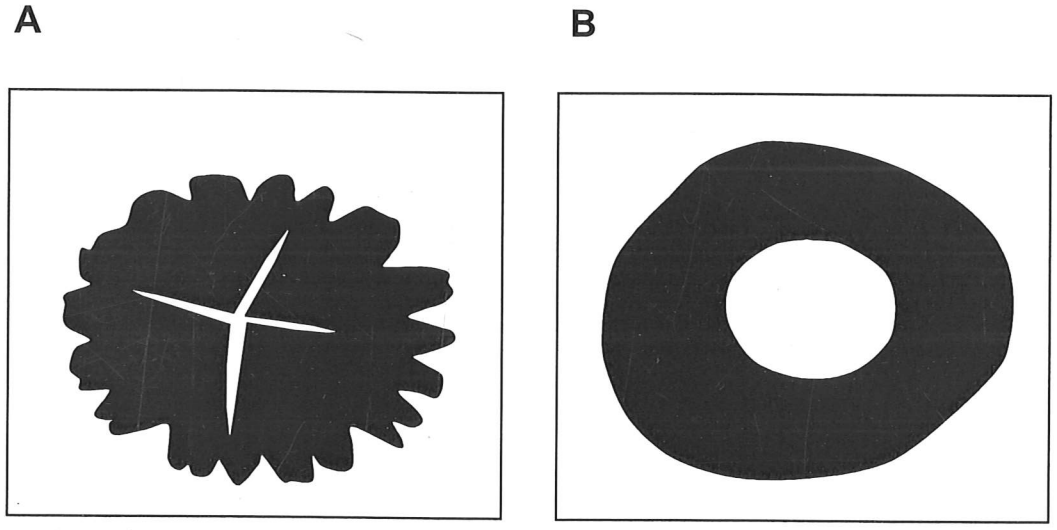


**Figure 6-5** **Star-like expansion pattern A (egg albumin, pepsin, tobacco seed globulin), smooth circular expansion pattern B (insulin, casein). Redrawn from data by Langmuir and Schaefer (1939).**

In an earlier paper Schaefer (1938) made the observation that "protein monolayers which produce expansion patterns of the star-like form are, in general, of the type described by Hughes and Rideal (1932) as a gel structure". Langmuir and Schaefer (1939) noted that protein films capable of providing a high degree of damping to a disk oscillating in the interfacial region tended to form star shaped patterns. Such observations provide evidence that protein films with a solid-like (rigid) structure can cause non-uniform stress distribution resulting in localised failure of the protein network, in an analogous fashion to crack propagation in conventional materials. There is a striking visual similarity between the work of Langmuir and Schaefer (1939) and recent work by Mackie *et al.* (1999) who investigated the displacement of protein from the air-water interface by the non-ionic surfactant Tween 20. The surfactant was found to adsorb at defects in the protein network, whereupon the protein network was compressed by the growing surfactant nucleation sites. The authors noted that "stress propagation through β-casein films is homogenous resulting in the growth of circular surfactant domains" while "β-lactoglobulin and α-lactalbumin form stronger networks and stress propagation is restricted resulting in the growth of irregular (fractal) surfactant domains".

Protein network formation appears to change the difficulty and mechanism of droplet disruption by causing a discontinuity in the tangential stresses across the interface. In the case of a liquid or emulsion droplet such a discontinuity is not present, as any film existing between the two phases merely transmits tangential stress from one fluid to the other. Therefore, oil droplets bounded by a rigid protein network may be better considered as capsules or even model mammalian cells where the membrane and internal cell properties are more easily characterised. Zhang *et al.* (1992) have considered the bursting of mouse hybridoma cells under mechanical stress using a micromanipulation technique and subsequently modelled the system as an elastic membrane surrounding an incompressible fluid. The membrane bursting tension for the cells was found to be 1.8 mN/m. This compares favourably with the 2.8 mN/m – 11.2 mN/m range of maximum tensile stress transmission found in this study for β-casein and β-lactoglobulin, respectively, at 0.1 mg/mL protein concentration. In the same year Born *et al.* (1992) developed a model to predict disruption of animal cells by laminar shear stresses. The cells were modelled as an emulsion of two immiscible

liquids using equations proposed by Taylor (1934) and assuming that cell membrane tension corresponds to droplet interfacial tension. The cell membrane tension is allowed to change during the deformation process using the approach of Born *et al.* (1992) but the dynamic behaviour of the cells is ignored and therefore the actual, or apparent, cell or droplet viscosity is neglected. However, the model achieved agreement with the experimental cell disruption data to within 30% and, therefore, demonstrates the useful predictive capability of this approach.

For a viscoelastic membrane the material properties depend on several parameters, so a model based upon full description of the interface will have improved accuracy over a model using a single value of bursting membrane tension. Barthes-Biesel (1991) has considered the influence of interfacial properties on the deformation and breakup of capsules in shear flow. The author develops a model based on normal and tangential stress balances coupled with a constitutive equation to describe the interfacial properties. The CIT is capable of generating full stress-strain plots at varying rates of strain for protein networks adsorbed at the oil-water interface, allowing the generation of an experimentally determined constitutive equation for the droplet interface (Figure 6-6). The exclusive ability of the CIT to generate an experimentally derived constitutive equation for an interfacial protein network will thus enable *a priori* prediction of droplet disruption to be made using numerical methods.

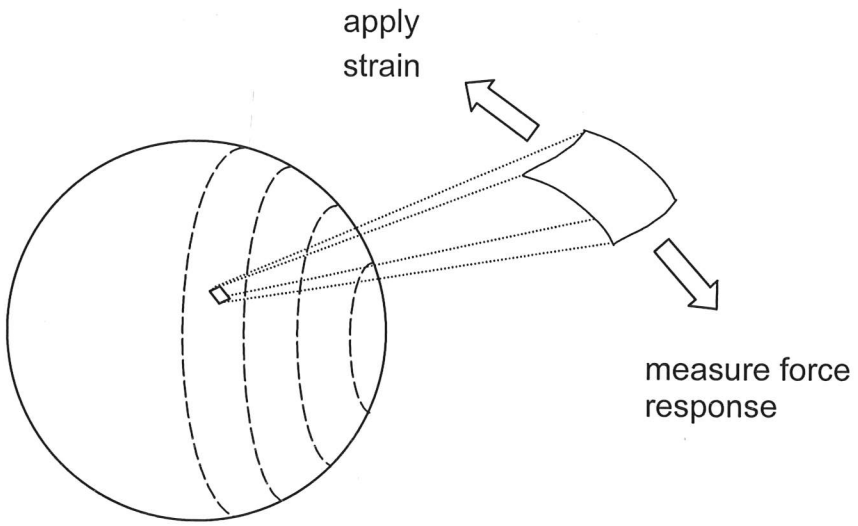


**Figure 6-6** **Requirement for material constitutive equation to predict droplet disruption.**

The data and supporting literature presented in this chapter strongly suggest that correlations based on interfacial energy alone are unsuitable in the case of a rigid interfacial network, and that the system is more accurately considered as a capsule bounded by a viscoelastic membrane. It seems this was first realised by Ascherson, in 1840, when he believed he had created momentarily viable cells by producing protein stabilised emulsions. Although the assertion that the emulsion droplet could be directly equated with living cells is incorrect, the analogy is useful as emulsion droplets surrounded by protein networks could be considered as "ghost" cells. Under these circumstances, independent and direct determination of the mechanical properties of the "cell membrane" is possible using the CIT. This would facilitate the development of further models to predict animal cell damage or disruption in more complex flow fields found in bioreactors, without additional complications arising from biological variability or cell age.

## 6.6. Conclusions

Droplets of silicone oil in glycerol solution have been successfully disrupted in a flow pattern that approximates simple shear. At low β-lactoglobulin concentrations ($\leq$ 0.01 mg/mL) droplet disruption can be predicted from the capillary number correlation using the shear rate, interfacial tension and bulk phase viscosity. At β-lactoglobulin concentrations greater than 0.01 mg/mL such an approach fails, and the maximum stable droplet size and critical capillary number are reduced below the expected value. This is shown in Figure 6-1, where the capillary ratio is less than 1 at the higher β-lactoglobulin concentrations. The experimental results are in good agreement with those of Williams *et al.* (1997) on larger single droplets where silicone oil was used as the continuous phase and a corn syrup solution was the dispersed phase. This suggests that the ability of β-lactoglobulin to modify droplet breakup at high bulk concentrations is a generic effect that is not system specific.

The CIT was used to probe the response of adsorbed protein layers to uniaxial strain in a way that eliminates the contribution from equilibrium interfacial tension. Such a technique is required as the droplet shearing results suggest that at high β-lactoglobulin concentrations, use of correlations based on the interfacial tension,

such as the capillary number, are incapable of predicting droplet disruption even if allowance is made for the dilatational elasticity modulus. The CIT also tackles the general paucity of literature regarding mechanical properties of protein films adsorbed at the oil-water interface when compared to the air-water interface, as the experimental technique can now be applied at both types of interface. The results show that at high concentrations of β-lactoglobulin (0.1 mg/mL) the adsorbed molecules can transmit a force in the plane of the interface. The results indicate the formation of a rigid β-lactoglobulin network at the octane-water interface at 0.1 mg/mL bulk protein concentration. Networks capable of transmitting significant forces laterally in the plane of the interface are not formed at the octane-water interface for 0.001 mg/mL β-lactoglobulin or 0.001 mg/mL β-casein. At 0.1 mg/mL concentration, β-casein is capable of forming a cohesive network but with a tensile rigidity much below that obtained for the same concentration of β-lactoglobulin.

Comparison of the droplet shearing data and those obtained using the CIT shows that droplet destabilisation occurs when a rigid interfacial network is formed. This suggests that a rigid interfacial network, capable of transmitting forces laterally in the plane of the interface, destabilises the liquid droplet by increasing localised network stress. Cyclic operation of the CIT provides a clear and quick test to show the presence of a rigid protein network, and can therefore indicate the suitability of the capillary number in prediction of droplet disruption. This work establishes the CIT as a useful predictive tool for determining the most appropriate theory for the prediction of droplet size after disruption in a known flow field. The richness of features in a full stress-strain plot of an interfacially adsorbed protein make the CIT an ideal instrument to provide detailed information regarding the macroscopic network properties that will be useful for the molecular design and testing of a wide range of emulsifiers and other interfacially adsorbed biomaterials. Furthermore, the stress-strain plots generated by the CIT provide full network constitutive information which could be coupled to equations describing the fluid behaviour, enabling *a priori* computational modelling of droplet deformation and disruption, as proposed by Barthes-Biesel (1991).

# 7. Molecular Design

## 7.1. Introduction

"If chemical engineers could assemble the basic ingredients of the material world with a hint of nature's ability the bounds would be limitless" (Loughran, 2001).

Previous chapters have demonstrated that improved understanding can be gained by regarding adsorbed protein films as thin layers of nanostructured biomaterials. The rapidly advancing and much publicised field of "nanotechnology" obviously requires knowledge of material structure, and the organisation or manipulation of molecules, on the nano-scale. Consumer demands will always drive work towards the low cost manufacture of such materials despite their potential sophistication. For these reasons, if new products or processes are to be brought to the consumer at an acceptable cost, improved understanding of molecular self-assembly is essential. Therefore, the field of nanotechnology rests implicitly on an ability to control molecular orientation and organisation to enable the manufacture of atomically precise structures.

Short peptides have been shown to assemble at the air-water interface to form a repeating β-sheet structure with a clearly defined characteristic spacing (Xu *et al.*, 2001). Leon *et al.* (1998) have successfully created a peptide-based, self-assembling, matrix capable of favourable interaction with cells. Such work provides the foundation for macroscopic applications such as biocompatible implants, tissue engineering, delivery of pharmaceuticals into the body and production of bio-mimetic membranes, through the design and control of materials at the molecular level. Short peptides are natural candidates for the production of new biomaterials as genetic engineering provides the possibility of large-scale production at low cost (Kempe *et al.*, 1985; Kuliopulos and Walsh, 1994; Artsaenko *et al.*, 1998; Daniell *et al.*, 1999) and peptides can be selected or designed to have a range of biologically relevant features. For example, through careful choice of the peptide sequence, biomaterials could be engineered for minimal toxicity and immunogenicity. Use of only L-amino acids would allow breakdown and reuse of material by the host organism, whilst at the same time peptides have been created that showed remarkable

resistance to heat, chemical denaturation agents and proteolytic degradation *in vitro* (Zhang *et al.*, 1993).

The twenty common, naturally occurring amino acids (Figure 7-1) provide an almost limitless number of design possibilities, yet there still exists the possibility of further enhancement of functionality through the use of non-natural "synthetic" amino acids. The amino acid type and sequence could be used to control the permeability, elasticity or thickness of peptide biofilms. Such films could then be used as membranes to encapsulate active reagents for medical applications, in cosmetic products, to target pesticide or herbicide use in agriculture, or as a substratum for cell attachment. For example, the peptide sequence RGD has been used to immobilise osteoblasts (bone cells) through integrin-type receptors on the cell surface (Anselme, 2000) demonstrating the unique possibilities made available by using peptide-based materials.

Self-assembly of peptides of known secondary structure is of particular interest as the peptides can represent clearly defined protein domains and may, therefore, improve knowledge of the conformational changes and protein-protein interactions occurring after protein adsorption. The issues discussed in the previous paragraphs have concentrated on the applications and new products that may be made possible in the future through an understanding of peptide molecular self-assembly. However, there is also a keen scientific interest in the interactions of peptides both with interfaces and other peptide molecules. Understanding the conformational changes of multidomain proteins upon adsorption at an interface is particularly complicated, so peptides could be used as simplified models of protein systems. The results of such studies would be "easier" to interpret than results generated using protein systems for two main reasons. Firstly the peptides can be chosen, or designed, initially to have a uniform secondary structure. Secondly the peptide structure can then be changed by altering the amino acid sequence based on rational design strategies, without the need to resort to point mutation studies often employed for investigations into protein structural variants. Fairman *et al.* (1995) have used peptide sequences based on the C-terminal oligomerisation domain of the Lac repressor to study the interactions of antiparallel four-chain coiled coils. The lengths of the peptide sequences were systematically varied to investigate the effect of chain length on the tetramer stability. This

knowledge of peptide behaviour is useful both as information on the specific peptide system considered and for interpreting the behaviour of proteins where four-helix bundles are present naturally, such as human growth hormone and T4 lysozyme (Kohn *et al.*, 1997).

Clearly studies of peptide systems representative of protein domains are a promising area for the development of new ideas and a greater understanding of protein folding and molecular interactions. In particular, such work may allow protein models or molecular dynamics simulations to be tested experimentally. For example, Chipot *et al.* (1999) have successfully performed a multinanosecond molecular dynamics study on the folding of an amphipathic peptide of eleven amino acids placed in the aqueous phase as a β-strand and allowed to adsorb at the hexane-water interface. In the future, with the advent of faster computers and higher resolution experimental techniques, it is expected that great synergistic benefits may accrue through the combined use of molecular dynamics simulations and experimental investigations, enabling valuable insights into the mechanisms of interfacial folding. Fundamental knowledge of protein or peptide interactions at an interface is required in an engineering environment for the *a priori* design of several downstream operations such as liquid-liquid extraction and chromatographic separations.

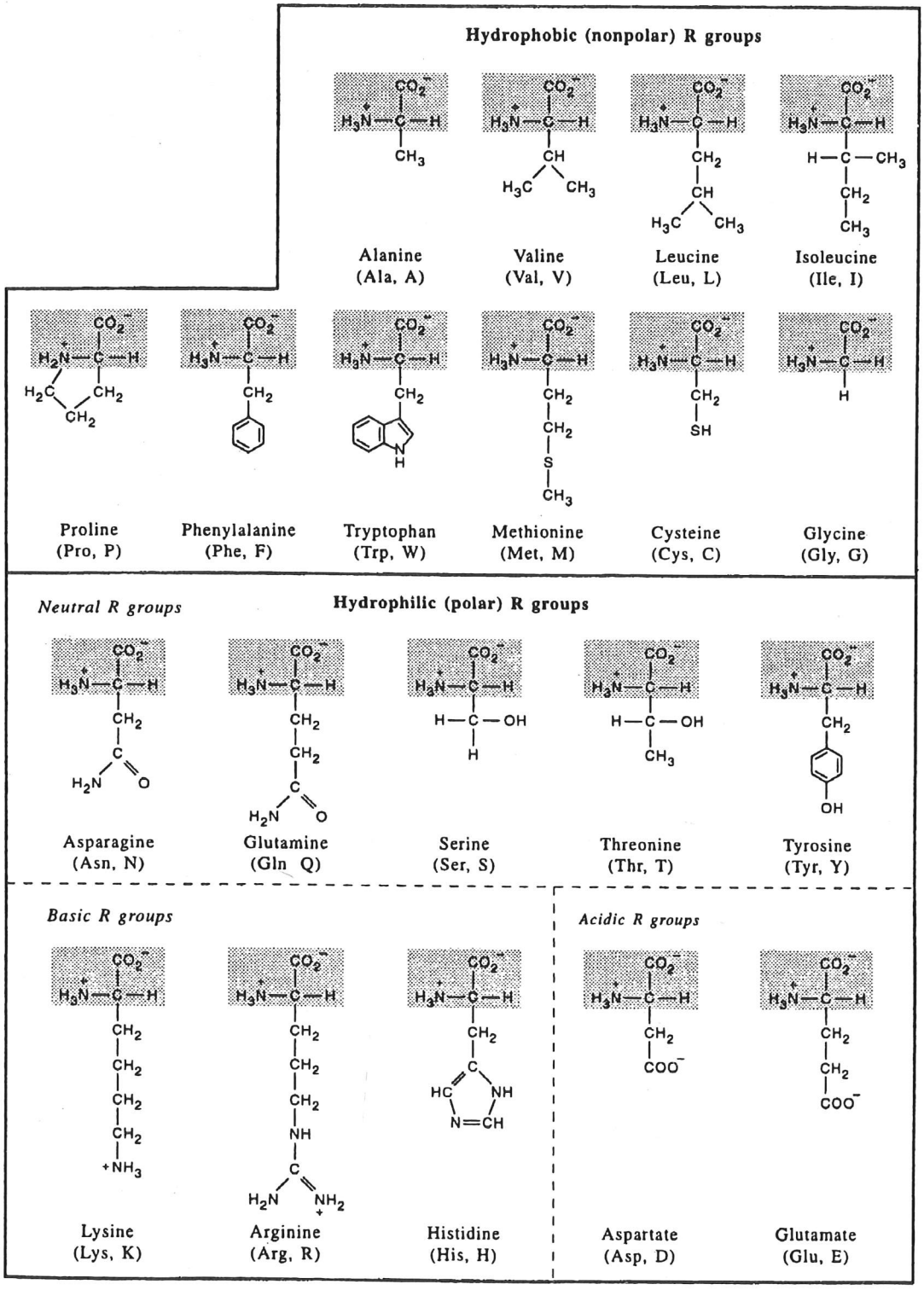


**Figure 7-1** **Structures, abbreviations, and classifications of the amino acids at pH 7.0. The shaded portions are those common to all amino acids. Taken from Rappé (1997).**

**Table 7-1** **Relative hydrophobicity of L-*alpha*-amino acids. Taken from Black and Mould (1991).**

| Amino Acid | 3-Letter Code | 1-Letter Code | Molecular Weight† | Hydrophobicity |
|---|---|---|---|---|
| Alanine | Ala | A | 89.09 | 0.616 |
| Cysteine | Cys | C | 121.16 | 0.680 |
| Aspartate | Asp | D | 133.18 | 0.028 |
| Glutamate | Glu | E | 147.13 | 0.043 |
| Phenylalanine | Phe | F | 165.19 | 1.000 |
| Glycine | Gly | G | 75.07 | 0.501 |
| Histidine | His | H | 155.16 | 0.165 |
| Isoleucine | Ile | I | 131.18 | 0.943 |
| Lysine | Lys | K | 146.19 | 0.283 |
| Leucine | Leu | L | 131.18 | 0.943 |
| Methionine | Met | M | 149.21 | 0.738 |
| Asparagine | Asn | N | 132.12 | 0.236 |
| Proline | Pro | P | 115.13 | 0.711 |
| Glutamine | Gln | Q | 146.15 | 0.251 |
| Arginine | Arg | R | 174.20 | 0.000 |
| Serine | Ser | S | 105.09 | 0.359 |
| Threonine | Thr | T | 119.12 | 0.450 |
| Valine | Val | V | 117.15 | 0.825 |
| Tryptophan | Trp | W | 204.23 | 0.878 |
| Tyrosine | Tyr | Y | 181.19 | 0.880 |

† **The molecular weights are those of neutral, free amino acids. Subtract molar weight of water (18 g/mol) to obtain residue weight.**

**Table 7-2** **The tendency of coded amino acids for α-helix promoting/breaking and β-structure promoting/breaking, when part of a peptide (neutral = ~0.8-1.00 = no tendency either way). Taken from Barrett (1998).**

| | | | | | | | | |
|---|---|---|---|---|---|---|---|---|
| **α-helix promoting (helicogenic)** | | | | | | | | |
| $Glu^-$ | Ala | Leu | $His^+$ | Met | Gln | Trp | Val | Phe |
| 1.53 | 1.45 | 1.34 | 1.24 | 1.20 | 1.17 | 1.14 | 1.14 | 1.12 |
| **Neutral** | | | | | | | | |
| $Lys^+$ | Ile | $Asp^-$ | Thr | Ser | $Arg^+$ | Cys | | |
| 1.07 | 1.00 | 0.98 | 0.82 | 0.79 | 0.79 | 0.77 | | |
| **α-helix breaking** | | | | | | | | |
| Asn | Tyr | Pro | Gly | | | | | |
| 0.73 | 0.61 | 0.59 | 0.53 | | | | | |
| **β-structure promoting** | | | | | | | | |
| Met | Val | Ile | Cys | Tyr | Phe | Gln | Leu | Thr | Trp |
| 1.67 | 1.65 | 1.60 | 1.30 | 1.29 | 1.28 | 1.23 | 1.22 | 1.20 | 1.19 |
| **Neutral** | | | | | | | | |
| Ala | $Arg^+$ | Gly | $Asp^-$ | | | | | |
| 0.97 | 0.90 | 0.81 | 0.80 | | | | | |
| **β-structure breaking** | | | | | | | | |
| $Lys^+$ | Ser | $His^+$ | Asn | Pro | $Glu^-$ | | | |
| 0.75 | 0.72 | 0.71 | 0.65 | 0.62 | 0.26 | | | |

## 7.2. α-Helical Peptide Structure

The amphipathic α-helix is a commonly encountered secondary structural motif found in many proteins and biologically active peptides. Pauling won a Nobel Prize in 1954 "for his research into the nature of the chemical bond and its application to the elucidation of the structure of complex substances". He used X-ray diffraction to deduce the chemical structures of small peptides, proving the existence of the α-helix structural element. Perutz *et al.* (1965) noted that α-helices in globular proteins often have a narrow non-polar edge running down the long axis of the helix. Perutz

also observed that this exposed hydrophobic strip often faces the non-polar interior of the protein. This observation is similar to one made by Clothia (1975), namely, that after the collapse of an unfolded protein molecule, many of the hydrophobic residues are not surface exposed but sequestered into the hydrophobic core of the protein. A study of amino acid sequences from the Lac repressor by Fairman *et al.* (1995) showed this effect very clearly as the peptides formed antiparallel four-helix bundles in solution, with the tetrameric form stabilised at the higher peptide lengths. Figure 7-2 is a helical wheel representation (Schiffer and Edmunson, 1967) of a tetramer of helices formed from residues 339-359 of the Lac repressor, showing the high degree of organisation of the hydrophobic amino acid residues. The tetramer is stabilised primarily by the association of the hydrophobic helix faces minimising disruption of the surrounding water structure.

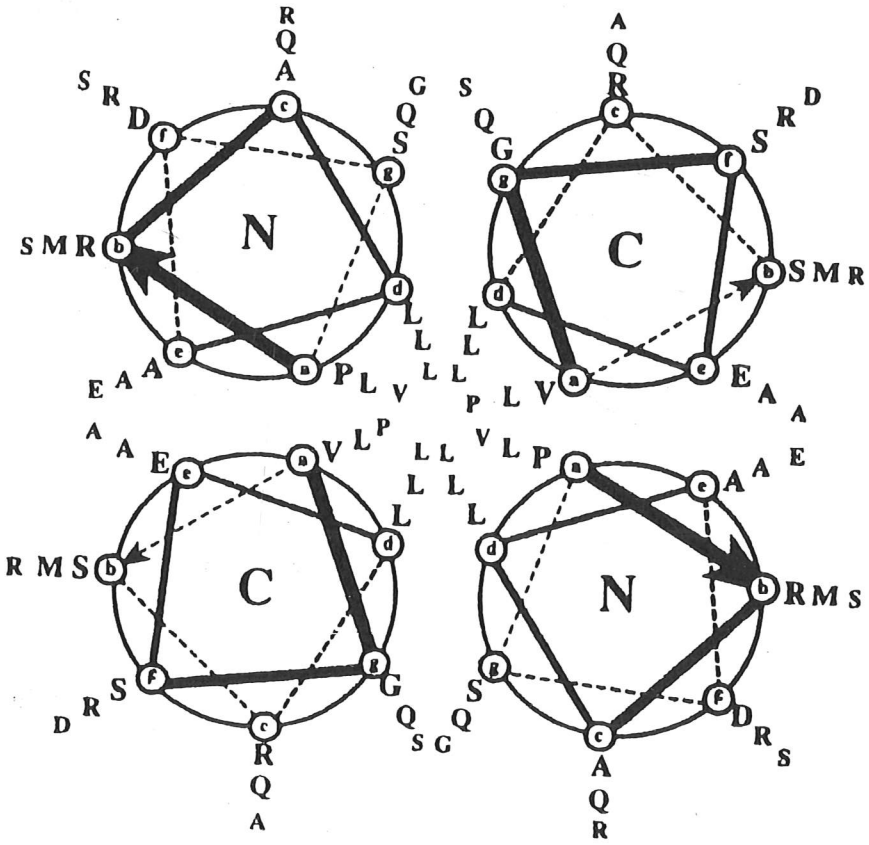


**Figure 7-2** **Helix wheel diagram of antiparallel four-helix bundle of C-terminal residues (339-359) from the Lac repressor showing hydrophobic residues hidden in bundle core. Taken from Fairman *et al.* (1995).**

The dynamic interfacial tension of two of the peptides originally used by Fairman *et al.* (1995) has been measured by Middelberg *et al.* (2000). The two peptides (Lac21 and Lac28) demonstrated very different interfacial behaviour. Lac21 was shown to exist in solution in mixed monomer-tetramer form and adsorb at the air-water interface with an interfacial pressure exceeding that of most proteins, including β-casein, bovine serum albumin (BSA) and lysozyme (Beverung *et al.*, 1999). Unusually for a peptide or protein, Lac21 demonstrated a well-defined equilibrium interfacial pressure even after long adsorption times. Lac28 was shown to exist primarily in a tetrameric form, even at low bulk concentrations, and showed a kinetic limitation to interfacial adsorption at moderate to high interfacial coverage that was not observed for Lac21.

Graham and Phillips (1979a; 1979b) identified three distinct regimes in protein interfacial adsorption: (1) diffusion to the interface; (2) penetration into the interfacial layer and (3) conformational rearrangement of the adsorbed molecules. Middelberg *et al.* (2000) showed that adsorption of tetrameric Lac28 was favourable only at low interfacial coverage and demonstrated that a thermodynamically stable tetramer exhibits a definite energy barrier to adsorption. This result is similar to the work of Boyd *et al.* (1973), discussed in Chapter 5, where the activation energy required to create a "hole" in the interfacial layer was found to correspond to a physical size much smaller than a whole protein molecule. Such a conclusion implies that units of peptide or protein secondary structure may be the elements penetrating the interfacial region to initially anchor the protein molecule at the interface. Therefore, the Lac28 tetramer could be thought to be representative of a simple protein where adsorption kinetics are determined, in part, by the thermodynamic stability of specific domains within the protein. Such work clearly demonstrates the enhanced understanding of protein behaviour that can be obtained through the use of peptides representative of protein domains or used as "model-protein" systems.

### *7.2.1. α-Helical Peptide Design Studies*

*De novo* design of α-helical peptides with the desired properties may be possible using the results of previous work and a knowledge of the size and physico-chemical properties of amino acids (Tables 7-1 & 7-2). The α-helical structure is based upon a

heptad repeat with the amino acid positions denoted by the letters **a - g** (see Figures 7-3 and 7-4). The coil has 3.6 residues per turn so if hydrophobic amino acids are present at positions **a** and **d**, a hydrophobic strip is created running longitudinally down the molecule. Hydrophobicity and hydrogen bonding are very important effects in determining the interaction of a peptide with a fluid-fluid interface. A review paper by Segrest *et al.* (1990) notes several studies where increasing the hydrophobicity of the hydrophobic face in a series of structurally related peptides has been found to increase the lipid affinity of the peptide. Hydrogen bonding will also affect the intermolecular interactions between adjacent peptide molecules. Adjacent hydrophobic residues will have a high affinity for each other as a result of the "anti-hydrogen" bond discussed in the Literature Review and, if a high degree of intermolecular hydrogen bonding is also possible, the result may be the formation of a "strong" interfacial peptide network.

Enser *et al.* (1990) have shown that raising the length of an α-helical peptide from 11 to 22 residues can increase the degree of helicity in aqueous solution and enhance emulsification activity. Su *et al.* (1994) have also shown that the helicity of α-helical peptides can be increased by lengthening the peptide chain. The paper of Segrest *et al.* (1990) mentioned above, also indicated that the degree of helicity was greater for longer peptides and that lipid association increases the degree of α-helicity of the peptides rather than denaturing them. This finding provides evidence that Lac21 will maintain an α-helical structure on adsorption at the air-water interface. Incorporation of the hydrophobic amino acids leucine and alanine has been shown to be another method of increasing the tendency of such a molecules to adopt α-helical conformations (Enser *et al.*, 1990). However, addition of a prolyl residue in a helical peptide structure has been shown to decrease both the helicity and lipid affinity of apolipoprotein analogues (Anantharamaiah, 1986).

The amino acid cysteine has a sulfur containing side chain. Under oxidising conditions, two sulfhydryl groups on cysteine residues in close proximity can form a disulfide bridge. Such bonding is a key stabilisation mechanism of proteins in their native state. This is demonstrated by the denaturant effect of reducing agents such as β-mercaptoethanol, which destroy the S-S bonds. Disulfide bonds have been shown to

stabilise proteins against denaturation by temperature (Heikoop *et al.*, 1997) and are attributed as the mechanism for intermolecular crosslinking of time aged protein films (Dickinson and Matsumura, 1991; McClements *et al.*, 1993). Electrostatic attractions such as salt bridging (at pH 7) between positively charged lysine residues and negatively charged glutamate residues is another mechanism for stabilisation of peptides and has been used specifically for the purpose of stabilising *de novo* designed helices (Marqusee and Baldwin, 1987). Employed in this manner, salt bridging may be useful for stabilising peptides via intramolecular bonding (Enser *et al.*, 1990) or potentially for the intermolecular binding of adjacent interfacially adsorbed peptide molecules.

Knowledge of the size and physico-chemical properties of amino acids has been used previously to design synthetic peptides that have no homology with naturally occurring proteins or peptides, yet still have the ability to form α-helices (Ho and Degrado, 1987; Lombardi *et al.*, 1996; Russell *et al.*, 1998). Ho and Degrado (1987) performed an important study demonstrating that peptides can be designed to give highly specific properties by their successful attempts to design a peptide forming a tetramer of α-helical bundles. Follow-up work performed by Guo and Thirumalai (1996) managed to produce a four-helix bundle using a very similar peptide system. Essentially this demonstrates the feasibility of designing a peptide system with similar conformational and self-associative properties to the naturally occurring Lac repressor sequences studied by Fairman *et al.* (1995) and Middelberg *et al.* (2000).

### 7.2.2. α-Helical Peptide Selection

Lac21 was chosen for study using the CIT because of its α-helical conformation and the rarity of peptides or proteins displaying a well-defined equilibrium interfacial pressure. In essence, this is a peptide capable of desorbing from the interface on a measurable time-scale. Although no studies have reported the conformation of interfacially adsorbed Lac21, evidence that such α-helices are stable at the oil-water interface is provided by the work of Loeb and Baier (1968) and Caessens *et al.* (1999) discussed in Chapter 5. Additional support for such a hypothesis can also be found in

papers by Malcolm (1968) and Boncheva and Vogel (1997) on the conformation of polypeptide monolayers.

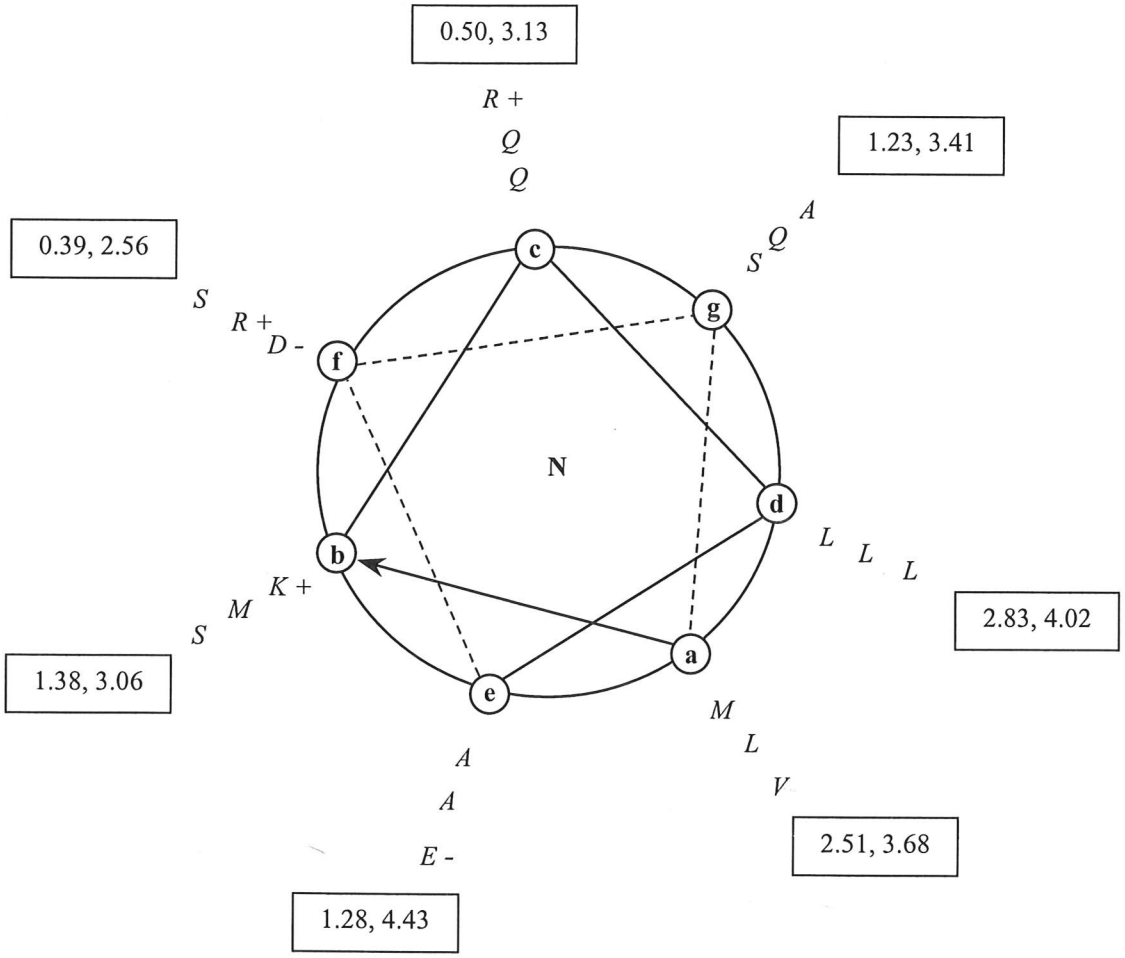


**Figure 7-3** **Monomer of Lac21 peptide showing distribution of charge, hydrophobicity and α-helix promoting amino acids. Figures in boxes show the total hydrophobicity and α-helix promoting tendency, respectively, of each peptide face. Values calculated from data in Tables 7-1 and 7-2.**

### 7.2.3. *α-Helical Peptide Design*

"Chemical engineers should be able to eventually design a wide variety of functional polymers based on their ability to fold and self-assemble." Professor Barron, Northwestern University, taken from Loughran (2001).

The key objective of this chapter is the *de novo* design of a peptide capable of adsorbing at the air-water interface to form an interfacial film with a high degree of mechanical strength. The results and literature discussed in Chapter 5 established that proteins with a high degree of secondary structure form more rigid interfacial films. Chapter 5 also provided experimental evidence, using Tween 20, that confirms the intuitive conclusion that an adsorbed molecular species incapable of forming intermolecular bonds results in a fluid-like interfacial region. Therefore, a peptide designed to form a strong interfacial network has two key requirements: an ability to form a high density of intermolecular interactions or bonds, and the adoption of a high level of secondary structure on adsorption at the air-water interface. Lac21 is expected to maintain a helical structure on adsorption at the air-water interface. Therefore, the sequence of the first twenty one amino acids of the *de novo* peptide, Dan25, was designed based on conservative changes to the Lac21 peptide.

Lac21 sequence : MKQLADS LMQLARQ VSRLESA

Dan25 sequence : CKQLADS LCQLAKQ VSKLESA GCDG

Four amino acids were then added to the C-terminus (right hand side) to balance the overall charge on the peptide and to enhance the intermolecular bonding characteristics. Both peptides were acetylated at the amino-termini (N) and amidated at the carboxy-termini (C) to minimise charge interactions resulting from the helix dipoles.

Two routes for intermolecular bonding were incorporated into the Dan25 design. The first is disulfide bridging via adjacent cysteine residues and the second is primary amine crosslinking between lysine residues. The former is expected to occur spontaneously under oxidising conditions while the latter allows control of the interfacial network mechanical properties through the introduction of formaldehyde as a crosslinking agent. These amino acid crosslinking mechanisms and other alternatives have been discussed in greater detail in the Literature Review. The Dan25 peptide incorporates three cysteine residues and three lysine residues to create a hetero-bifunctional peptide with the potential to form a high density of intermolecular covalent bonds. Such a design required the addition of three cysteine residues and two

lysine residues. Glycine was selected for residue 22 as this amino acid is known to "break" α-helices. This addition was performed to create a four amino acid pendant anchored to the interface by the helical structure, providing a more conformationally flexible region of the molecule to minimise any steric limitations to intermolecular bonding. One cysteine residue was contained in this pendant region, leaving four substitutions to be made to the original Lac21 sequence. These substitutions were selected to maintain the overall charge and hydrophobicity distribution as well as the tendency of the sequence to adopt an α-helical conformation. See Tables 7-1 and 7-2 and Figures 7-3 and 7-4.

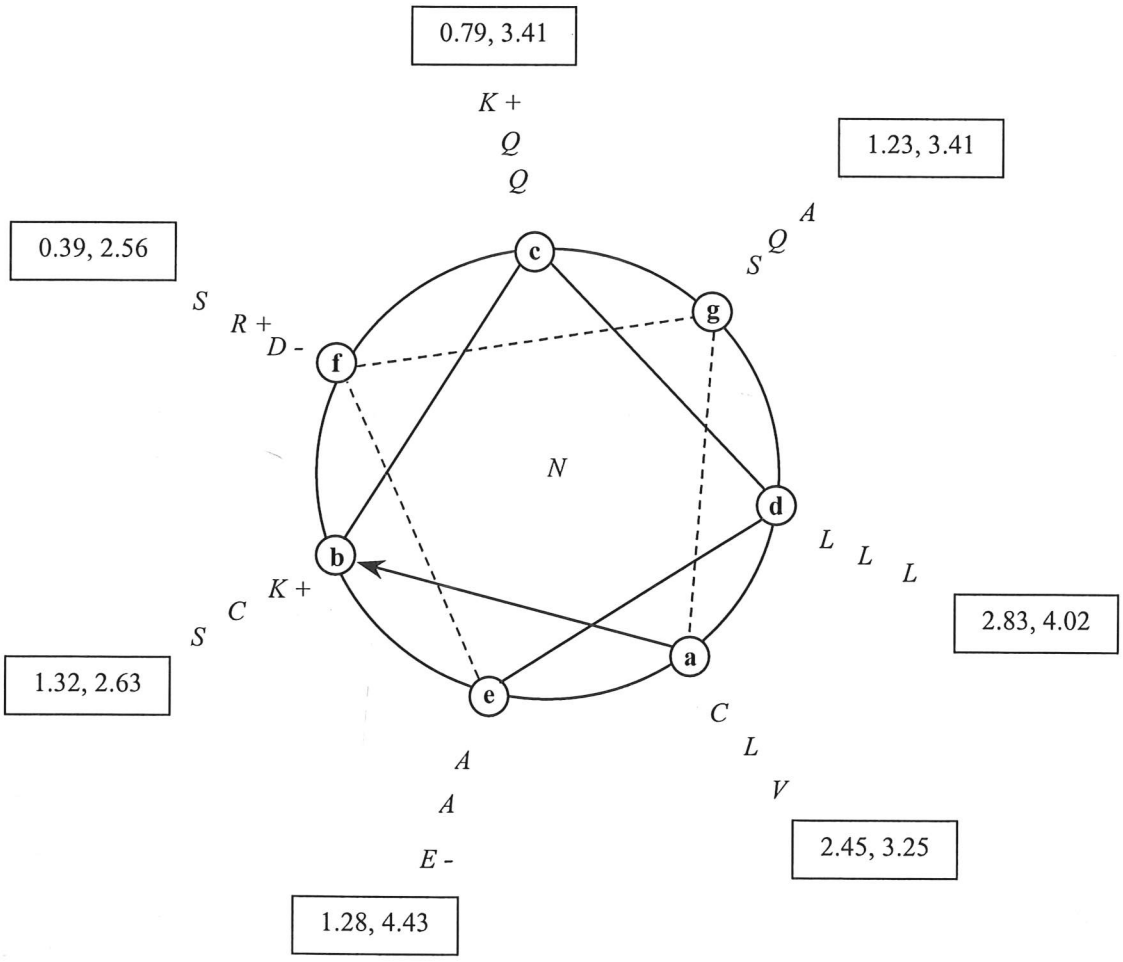


**Figure 7-4** **Section of Dan25 peptide expected to adopt a helical conformation. Diagram shows distribution of charge, hydrophobicity and α-helix promoting amino acids. Figures in boxes show the total hydrophobicity and α-helix promoting tendency, respectively, of each peptide face. Values calculated from data in Tables 7-1 and 7-2.**

## 7.3. β-Sheet Peptide Structure

β-sheet structure is of interest as a common structural motif of globular proteins and as a cause, or diagnostic indicator, of certain neurological disorders. For example, the presence of "β-amyloid plaques" with a predominantly β-sheet structure has been used as an indicator of Alzheimer's disease (Barrow and Zagorski, 1991). β-sheet formation is also implicated in other brain disorders. The human form of bovine spongiform encephalopathy, Creutzfeld-Jakob disease, is thought to involve a protein mutation resulting in raised levels of β-domains and the formation of oligopeptide "β-plaques" (Prusiner, 1991).

### *7.3.1. β-Sheet Peptide Design Studies*

Xu *et al.* (2001) have successfully created self-assembled β-sheet monolayers from a combinatorial library of *de novo* peptides. All the peptides in the library were sixty three amino acids long and the authors selected three peptides, at random, for further experimental study. These three sequences were expressed in *Escherichia coli*, purified, dialysed into water at pH 11.0 and finally lyophilised. Despite the different amino acid sequences of the peptides, all shared the ability to assemble into β-sheet monolayers at the air-water interface, as shown by circular dichroism and infrared spectroscopies. It is essential that rational design methodologies be used to guide the production of such a collection of *de novo* designed peptides that are capable of self-assembly. In this paper each peptide had a unique sequence, but all shared an identical binary pattern of polar and non-polar residues designed to favour the formation of six-stranded amphiphilic β-sheets. Each of the six β-strands was seven residues long with polar and non-polar amino acids arranged in an alternating pattern and each strand was separated by four amino acids designed to form a reverse turn. Therefore, the total peptide length is sixty three amino acids (6 strands x 7 amino acids, 5 turns x 4 amino acids, + 1 methionine initiator).

A shorter peptide, DN1, capable of self-assembly in bulk solution to form β-sheet tapes has been designed and studied by Aggeli *et al.* (1997a). The *de novo* 11-residue peptide DN1 ($CH_3CO$-Gln-Gln-Arg-Phe-Gln-Trp-Gln-Phe-Glu-Gln-Gln-$NH_2$) was designed to form β-sheet polymer tapes in water. The antiparallel β-sheet arrangement

is similar to that of the peptides studied by Xu *et al.* (2001) with successive side chains pointing up and down (Figure 7-5). In the centre of the sequence the same binary pattern of polar and non-polar amino acids can be observed (Phe4, Trp6, Phe8), although a degree of stabilisation is also predicted to occur between the $(-CH_2-)_2$ moieties on the side chains of the six glutamine residues. Studies on DN1 using circular dichroism spectroscopy reveal a low level of DN1 self-association up to a concentration of 40 μM where a sudden increase in the level of β-sheet structure occurs via a two step self-assembly process (Aggeli *et al.*, 1997b). The first transition is from a random coil configuration to an extended β-strand, this then allows addition of each peptide monomer to a growing β-sheet.

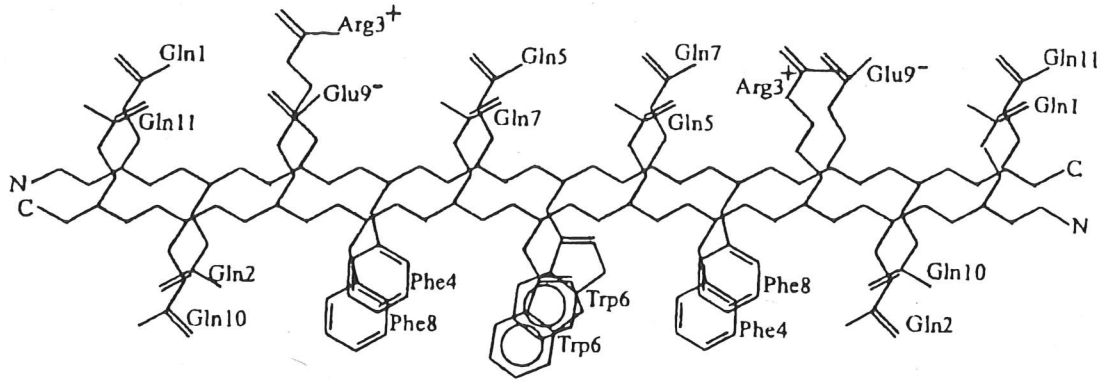


**Figure 7-5** **Antiparallel β-sheet arrangement of two DN1 molecules. Zig-zag lines represent peptide backbone. Taken from Aggeli *et al.* (1997a).**

### 7.3.2. *β-Sheet Peptide Selection*

DN1 and the peptides studied by Xu *et al.* (2001) are not the only examples of self-assembling β-sheet peptides. Rapaport *et al.* (2000) have demonstrated the ability of periodic peptides with an alternating Pro-Glu-$(Phe-Glu)_n$-Pro sequence to form β-sheet films at the air-water interface. However, DN1 was selected for further study predominantly for its short length, as solid-phase peptide synthesis shows a rapid decrease in peptide purity and yield as the peptide length rises. Solid-phase synthesis was favoured for this work, rather than the expression of longer peptides in a bacterial host, due to the faster peptide development timescale via the synthetic route. If

β-sheet self-assembly is not required, other peptides from β-sheet regions of proteins could be studied. For example, Middelberg *et al.* (1998) have measured the dynamic interfacial tension of a peptide from the β-sheet region of human lysozyme. This twenty-four amino acid peptide adsorbed rapidly at the octane-water interface and a long-term trend towards decreasing interfacial tension was observed. This was thought to be due to further self-association and aggregation at the interface, resulting in the formation of a film with mechanical strength.

Based on the information presented in this section, it is expected that the peptide DN1 will adsorb strongly at the air-water interface. The adsorbed layer may contain some degree of β-sheet structure, either from self-assembly of adsorbed molecules in the interface or through tape formation in the bulk solution at higher concentrations. It is also possible that surface exposed hydrophobicity of the adsorbed species will result in the continuing build up of interfacially adsorbed DN1 beyond monolayer coverage. In summary, it is expected that DN1 adsorption will result in the formation of an interfacial film with some mechanical strength, either through the assembly of β-sheet tapes or non-specific binding of multiple peptide layers at the interface.

## 7.4. Peptide Design and Selection Summary

In this chapter the mechanical properties of adsorbed layers of three different peptides are presented. The peptide networks were tested at the air-water interface using the CIT in the same way as the proteins presented in earlier chapters. These peptide networks were tested to provide insight into protein behaviour and to generate data to guide molecular design. Therefore, two of the peptides selected are known to form secondary structures that are common in native proteins. The first peptide selected was Lac21, as this has been shown to adopt the commonly occurring α-helix structure in bulk solution (Fairman *et al.*, 1995; Middelberg *et al.*, 2000) and was expected to retain this conformation on adsorption at the air-water interface. Aggeli *et al.* (1997a; 1997b) have performed *de novo* peptide design to create DN1, a peptide capable of self-assembly in solution to form β-sheet tapes. This peptide was chosen as it was expected to form a film at the air-water interface with a degree of mechanical strength containing some β-structure. The final peptide is a hetero-bifunctional peptide based

on the Lac21 structure, and was designed specifically for this work. The objective was to generate an amphipathic α-helix capable of forming an interfacial network with a high mechanical strength that could be used as a basic scaffold for further peptide design.

## 7.5. Materials and Methods

### *7.5.1. Mechanical Testing with the CIT*

All peptide tests were performed at the air-water interface in the same manner as those in Chapters 4 and 5. T-bar separation = 1.0 mm, displacement speed = 200 μm/s. Peptides were allowed to adsorb for a period of 1 h from PBS buffer at pH 7.4. Formaldehyde was added in one experiment after 30 min of peptide adsorption, leaving another 30 min for further adsorption and amine crosslinking to occur.

### *7.5.2. Peptide Synthesis*

Peptides were synthesised using Fmoc (fluoren-9-ylmethoxycarbonyl) solid-phase chemistry and purified using reversed-phase high performance liquid chromatography (RP-HPLC). All peptides were acetylated at the amino-termini (N) and amidated at the carboxy-termini (C) to minimise charge interactions resulting from the helix dipoles. Syntheses and initial purifications were performed by the Microchemical Facility, Babraham Institute, Babraham, Cambridgeshire, UK.

### *7.5.3. Purification*

The peptides Lac21 and Dan25 were further purified by reversed-phase chromatography using a water-acetonitrile (Sigma-Aldrich, UK) gradient with 0.1% trifluoroacetic acid (TFA, Fluka, UK) counterion. Peptide was injected onto a C5 semi-prep scale column (5 μm particle size, 300 Å pore size, 250 mm length, 10 mm diameter) in 10 mg quantities (1000 μL at 10 mg/mL). Product purity was confirmed by injecting ~80 μg (120 μL at ~0.65 mg/mL) of each fraction eluted from the semi-prep column onto an analytical column of smaller dimensions (5 μm particle size,

300 Å pore size, 150 mm length, 4.6 mm diameter) before pooling the purified peptide fractions. Figures 7-6 and 7-7 show chromatograms from the analytical column for the peptide samples as received and after further purification. Chromatograms show UV absorption at 214 nm versus retention time on the column.

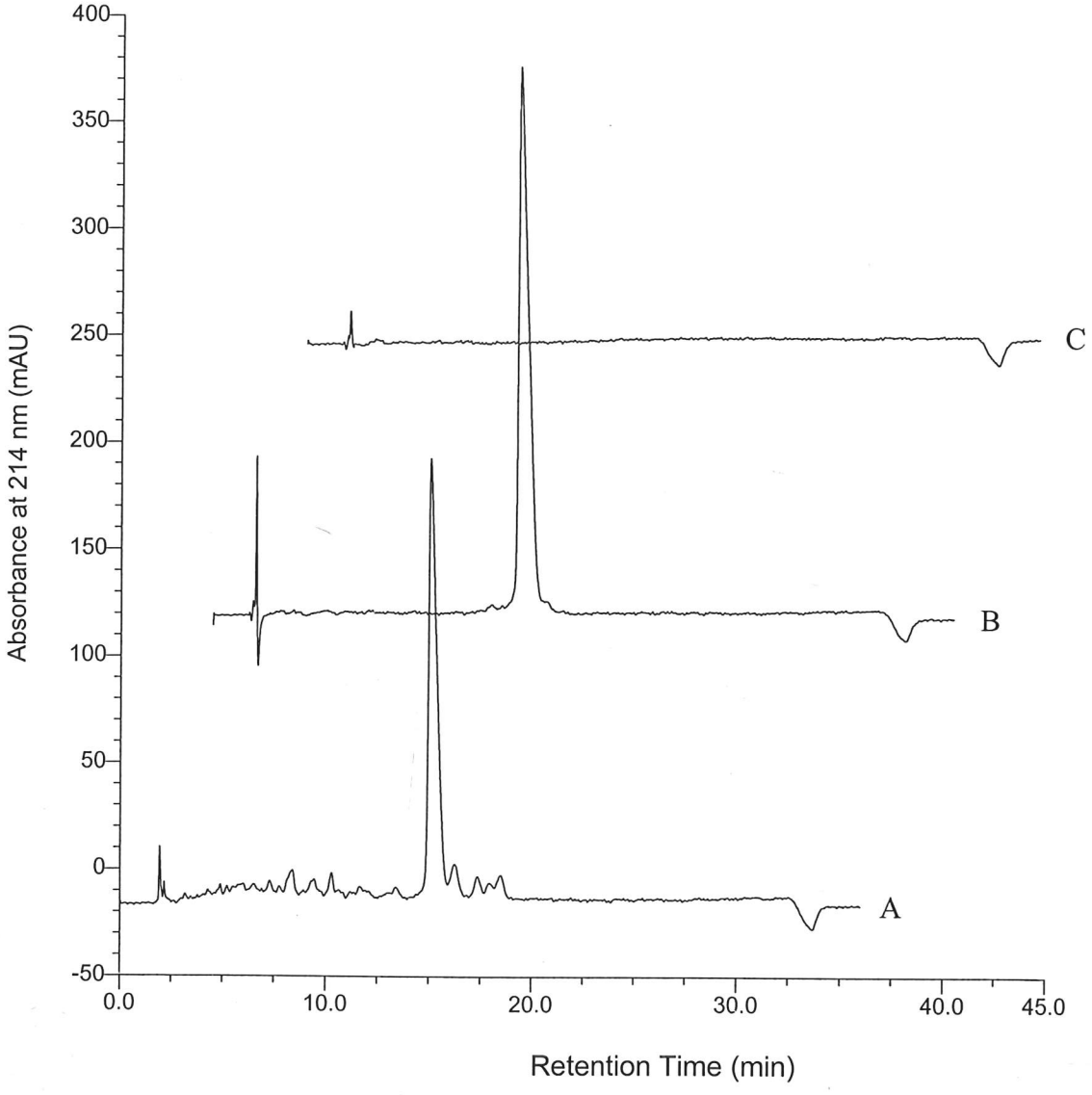


**Figure 7-6** **Validation of Lac21 peptide purification. A = peptide sample as received, B = further purified peptide, C = blank injection.**

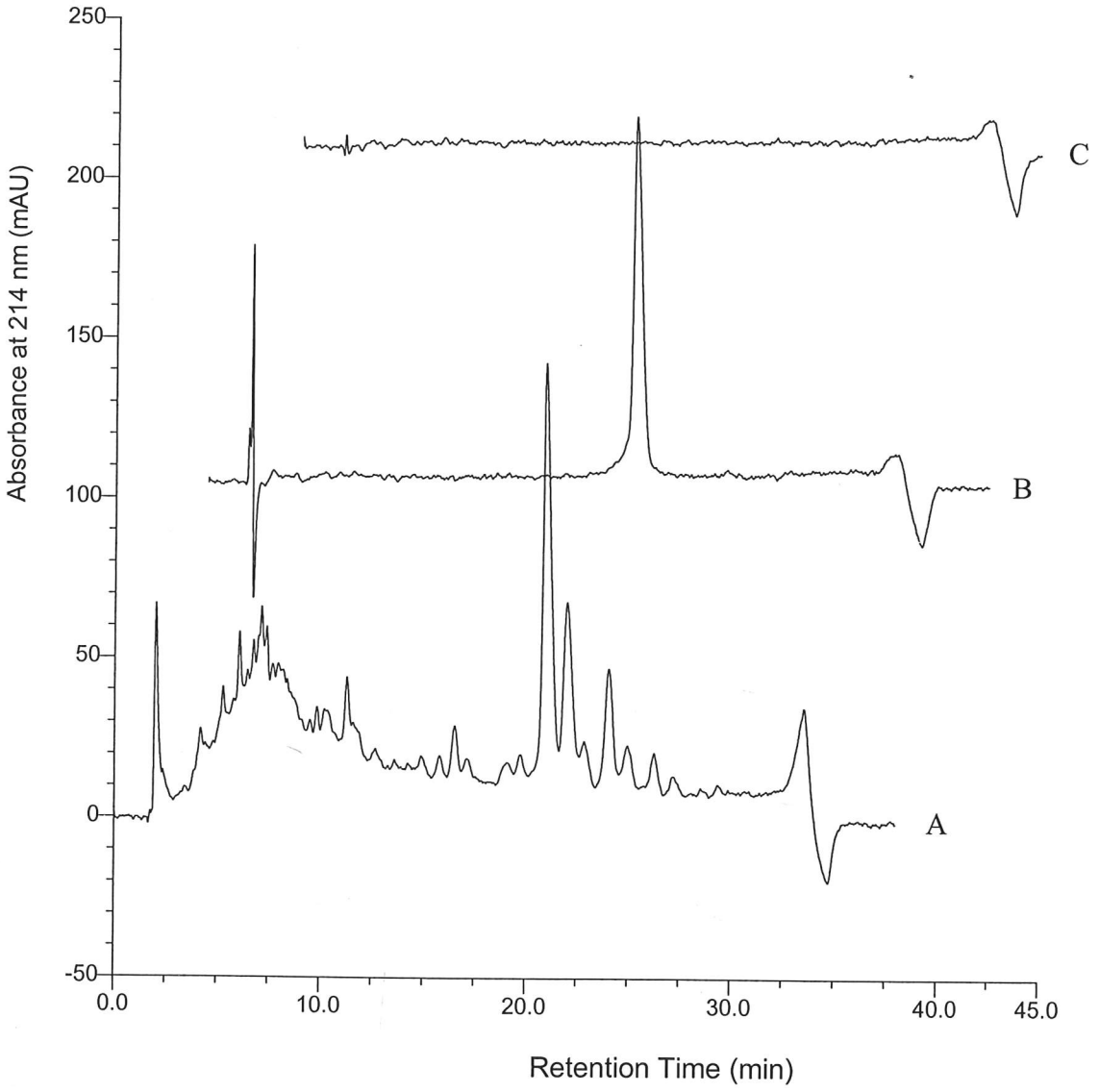


**Figure 7-7** **Validation of Dan25 peptide purification. A = peptide sample as received, B = further purified peptide, C = blank injection.**

### 7.5.4. Storage

The pooled peptide fractions were lyophilised to concentrate the samples after exiting the chromatography column. The samples were then re-dissolved in 50% water/acetonitrile (No TFA), divided into aliquots and lyophilised for a second time. These lyophilised samples were stored under nitrogen, at –20 °C, in a light-proof container.

### 7.5.5. Validation

Identities and aliquot sizes of the purified peptide samples were confirmed by quantitative amino acid analysis (PNAC - Protein and Nucleic Acid Facility, Biochemistry Department, University of Cambridge). Molecular weights of the lyophilised peptide samples were confirmed by matrix assisted laser desorption and ionisation – time of flight (MALDI-TOF) mass spectrometry (PNAC facility).

## 7.6. Results and Discussion

Figures 7-8 and 7-9 show plots of stress versus strain for the three different peptides that were studied. At a bulk concentration of 0.55 μM, only the *de novo* peptide Dan25 is capable of transmitting a significant force laterally in the plane of the interface. Data extracted from these plots are summarised in Table 7-3. The maximum interfacial stress obtained for Dan25 is 15.0 mN/m, whilst for Lac21 and DN1 the values are 0.3 mN/m and 0.2 mN/m, respectively. The null result obtained with Lac21 has been confirmed at higher peptide concentrations and is highly significant as it provides direct support for the idea put forward in Chapter 5 to explain the results obtained with Tween 20. The hypothesis was that interfacially adsorbed molecules with a clearly defined separation of the hydrophilic and hydrophobic sections of the molecule do not support the level of intermolecular interactions required to transmit a significant force in the plane of the interface. An amphipathic α-helix, that maintains a high level of secondary structure after adsorption, satisfies this condition as the hydrophobic amino acids reside predominantly on two of the seven available positions on the repeating heptad structure (Figure 7-3). These experimental results are highly significant because the peptides Lac21 and Dan25 have been shown to

demonstrate behaviour at the extremes of that observed for the protein systems tested. Lac21 is highly surface-active (Middelberg *et al.*, 2000) and capable of reducing interfacial tension below that for β-lactoglobulin, yet a negative result is returned by the CIT. The peptide demonstrates behaviour that is highly unusual for a protein or peptide system and behaves more like a conventional low molecular weight surfactant than a protein. This shows conclusively that the CIT is an excellent tool to separate network effects from interfacial energy effects. As discussed previously this is a key requirement to enable droplet disruption to be predicted in the presence of an adsorbed protein or peptide layer.

**Table 7-3** **Comparison of the mechanical properties determined by the CIT for peptide and β-lactoglobulin networks adsorbed at the air-water interface. All peptide and protein concentrations were 0.55 μM except for "DN1 high" where the concentration was 8 μM. Formaldehyde was added to give a 1% v/v bulk solution, column "Dan25 + HCHO".**

| Peptide or protein | Lac21 | DN1 | DN1 high | Dan25 | Dan25 + HCHO | β-lacto-globulin |
|---|---|---|---|---|---|---|
| Maximum interfacial stress (mN/m) | 0.3 | 0.2 | 3.8 | 15.0 | 18.0 | 12.3 |
| Minimum interfacial stress (mN/m) | -0.2 | -0.1 | -16.5 | -16.6 | -16.1 | -28.1 |
| Interfacial low-strain rigidity parameter (5% strain, mN/m) | 3.8 | 0.0 | 52.0 | 72.8 | 90.3 | 104.9 |
| Force transmission (5% cyclic strain, μN) | 0 | 0 | 120 | 175 | N/A | N/A |
| Interfacial elasticity modulus (1% strain, mN/m) | 20.5 | 7.2 | 116.8 | 71.9 | 93.6 | 124.3 |

An interfacial layer of DN1 was unable to transmit a significant lateral force when adsorbed for 1 h from a 0.55 μM solution. This may be due to slow adsorption kinetics or the formation of a thin, relatively unstructured, peptide layer. The process

of DN1 adsorption is unlikely to be diffusion limited as the results for the larger Dan25 peptide indicate strong film formation within 1 h. Based on the small peptide size and literature discussed earlier in this chapter, the adsorption of DN1 is not expected to be sufficiently slow to explain such a low level of lateral force transmission. The bulk concentration was, therefore, increased to see if the results showed the concentration dependence that was suggested earlier in this chapter. At a concentration 14.5 times higher (8 μM), forces of sufficient magnitude were detected to allow the production of a full stress-strain plot (Figure 7-8).

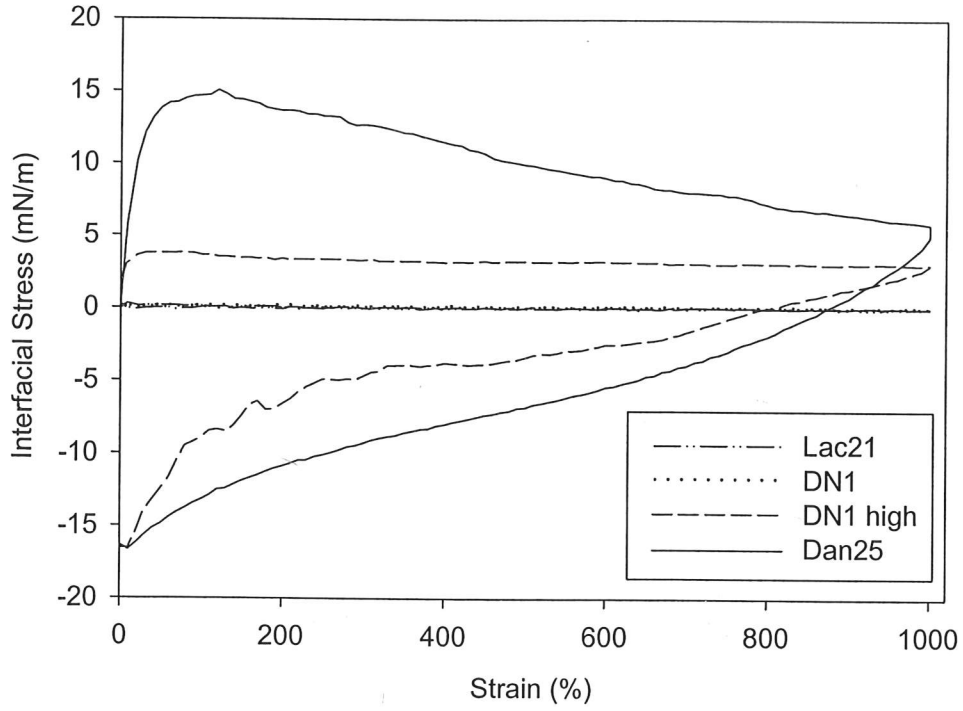


**Figure 7-8** **Stress versus strain response of peptide networks adsorbed at the air-water interface from PBS buffer (pH 7.4). All peptide concentrations were 0.55 μM except for "DN1 high" where the concentration was 8 μM.**

This confirms the dependence of the structure and/or thickness of the adsorbed DN1 layer on bulk peptide concentration. Such a result may be explained by continuing with the concept of peptides as model protein systems. The Lac21 peptide adopts an α-helical conformation in bulk solution. This is also likely to be the case for the Dan25 peptide. These peptides then adsorb at the interface and associate with other

peptide molecules to form an interfacial layer that may or may not be capable of lateral force transmission. In essence the peptides already have a secondary structure in bulk solution and a type of tertiary structure could be considered to be formed after adsorption at the interface. In contrast, the DN1 peptide is simply a short β-strand in bulk solution and is unlikely to self-associate significantly at such low peptide concentrations (Aggeli *et al.*, 1997b). Therefore, the DN1 peptide secondary structure (β-sheet in this case) is probably only formed after adsorption when the local concentration is much higher. However, at this point the DN1 molecules are already tethered to the interface so a significant energy barrier to conformational rearrangement in the interface may exist, explaining the relatively slow kinetics and concentration dependence of rigid film formation.

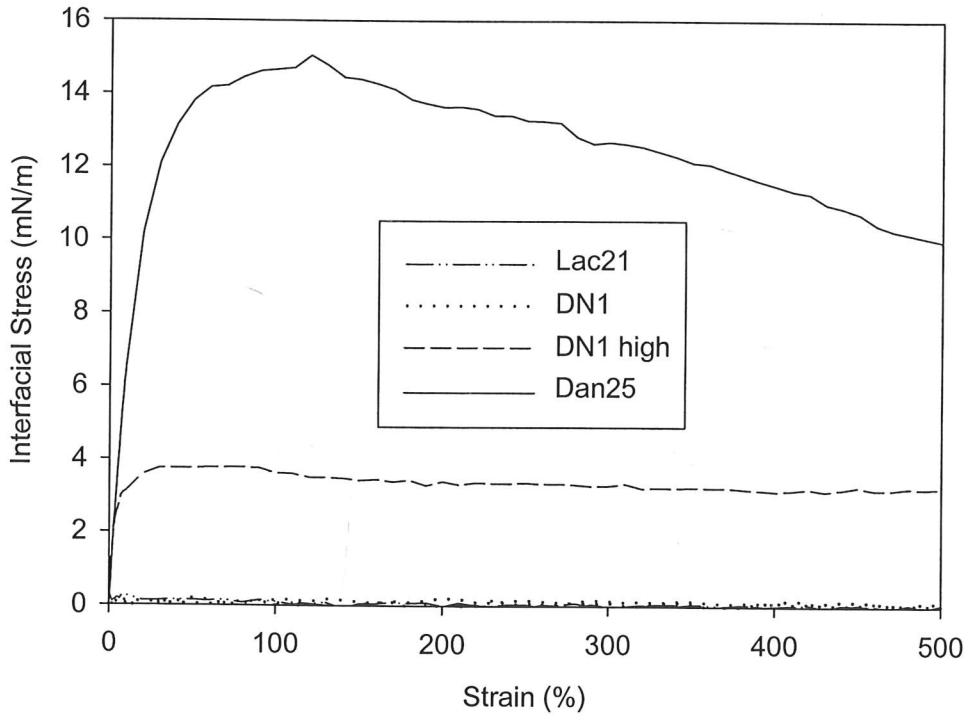


**Figure 7-9** **Tensile, low-strain, stress versus strain response of peptide networks adsorbed at the air-water interface from PBS buffer (pH 7.4). All peptide concentrations were 0.55 μM except for "DN1 high" where the concentration was 8 μM.**

Figure 7-10 shows the low strain (5%) network rigidity as a function of time. The results at peptide concentrations of 0.55 μM generally show the same pattern as those presented in Figures 7-8 and 7-9, discussed above. However, results for the higher DN1 concentration are of interest as they show time dependence for the film rigidity after initial detection at 20 min. For comparison, Dan25 forms a rigid network within 2 min at 0.55 μM bulk concentration and reaches 95% of the ultimate strength within 10 min. The results for the high DN1 concentration could indicate either continued build-up of DN1 at the interface with time, or the formation of a more structured film through a relatively slow self-assembly process. The rapidly increasing value of compressive force measured in the second half of the stress-strain test (Figure 7-8, dashed line) may be indicative of multilayer adsorption, but further testing with an independent experimental technique capable of measuring interfacial peptide concentration is required to confirm this assertion.

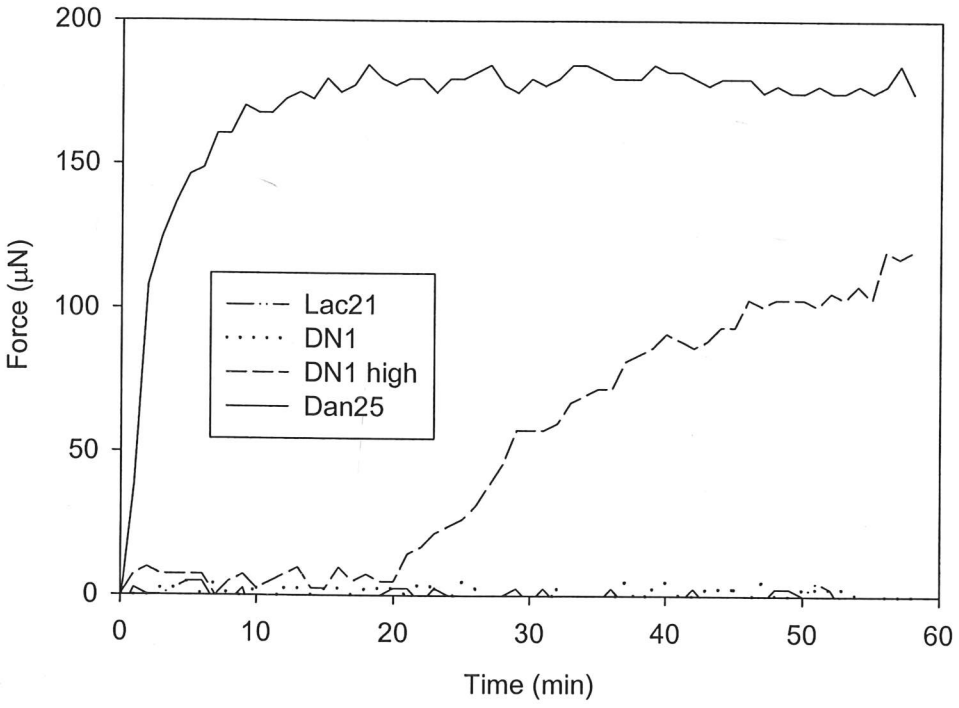


**Figure 7-10** **Cyclic testing, to 5% strain, of peptide networks adsorbed at the air-water interface from PBS buffer (pH 7.4). The data represent the increase in tensile force after application of 5% tensile displacement. All peptide concentrations were 0.55 μM except for "DN1 high" where the concentration was 8 μM.**

Comparison of the low strain data presented in Table 7-3 provides an insight into the level of interfacial network structure present at the interface. Differences in the relative values of the elasticity modulus at 1% strain and the 5% low-strain rigidity parameter show the ease of network disruption at low strain, although results at 1% strain must be interpreted with care as they are generated from a small number of data points. The results for Dan25 are suggestive of an elastic film with high rigidity, whilst the data obtained for DN1 at 8 μM concentration may indicate a loss of structure at low strain. The interfacial elasticity obtained at 1% for Lac21 and DN1 at 0.55 μM concentration show that some build-up of interfacial material has occurred but that any structure is virtually destroyed after straining to 5%.

The Dan25 peptide was designed to form intermolecular covalent bonds once two molecules are anchored in close proximity through adsorption at the interface. The primary bonding route was selected to be intermolecular disulfide bond formation, under oxidising conditions, via the sulfhydryl groups of the three cysteine residues in each Dan25 molecule. However, the peptide was also engineered to contain three lysine amino acids to allow formaldehyde crosslinking between the primary amines. Figure 7-11 shows the mechanical properties of a Dan25 network adsorbed at the air-water interface with and without amine crosslinking. Increasing the number of intermolecular bonds between the adsorbed peptide molecules by amine crosslinking increases the maximum force that can be transmitted laterally through the peptide network by 20%. However, this peak interfacial stress is followed by a region where the interfacial stress decreases more rapidly than for the non-crosslinked Dan25. Such behaviour probably indicates brittle fracture and subsequent reforming, by adsorption from the bulk solution, of the highly crosslinked network. This explains the rapid decay and erratic behaviour of the stress response as the material strain is increased.

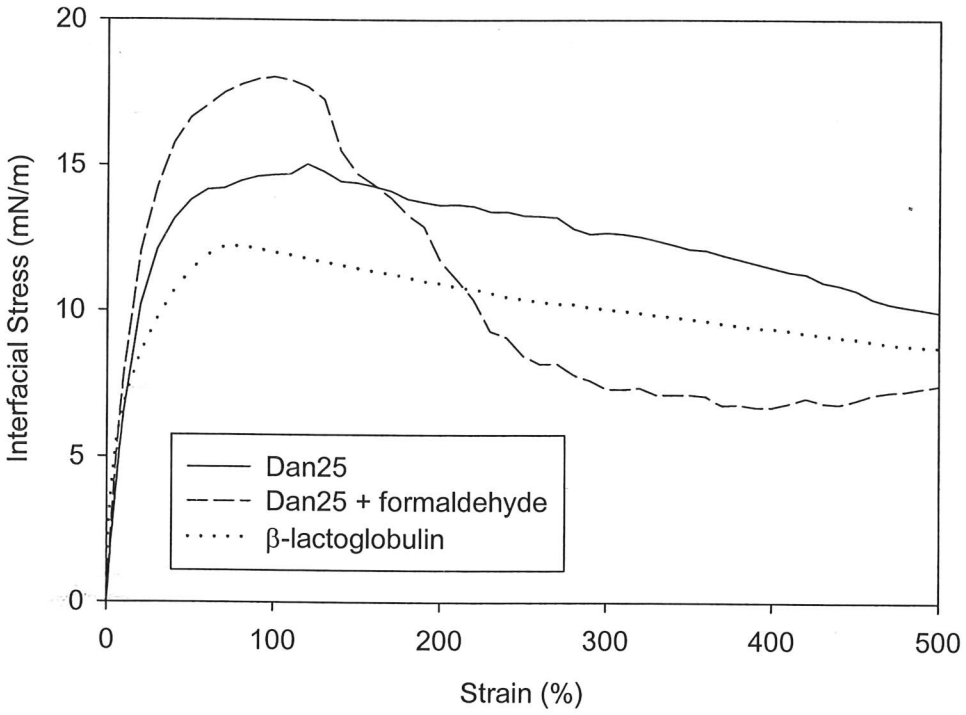


**Figure 7-11** **Tensile, low-strain, stress versus strain response of Dan25 networks adsorbed at the air-water interface from PBS buffer (pH 7.4). Dashed line shows stress-strain response after crosslinking Dan25 with 1% v/v formaldehyde in bulk solution. β-lactoglobulin response is given for reference. All protein and peptide concentrations were 0.55 μM.**

The absolute values of peak force transmitted are higher for the crosslinked and non-crosslinked Dan25 films than all the β-lactoglobulin networks tested. Figure 7-11 shows a plot for 0.55 μM β-lactoglobulin adsorbed at the air-water interface as a reference sample. Taking 5 nm as the thickness of the β-lactoglobulin network (Graham and Phillips, 1979b) and assuming monolayer adsorption for Dan25, the elastic modulus of the adsorbed material is many times higher for the peptide due to the lower network thickness. Using the figure for α-helix diameter of 0.4 nm (Idiris *et al.*, 2000) a value for the elastic modulus of the material can be calculated. For the β-lactoglobulin film shown in Figure 7-11 and included in Table 7-3, the value is 24.9 MPa using the 1% strain data. However, the Dan25 network exhibits a much higher elastic modulus of 180 MPa in the non-crosslinked case, increasing to

234 MPa after amine crosslinking. These values compare favourably with the elastic modulus of 14.7 kPa obtained by Leon *et al.* (1998) for three-dimensional matrices of short peptides assembled from 10 mg/mL aqueous solution. Normalisation using the α-helix diameter indicates that the ultimate tensile strength of the non-crosslinked Dan25 network is around 38 MPa. Comparison with other common materials shows that Dan25 networks exhibit mechanical characteristics similar to, but exceeding, those of low-density polyethylene. For low-density polyethylene, the modulus of elasticity in tension = 140 MPa – 190 MPa and the tensile strength = 9 MPa – 17 MPa (Perry and Green, 1984). Such results demonstrate both the high material strength and degree of control that can be achieved through interfacial self-assembly of novel peptide-based biomaterials.

## 7.7. Conclusions

A *de novo* peptide, Dan25, has been designed that can assemble at the air-water interface to form a network capable of transmitting a force laterally in the plane of the interface. The Dan25 peptide has dual mechanisms for covalent intermolecular bonding: disulfide linkages via cysteine sulfhydryl groups and formaldehyde crosslinking between lysine residues. Amine crosslinking of an interfacially adsorbed network of the Dan25 peptide increases both the interfacial elasticity modulus and the maximum interfacial stress that can be transmitted laterally through the network. This provides a mechanism for the control of interfacial mechanical properties. Mechanical characteristics of interfacial films of Dan25 are similar to those of other polymeric materials such as low-density polyethylene.

Interfacially adsorbed Lac21 cannot transmit a significant force in the plane of the interface due to the low level of intermolecular bonding between adsorbed peptide molecules. The low degree of peptide intermolecular interaction is likely to be a result of the retention of the amphipathic α-helical structure after adsorption at the interface. This allows the bulk of the hydrophobic amino acid side chains to be ejected from the aqueous phase into the air. The DN1 peptide shows a time and concentration dependent force response, probably as a result of the continued build up of interfacial material beyond monolayer coverage and a possible increase in the level of β-sheet structure.

# 8. Conclusions and Future Work

"As is clear from the literature, a step forward in the study of the interfacial properties of surface-active species is usually brought about by the development of a novel technique." (Bos and van Vliet, 2001).

## 8.1. Conclusions

### *8.1.1. Cambridge Interfacial Tensiometer Design*

Novel equipment, the Cambridge Interfacial Tensiometer (CIT) has been designed and constructed to facilitate the micro-mechanical characterisation of interfacial films. This work has focused mainly on the mechanical testing of interfacially adsorbed protein networks at the air-water and octane-water interfaces. The CIT uniaxially strains the adsorbed film, in the plane of the interface, and measures the lateral force transmission. In essence, the test can be thought of as a two-dimensional analogy of the "Instron" test used for conventional materials testing.

The CIT has been used to clearly demonstrate the ability of adsorbed protein and peptide layers to transmit forces laterally in the plane of a flat interface, over distances greater than 11 000 μm (c.f. protein diameter ~0.005 μm, see Table 2-1). In contrast with many existing techniques for measuring interfacial rheology, the CIT approach is not limited to small deformation studies as no assumptions are made about the preservation of network structure during the tests. Therefore, the CIT has the unique ability to produce stress-strain curves up to the point of material failure. In addition the CIT can be operated in a low strain, minimally invasive, mode that allows network rigidity to be recorded as a function of time.

The CIT was tested and validated using β-lactoglobulin networks adsorbed at the air-water interface. The instrument was validated by systematic changes in equipment dimensions and operating parameters. The influences of equipment size and geometry were found to be minimal and β-lactoglobulin networks were shown to exhibit a strain-rate dependent response, as would be expected for a polymer-like material. Visualisation of the interfacial region showed that significant detachment of the

protein networks from the silica T-bars did not occur during the test procedure. The multitude of experimental parameters yielded by the CIT, and lack of simplifying assumptions in the analysis, make it an ideal instrument to resolve the complex interplay between factors determining the mechanical properties of an interfacially adsorbed protein or peptide network.

### 8.1.2. *Mechanical Properties of β-lactoglobulin Networks at the Air-Water Interface*

Networks of β-lactoglobulin molecules adsorbed at the air-water interface and aged for a period of 1 h show an initial region of high rigidity or high elastic modulus at low tensile strain. The interfacial elasticity modulus was found to rise with bulk protein concentration. Between 10% and 50% strain substantial yielding of the network occurs and peak interfacial stress is reached at around 100% strain. The maximum force that can be transmitted through adsorbed β-lactoglobulin networks increases by over 30% when the bulk concentration is reduced below 1.0 mg/mL, to 0.1 mg/mL or 0.01 mg/mL. Less initial competition for interfacial space may allow a greater degree of conformational changes in the β-lactoglobulin molecules on adsorption, enabling more extensive polymer chain interaction and entanglement. After the peak interfacial stress the β-lactoglobulin networks show a long plateau in transmitted stress levels, indicating "repair" of the network through the transport of additional protein molecules to the interface.

### 8.1.3. *Molecular Structure and Mechanisms of Intermolecular Interaction*

In Chapter 6 it was shown that the magnitude of the interfacial elasticity modulus could be predicted from Atomic Force Microscopy (AFM) studies on the unfolding of single protein molecules. The low strain (1%) interfacial elasticity modulus was, therefore, shown to represent an ensemble average unfolding force for the adsorbed protein molecules. This clearly established a link between the mechanical properties of the interfacial protein network and the structure at a molecular level.

Experiments performed using β-casein at the oil-water and air-water interfaces demonstrate drastically reduced values of interfacial elasticity modulus when compared with β-lactoglobulin networks adsorbed under the same conditions. β-lactoglobulin is a globular protein, with a high level of secondary structure, whilst β-casein is a relatively disordered random coil protein. The large difference in elasticity modulus provides further experimental evidence of a correlation between molecular structure and ensemble interfacial mechanical properties.

Tests performed using the reducing agent dithiothreitol (DTT) in the aqueous phase indicate that disulfide bond formation is not the dominant mechanism of intermolecular bonding between interfacially adsorbed protein molecules aged for periods up to 1 h. Disruption of the protein hydrophobic bonding ability with Tween 20 resulted in the complete loss of ability to transmit force laterally through the layer of interfacially bound material. An interfacially adsorbed layer with no crosslinking capacity is unable to resist the tensile stress generated by the CIT and, therefore, no force transmission is observed.

### *8.1.4. Droplet Disruption*

Droplets of silicone oil in glycerol solution were successfully disrupted in custom designed and built apparatus that generated a flow pattern approximating simple shear. At low β-lactoglobulin concentrations (≤ 0.01 mg/mL) droplet disruption can be predicted from the capillary number correlation using the shear rate, interfacial tension and fluid viscosities. At β-lactoglobulin concentrations greater than 0.01 mg/mL such an approach fails, and the maximum stable droplet size and capillary number are reduced below the expected value. The CIT was used to probe the mechanical properties of β-lactoglobulin and β-casein interfacial networks above and below the 0.01 mg/mL threshold protein concentration discussed above. Rigid protein networks were not formed at the octane-water interface for 0.001 mg/mL β-lactoglobulin or 0.001 mg/mL β-casein. At 0.1 mg/mL concentration, β-casein is capable of forming a cohesive network, but with a tensile rigidity much below that obtained for the same concentration of β-lactoglobulin. Comparison of the droplet disruption data and those obtained using the CIT indicates that droplet destabilisation

occurs when a rigid interfacial network is formed. Rigid network formation invalidates the use of the capillary number approach and destabilises the liquid droplet, probably by increasing localised network stresses. The CIT is, therefore, a useful predictive tool for determining the validity of engineering correlations based on interfacial energy for the prediction of droplet disruption. The unique ability of the CIT to generate full stress-strain plots at varying rates of strain facilitates the derivation of a network constitutive equation. A material constitutive equation could be coupled with equations describing fluid motion for the case of disruption without an interfacial film, enabling *a priori* computational modelling of droplet deformation and disruption under the influence of a rigid interfacial network.

### *8.1.5. Mechanical Properties of Interfacial Peptide Networks*

An interfacially adsorbed layer of the α-helical peptide Lac21 was not found to transmit a significant force in the plane of the interface. This is due to a low level of intermolecular bonding between the adsorbed peptide molecules and is thought to result from the retention of an α-helical structure after adsorption at the air-water interface. The experimental data provide evidence of the importance of hydrophobic amino acids that are exposed to the aqueous phase in determining the degree of intermolecular interaction. In addition, the result confirms that interfacial layers with no crosslinking ability are unable to directly transmit forces laterally in the plane of the interface. A β-sheet peptide, DN1, exhibited a time and concentration dependent force transmission, probably caused by the continued build up of interfacial material beyond monolayer coverage and a possible increase in the level of β-sheet structure.

A *de novo* peptide, Dan25, was designed with the explicit aim of creating an interfacial network capable of forming a solid-like structure and transmitting a force laterally in the plane of the interface. The Dan25 peptide was designed to adopt an α-helical structure and have dual mechanisms for covalent intermolecular bonding. Firstly, disulfide bonding between sulfhydryl groups of cysteine residues under oxidising conditions, and secondly crosslinking of lysine residues using formaldehyde. Amine crosslinking of an interfacially adsorbed network of Dan25 increased both the interfacial elasticity modulus and the maximum interfacial stress

that could be transmitted, providing a mechanism for control of the interfacial mechanical properties. The mechanical characteristics of Dan25 networks adsorbed at the air-water interface were found to be similar to those of other polymeric materials such as low-density polyethylene.

The experimental results obtained for peptides at the air-water interface, links made between interfacial and molecular structures, and progress made to elucidate the dominant mechanisms of intermolecular interaction at the interface, provide a foundation for the continued development of self-assembling peptide-based systems.

## 8.2. Future Work

The further work suggested in this section can be broadly separated into improved equipment design, and continued molecular design. Improvements to the CIT in its current form could be made relatively simply to enhance data reproducibility and allow faster and more flexible operation. Coupling the CIT with an experimental technique providing information on the thickness or conformation of the adsorbed protein layer would facilitate rapid advances in the understanding of interfacial molecular assembly at a fundamental level. Continued molecular design should initially focus on elucidating the possible mechanisms for intermolecular interactions between proteins or peptides adsorbed at a fluid-fluid interface. Such work should be used to proceed with additional *de novo* peptide design beyond the Dan25 peptide already developed. This peptide design should be performed with the explicit aim of demonstrating the self-assembling characteristics of a peptide-based system.

### *8.2.1. Improvements to the Existing CIT*

The single largest problem in the development of the CIT was the difficulty in obtaining reproducible results. The main source of error was found to be the cleanliness of the silica T-bars. The problem was greatly reduced through the introduction of a rigorous cleaning protocol. However, many interfacial rheological techniques suffer from poor reproducibility and the drive to improve quality of the CIT data is still present. The most significant remaining source of variance in the data is likely to be air currents across the fluid interface and localised temperature

variations. Encasing the CIT in an airtight, temperature controlled, enclosure would alleviate such problems. Although the sample size is rather small, the duplicate experimental results obtained at the oil-water interface in Chapter 6 appear to be highly reproducible, and no anomalous results were found for any of the experiments performed in this way. Therefore, recommendations to improve data reproducibility are to construct a cabinet to encase the CIT, ideally with Peltier-cell temperature control, and to perform the bulk of future experiments at the oil-water interface.

Several experiments performed in this work required the injection of concentrated chemicals or protein solution in the CIT dish whilst it already contained buffer solution. The result is an imprecise definition of localised concentrations and poorly characterised mixing times in this case of combined diffusion and bulk fluid motion. The addition of a liquid mixing facility to the CIT would allow easier interpretation of the results from experiments such as those presented in Chapter 5 where Tween 20 or DTT was added to the aqueous phase after the start of the experiment. Specifically, if the system could be assumed to be well mixed on a short time-scale, further dynamic changes in the mechanical properties of the adsorbed protein layer could be attributed to structural changes resulting from the change in chemical environment. Such mixing could be achieved by thinning the base of the CIT dish and placing one or more magnets connected to 12 Volt electric motors below the dish. Use of variable resistors to control the motor speed would allow fluid mixing in the same fashion as conventional magnetic stirrers, but on a smaller scale.

The final enhancement of the CIT, that could be made relatively easily, is connection of two peristaltic pumps for loading and removing the washing solutions. As present the CIT dish has to be removed and emptied after each washing step (9 times per experiment). Incorporation of pumps for *in situ* washing of the dish and silica T-bars would decrease the experimental cycle time allowing more proteins, peptides or buffer conditions to be investigated. Use of peristaltic pumps avoids limitation on the solutions that can be pumped, as the liquids do not contact the moving parts of the pump and the type of tubing can be easily changed.

### 8.2.2. In Situ *Measurements of Network Thickness and Molecular Conformation*

In a review of protein and surfactant interfacial rheology Bos and Vliet (2001) concluded that "there is a need for new measuring devices that monitor several interfacial properties on a mesoscopic and microscopic scale at the same time". One of the key targets in this work has been the correlation of the mechanical properties of an interfacially adsorbed layer with the structure at a molecular level. So far this has been conducted through re-interpretation and analysis of studies performed by other workers. Combining the CIT with a technique to measure the adsorbed layer thickness and conformation is likely to yield synergistic benefits beyond the continued application of a single experimental procedure to many different proteins or peptides. Such an equipment combination may allow the investigation of structural changes in the adsorbed layer resulting from the application of an external force. This work is required because in many applications, such as the case of droplet disruption investigated in Chapter 6, the interfacial network is not at mechanical equilibrium. Possible techniques to non-invasively investigate adsorption phenomena at the fluid-fluid interface include ellipsometry, infrared reflection absorption spectroscopy (IRRAS) and total internal reflection fluorescence spectroscopy (TIRFS).

TIRFS has been used by Tupy *et al.* (1998) to study the adsorption/desorption dynamics of β-casein at a liquid-liquid interface. The apparatus non-invasively measures the arrival of fluorescing surface-active molecules at the oil-water interface. This was achieved by shining light, with a wavelength 490 nm, on the interface at the angle of total internal reflection. One of the key requirements for the TIRFS technique was the development of a new type of flow cell. The flow cell and experimental setup developed could be adapted relatively easily to other optical techniques that are more sensitive to molecular conformation, such as fluorescence resonance energy transfer (FRET) and tryptophan fluorescence.

Ellipsometric measurements of β-lactoglobulin adsorbed at the air-water interface have been carried out by Gauthier *et al.* (2001). Their experimental technique is based around a He-Ne laser operating at 632.8 nm with an incidence angle around 1°. "Basically, ellipsometric angle, related to the phase difference between vertical and horizontal beam polarisations, is proportional to the amount of protein adsorbed at the

interface." This experimental setup allowed the quantity of adsorbed protein to be plotted as a function of time over the course of several hours.

An important development in ellipsometry is the use of infrared, rather than visible light, enabling other possibilities for the simultaneous structural and chemical interrogation of the interfacial layer (Keddie, 2001). IRRAS has been used by Meinders *et al.* (2001) to characterise the molecular behaviour of β-casein at and near the air-water interface. The technique is similar to Fourier Transform Infrared Spectroscopy (FTIRS) but can be performed at a fluid-fluid interface, provided that the molecular species of interest resides in the more optically dense medium. "Molecular properties can be measured together with system parameters, such as surface pressure, pH and ionic strength, and as a function of processes, like expansion or compression of the surface" (Meinders *et al.*, 2000). IRRAS is, therefore, a promising candidate for coupling with the CIT to generate high quality data on the mechanical properties of an adsorbed film of defined thickness and structure.

### *8.2.3. Further Molecular Design*

Improved understanding of the dominant mechanisms that determine the level of protein or peptide intermolecular interactions is required to facilitate further peptide design. Enhancements to the CIT that improve fluid mixing should allow better interpretation of experiments performed to probe interaction mechanisms. The most pressing need is for further investigations into the role of disulfide bonding in the determination of mechanical properties of the interfacial protein or peptide layer. Experiments investigating the role of disulfide bonding performed with DTT should be repeated using N-ethylmaleimide (NEM) in the aqueous phase, as this has been used previously to permanently block the sulfhydryl groups of cysteine residues (Riordan and Vallee, 1972). Use of NEM would remove any doubts regarding the efficacy of disulfide reduction with DTT due to localised oxidation at the interface. Such experiments were not performed due to the toxicity of NEM. However, these tests would be made easier and safer to perform if the ability to wash the CIT *in situ* was improved by the measures discussed previously.

The design of a β-sheet peptide should follow the creation of the Dan25 peptide. This would be best performed by following the approach of Xu *et al.* (2001) to generate self-assembling β-sheet peptides with a repeating structure of hydrophobic and hydrophilic residues. A molecule designed to adsorb at the air-water interface to create a repeating β-sheet structure is an ideal case to demonstrate useful self-assembly properties through the creation of a nano-patterned solid surface. Cysteine residues could be incorporated into the sequence at appropriate locations to create an interfacial layer patterned with sulfhydryl groups spaced a few nanometers apart. The peptides of Xu *et al.* (2001) folded at the air-water interface to create β-sheet structures through the self-association of six amphiphilic β-strands, each consisting of a seven amino acids. The result is a lattice structure with overall dimensions of 27.2 Å by 23.6 Å. This type of interfacial peptide layer could be used to organise gold nanoparticles (currently available down to 5 nm diameter, Sigma-Aldrich, UK) by addition to the aqueous phase at low concentration. After sufficient time for binding of the gold to the cysteine residues, the interfacial layer could be immobilised on a solid support by conventional Langmuir-Blodgett methods. The immobilised film could be imaged using Atomic Force Microscopy (AFM) or Transmission Electron Microscopy (TEM) to confirm the powerful ability of peptide-based systems to create structures organised on the nanometer scale.

## References


Aggeli, A., Bell, M., Boden, N., Keen, J. N., Knowles, P. F., McLeish, T. C. B., Pitkeathly, M., and Radford, S. E. (1997a). Responsive gels formed by the spontaneous self-assembly of peptides into polymeric beta-sheet tapes. *Nature, 386*(6622), 259-262.

Aggeli, A., Bell, M., Boden, N., Keen, J. N., McLeish, T. C. B., Nyrkova, I., Radford, S. E., and Semenov, A. (1997b). Engineering of peptide beta-sheet nanotapes. *Journal of Materials Chemistry, 7*(7), 1135-1145.

Anantharamaiah, G. M. (1986). Synthetic peptide analogs of apolipoproteins. *Methods in Enzymology, 128*, 627-647.

Anderson, R. E., Pande, V. S., and Radke, C. J. (2000). Dynamic lattice Monte-Carlo simulation of a model protein at an oil/water interface. *Journal of Chemical Physics, 112*(20), 9167-9185.

Anselme, K. (2000). Osteoblast adhesion on biomaterials. *Biomaterials, 21*(7), 667-681.

Artsaenko, O., Kettig, B., Fiedler, U., Conrad, U., and During, K. (1998). Potato tubers as a biofactory for recombinant antibodies. *Molecular Breeding, 4*(4), 313-319.

Ascherson (1840). Ueber den physiologischen Nutzen der Fettstoffe und über eine neue auf deren Mitwirkung begründete und durch mehrere neue Thatsachen unterstützte Theorie der Zellenbildung. *Archiv für Anatomie und Physiologie*, 44-68.

Barrett, G. C. (1998). *Amino Acids and Peptides*, pp. 22. Cambridge University Press, Cambridge.

Barrow, C. J., and Zagorski, M. G. (1991). Solution structures of beta peptide and its constituent fragments - Relation to amyloid deposition. *Science, 253*(5016), 179-182.

Barthes-Biesel, D. (1991). Role of interfacial properties on the motion and deformation of capsules in shear-flow. *Physica A, 172*(1-2), 103-124.

Becher, P. (1991). Food emulsions - An introduction. *ACS Symposium Series, 448*, 1-6.

Benjamins, J., and Vader, F. V. (1992). The determination of the surface shear properties of adsorbed protein layers. *Colloids and Surfaces, 65*(2-3), 161-174.

Bentley, B. J., and Leal, L. G. (1986). An experimental investigation of drop deformation and breakup in steady, two-dimensional linear flows. *Journal of Fluid Mechanics, 167*, 241-283.

Best, R. B., Li, B., Steward, A., Daggett, V., and Clarke, J. (2001). Can non-mechanical proteins withstand force? Stretching barnase by atomic force microscopy and molecular dynamics simulation. *Biophysical Journal, 81*(4), 2344-2356.

Beverung, C. J., Radke, C. J., and Blanch, H. W. (1999). Protein adsorption at the oil/water interface: Characterization of adsorption kinetics by dynamic interfacial tension measurements. *Biophysical Chemistry, 81*(1), 59-80.

Black, S. D., and Mould, D. R. (1991). Development of hydrophobicity parameters to analyze proteins which bear posttranslational or cotranslational modifications. *Analytical Biochemistry, 193*(1), 72-82.

Boncheva, M., and Vogel, H. (1997). Formation of stable polypeptide monolayers at interfaces: Controlling molecular conformation and orientation. *Biophysical Journal, 73*(2), 1056-1072.

Born, C., Zhang, Z., Alrubeai, M., and Thomas, C. R. (1992). Estimation of disruption of animal cells by laminar shear stress. *Biotechnology and Bioengineering, 40*(9), 1004-1010.

Bos, M. A., and van Vliet, T. (2001). Interfacial rheological properties of adsorbed protein layers and surfactants: A review. *Advances in Colloid and Interface Science, 91*(3), 437-471.

Boussinesq, M. J. (1913). Sur l'existence d'une viscosite superficielle, dans la mince couche de transition separant un liquide d'un autre fluid contigu. *Comptes Rendus [Hebdomadaires] des Seances de l'Academie des Sciences, 156*, 983.

Boyd, J., and Sherman, P. (1970). Two-dimensional rheological studies on surfactant films at interfaces. *Journal of Colloid and Interface Science, 34*(1), 76-80.

Boyd, J., Mitchell, J. R., Irons, L., Musselwhite, P. R., and Sherman, P. (1973). The mechanical properties of milk protein films spread at the air-water interface. *Journal of Colloid and Interface Science, 45*(3), 478-486.

Burgess, D. J., and Sahin, N. O. (1997). Interfacial rheological and tension properties of protein films. *Journal of Colloid and Interface Science, 189*(1), 74-82.

Caessens, P. W. J. R., DeJongh, H. H. J., Norde, W., and Gruppen, H. (1999). The adsorption-induced secondary structure of beta-casein and of distinct parts of its sequence in relation to foam and emulsion properties. *Biochimica Et Biophysica Acta-Protein Structure and Molecular Enzymology, 1430*(1), 73-83.

Carrion-Vazquez, M., Oberhauser, A. F., Fowler, S. B., Marszalek, P. E., Broedel, S. E., Clarke, J., and Fernandez, J. M. (1999). Mechanical and chemical unfolding of a single protein: A comparison. *Proceedings of the National Academy of Sciences of the United States of America, 96*(7), 3694-3699.

Chipot, C., Maigret, B., and Pohorille, A. (1999). Early events in the folding of an amphipathic peptide: A multinanosecond molecular dynamics study. *Proteins: Structure Function and Genetics, 36*(4), 383-399.

Chothia, C. (1975). Structural invariants in protein folding. *Nature, 254*, 304-308.

Clark, D. C., Mackie, A. R., Wilde, P. J., and Wilson, D. R. (1994). Differences in the structure and dynamics of the adsorbed layers in protein-stabilized model foams and emulsions. *Faraday Discussions, 98*, 253-262.

Cooper, A. (2000). Heat capacity of hydrogen-bonded networks: An alternative view of protein folding thermodynamics. *Biophysical Chemistry, 85*(1), 25-39.

Costello, B. A., Luckham, P. F., and Manimaaran, S. (1994). The viscoelastic properties of confined polymer layers. *Colloids and Surfaces A-Physicochemical and Engineering Aspects, 86*, 291-293.

Courthaudon, J. L., Dickinson, E., Matsumura, Y., and Clark, D. C. (1991). Competitive adsorption of beta-lactoglobulin + Tween 20 at the oil-water interface. *Colloids and Surfaces, 56*, 293-300.

Daniell, H., McPherson, D. T., Urry, D. W., and Xu, J. (1999). Hyperexpression of bioelastic polypeptides. United States Patent: Bioelastics Research Ltd. (Birmingham, AL); The UAB Research Foundation (Birmingham, AL).

de Bruijn, R. A. (1989). Deformation and breakup of droplets in simple shear flow, *Ph.D. Thesis*, University of Eindhoven.

Dickinson, E. (1992). *An Introduction to Food Colloids*. Oxford University Press, Oxford.

Dickinson, E. (1997). Properties of emulsions stabilized with milk proteins: Overview of some recent developments. *Journal of Dairy Science, 80*(10), 2607-2619.

Dickinson, E., and Euston, S. R. (1992). Monte-Carlo simulation of colloidal systems. *Advances in Colloid and Interface Science, 42*, 89-148.

Dickinson, E., and Matsumura, Y. (1991). Time-dependent polymerization of beta-lactoglobulin through disulfide bonds at the oil-water interface in emulsions. *International Journal of Biological Macromolecules, 13*(1), 26-30.

Dickinson, E., Murray, B. S., and Stainsby, G. (1985). Time-dependent surface viscosity of adsorbed films of casein + gelatin at the oil-water interface. *Journal of Colloid and Interface Science, 106*(1), 259-262.

Dickinson, E., Murray, B. S., and Stainsby, G. (1988). Coalescence stability of emulsion-sized droplets at a planar oil-water interface and the relationship to protein film surface rheology. *Journal of the Chemical Society-Faraday Transactions I, 84*(3), 871-883.

Dickinson, E., Rolfe, S. E., and Dalgleish, D. G. (1990). Surface shear viscometry as a probe of protein-protein interactions in mixed milk protein films adsorbed at the oil-water interface. *International Journal of Biological Macromolecules, 12*(3), 189-194.

Dill, K. A. (1990). Dominant forces in protein folding. *Biochemistry, 29*(31), 7133-7155.

Enser, M., Bloomberg, G. B., Brock, C., and Clark, D. C. (1990). De novo design and structure-activity relationships of peptide emulsifiers and foaming agents. *International Journal of Biological Macromolecules, 12*(2), 118-124.

Faergemand, M., and Murray, B. S. (1998). Interfacial dilatational properties of milk proteins cross-linked by transglutaminase. *Journal of Agricultural and Food Chemistry, 46*(3), 884-890.

Faergemand, M., Murray, B. S., and Dickinson, E. (1997). Cross-linking of milk proteins with transglutaminase at the oil-water interface. *Journal of Agricultural and Food Chemistry, 45*(7), 2514-2519.

Faergemand, M., and Qvist, K. B. (1999). On the importance of using a $Ca^{2+}$ independent transglutaminase for cross-linking of beta-lactoglobulin. *Food Hydrocolloids, 13*(3), 199-201.

Fairman, R., Chao, H. G., Mueller, L., Lavoie, T. B., Shen, L. Y., Novotny, J., and Matsueda, G. R. (1995). Characterization of a new 4-chain coiled-coil: Influence of chain-length on stability. *Protein Science, 4*(8), 1457-1469.

Fisher, L. R., and Mitchell, E. E. (1988). *Effect of adsorbed proteins on interactions between emulsion droplets.* Paper presented at the International Symposium on Food Colloids, Unilever Reseach, Colworth, UK.

Fisher, T. M., Stohr, M., and Schmid-Schonbein, H. (1978). Red blood cell (RBC) microrheology: Comparison of the behaviour of single RBC and liquid droplets in shear flow. *AIChE Symposium Series, 74*(182), 38-45.

Fourt, L. (1939). Lateral cohesion in protein monolayers. *Journal of Physical Chemistry, 43*, 887-899.

Gauthier, F., Bouhallab, S., and Renault, A. (2001). Modification of bovine beta-lactoglobulin by glycation in a powdered state or in aqueous solution: Adsorption at the air-water interface. *Colloids and Surfaces B-Biointerfaces, 21*(1-3), 37-45.

Geiger, S., JagerLezer, N., Tokgoz, S., Seiller, M., and Grossiord, J. L. (1999). Characterization of the mechanical properties of a water/oil/water multiple emulsion oily membrane by a micropipette aspiration technique. *Colloids and Surfaces A-Physicochemical and Engineering Aspects, 157*(1-3), 325-332.

Georgiadis, R., Peterlinz, K. P., and Peterson, A. W. (2000). Quantitative measurements and modeling of kinetics in nucleic acid monolayer films using SPR spectroscopy. *Journal of the American Chemical Society, 122*(13), 3166-3173.

Grace, H. P. (1982). Dispersion phenomena in high-viscosity immiscible fluid systems and application of static mixers as dispersion devices in such systems. *Chemical Engineering Communications, 14*(3-6), 225-277.

Graham, D. E., and Phillips, M. C. (1979a). Proteins at liquid interfaces I. Kinetics of adsorption and surface denaturation. *Journal of Colloid and Interface Science, 70*(3), 403-414.

Graham, D. E., and Phillips, M. C. (1979b). Proteins at liquid interfaces II. Adsorption isotherms. *Journal of Colloid and Interface Science, 70*(3), 415-426.

Graham, D. E., and Phillips, M. C. (1979c). Proteins at liquid interfaces III. Molecular structures of adsorbed films. *Journal of Colloid and Interface Science, 70*(3), 427-439.

Graham, D. E., and Phillips, M. C. (1980a). Proteins at liquid interfaces IV. Dilatational properties. *Journal of Colloid and Interface Science, 76*(1), 227-239.

Graham, D. E., and Phillips, M. C. (1980b). Proteins at liquid interfaces V. Shear properties. *Journal of Colloid and Interface Science, 76*(1), 240-250.

Guo, Z., and Thirumalai, D. (1996). Kinetics and thermodynamics of folding of a de novo designed four-helix bundle protein. *Journal of Molecular Biology, 263*(2), 323-343.

Heikoop, J. C., van den Boogaart, P., Mulders, J. W. M., and Grootenhuis, P. D. J. (1997). Structure-based design and protein engineering of intersubunit disulfide bonds in gonadotropins. *Nature Biotechnology, 15*(7), 658-662.

Hickel, A., Radke, C. J., and Blanch, H. W. (1999). Hydroxynitrile lyase at the diisopropyl ether/water interface: Evidence for interfacial enzyme activity. *Biotechnology and Bioengineering, 65*(4), 425-436.

Ho, S. P., and Degrado, W. F. (1987). Design of a 4-helix bundle protein - Synthesis of peptides which self-associate into a helical protein. *Journal of the American Chemical Society, 109*(22), 6751-6758.

Hughes, A. H., and Rideal, E. K. (1932). On protein monolayers. *Proceedings of the Royal Society of London, A137*, 62-77.

Idiris, A., Alam, M. T., and Ikai, A. (2000). Spring mechanics of alpha-helical polypeptide. *Protein Engineering, 13*(11), 763-770.

Improta, S., Politou, A. S., and Pastore, A. (1996). Immunoglobulin-like modules from titin I-band: Extensible components of muscle elasticity. *Structure, 4*(3), 323-337.

Janssen, J. J. M., Boon, A., and Agterof, W. G. M. (1994). Influence of dynamic interfacial properties on droplet breakup in simple shear-flow. *AIChE Journal, 40*(12), 1929-1939.

Janssen, J. J. M., Boon, A., and Agterof, W. G. M. (1997). Influence of dynamic interfacial properties on droplet breakup in plane hyperbolic flow. *AIChE Journal, 43*(6), 1436-1447.

Kauzmann, W. (1959). Some factors in the interpretation of protein denaturation. *Advances in Protein Chemistry, 14*, 1-63.

Keddie, J. L. (2001). Structural analysis of organic interfacial layers by ellipsometry. *Current Opinion in Colloid & Interface Science, 6*(2), 102-110.

Kempe, T., Kent, S. B. H., Chow, F., Peterson, S. M., Sundquist, W. I., Litalien, J. J., Harbrecht, D., Plunkett, D., and Delorbe, W. J. (1985). Multiple-copy genes - Production and modification of monomeric peptides from large multimeric fusion proteins. *Gene, 39*(2-3), 239-245.

Kohn, W. D., Mant, C. T., and Hodges, R. S. (1997). alpha-Helical protein assembly motifs. *Journal of Biological Chemistry, 272*(5), 2583-2586.

Kuliopulos, A., and Walsh, C. T. (1994). Production, purification, and cleavage of tandem repeats of recombinant peptides. *Journal of the American Chemical Society, 116*(11), 4599-4607.

Lakowicz, J. R. (1999). *Principles of Fluorescence Spectroscopy* (2nd ed.), pp. 461-497. Kluwer Academic / Plenum Publishers, New York.

Langmuir, I. (1936). Two-dimensional gases, liquids and solids. *Science, 84*(2183), 379-383.

Langmuir, I., and Schaefer, V. J. (1939). Properties and structure of protein monolayers. *Chemical Reviews, 24*, 181-202.

Leon, E. J., Verma, N., Zhang, S. G., Lauffenburger, D. A., and Kamm, R. D. (1998). Mechanical properties of a self-assembling oligopeptide matrix. *Journal of Biomaterials Science-Polymer Edition, 9*(3), 297-312.

Loeb, G. I., and Baier, R. E. (1968). Spectroscopic analysis of polypeptide conformation in polymethyl glutamate monolayers. *Journal of Colloid and Interface Science, 27*(1), 38-45.

Lombardi, A., Bryson, J. W., and DeGrado, W. F. (1996). De novo design of heterotrimeric coiled coils. *Biopolymers, 40*(5), 495-504.

Loughran, O. (2001). Molecular self-assembly - the chemical engineer's final frontier. *The Chemical Engineer, 717*, 38-40.

Lu, J. R., Su, T. J., and Thomas, R. K. (1999). Structural conformation of bovine serum albumin layers at the air-water interface studied by neutron reflection. *Journal of Colloid and Interface Science. 213*(2), 426-437.

Lomax, C. (2001). Protein interfacial aggregation and its effect on droplet disruption. *Undergraduate Research Project*, Department of Chemical Engineering, Cambridge University, Cambridge.

Lucassen-Reynders, E. H. (1996). *Encyclopedia of Emulsion Technology*, Vol. 4(2). Marcel Dekker, New York.

Mackie, A. R., Gunning, A. P., Wilde, P. J., and Morris, V. J. (1999). Orogenic displacement of protein from the air/water interface by competitive adsorption. *Journal of Colloid and Interface Science, 210*(1), 157-166.

MacRitchie, F. (1970). Bonding in protein and polypeptide monolayers. *Journal of Macromolecular Science: Pure and Applied Chemistry, A4*(5), 1169-1176.

Makievski, A. V., Fainerman, V. B., Miller, R., Bree, M., Liggieri, L., and Ravera, F. (1997). Determination of equilibrium surface tension values by extrapolation via long time approximations. *Colloids and Surfaces A-Physicochemical and Engineering Aspects, 122*(1-3), 269-273.

Malcolm, B. R. (1968). Molecular structure and deuterium exchange in monolayers of synthetic polypeptides. *Proceedings of the Royal Society of London, A305*, 363-385.

Marquie, C., Tessier, A. M., Aymard, C., and Guilbert, S. (1997). HPLC determination of the reactive lysine content of cottonseed protein films to monitor the extent of cross-linking by formaldehyde, glutaraldehyde, and glyoxal. *Journal of Agricultural and Food Chemistry, 45*(3), 922-926.

Marqusee, S., and Baldwin, R. L. (1987). Helix stabilization by Glu- ... Lys+ salt bridges in short peptides of de novo design. *Proceedings of the National Academy of Sciences of the United States of America, 84*(24), 8898-8902.

Mauguen, Y., Hartley, R. W., Dodson, E. J., Dodson, G. G., Bricogne, G., Chothia, C., and Jack, A. (1982). Molecular-structure of a new family of ribonucleases. *Nature, 297*(5862), 162-164.

McClements, D. J., Monahan, F. J., and Kinsella, J. E. (1993). Disulfide bond formation affects stability of whey-protein isolate emulsions. *Journal of Food Science, 58*(5), 1036-1039.

McKenzie (1972). Location of sulfhydryl and disulfide groups in bovine lactoglobulins and effects of urea. *Biochemistry, 11*(24), 4539-4547.

McLeish, M. J., Nielsen, K. J., Najbar, L. V., Wade, J. D., Lin, F., Doughty, M. B., and Craik, D. J. (1994). Conformation of a peptide corresponding to T4 lysozyme residues 59-81 by NMR and CD spectroscopy. *Biochemistry, 33*(37), 11174-11183.

Meinders, M. B. J., van den Bosch, G. G. M., and de Jongh, H. H. J. (2000). IRRAS, a new tool in food science. *Trends in Food Science & Technology, 11*(6), 218-225.

Meinders, M. B. J., van den Bosch, G. G. M., and de Jongh, H. H. J. (2001). Adsorption properties of proteins at and near the air/water interface from IRRAS spectra of protein solutions. *European Biophysics Journal with Biophysics Letters, 30*(4), 256-267.

Middelberg, A. P. J. (1998). *The influence of peptide adsorption on interfacial tension.* Paper presented at the 2nd European Symposium on Biochemical Engineering Science, Porto.

Middelberg, A. P. J., Radke, C. J., and Blanch, H. W. (2000). Peptide interfacial adsorption is kinetically limited by the thermodynamic stability of self association. *Proceedings of the National Academy of Sciences of the United States of America, 97*(10), 5054-5059.

Miller, R., Wustneck, R., Kragel, J., and Kretzschmar, G. (1996). Dilational and shear rheology of adsorption layers at liquid interfaces. *Colloids and Surfaces A-Physicochemical and Engineering Aspects, 111*(1-2), 75-118.

Mohammed, R. A., Bailey, A. I., Luckham, P. F., and Taylor, S. E. (1993). Dewatering of crude-oil emulsions. 1. Rheological behavior of the crude-oil water interface. *Colloids and Surfaces A-Physicochemical and Engineering Aspects, 80* (2-3), 223-235.

Moore, W. J., and Eyring, H. (1938). Theory of the viscosity of unimolecular films. *Journal of Chemical Physics, 6*, 391-394.

Pace, C. N., Vajdos, F., Fee, L., Grimsley, G., and Gray, T. (1995). How to measure and predict the molar absorption-coefficient of a protein. *Protein Science, 4*(11), 2411-2423.

Perry, R. H., and Green, D. (1984). *Perry's Chemical Engineers' Handbook* (6th ed.), pp. 22:53 - 22:55. McGraw-Hill Book Company, New York.

Perutz, M. F., Kendrew, J. C., and Watson, H. C. (1965). Structure and function of haemoglobin. II. Some relations between polypeptide chain configuration and amino acid sequence. *Journal of Molecular Biology, 13*, 669-678.

Petkov, J. T., Gurkov, T. D., Campbell, B. E., and Borwankar, R. P. (2000). Dilatational and shear elasticity of gel-like protein layers on air/water interface. *Langmuir, 16*(8), 3703-3711.

Polson, A. (1950). Some aspects of diffusion in solution and a definition of a colloidal particle. *Journal of Physical and Colloid Chemistry, 54*, 649-654.

ProtParam. (2000). *Sequence beta-lactoglobulin and lysozyme*, [Web site]. Available: http://expasy.cbr.nrc.ca/cgi-bin/protparam [2000, 31st August].

Prusiner, S. B. (1991). Molecular biology of prion diseases. *Science, 252*(5012), 1515-1522.

Rapaport, H., Kjaer, K., Jensen, T. R., Leiserowitz, L., and Tirrell, D. A. (2000). Two-dimensional order in beta-sheet peptide monolayers. *Journal of the American Chemical Society, 122*(50), 12523-12529.

Rappé, A. K. (1997). *Molecular Mechanics across Chemistry*, pp. 89. University Science Books, Sausalito, California.

Riordan, J. F., and Vallee, B. L. (1972). Reactions with N-ethylmaleimide and p-mercuribenzoate. *Methods in Enzymology, 25*, 449-456.

Russell, C. J., King, D. S., Thorgeirsson, T. E., and Shin, Y. K. (1998). De novo design of a peptide which partitions between water and phospholipid bilayers as a monomeric alpha-helix. *Protein Engineering, 11*(7), 539-547.

Schaefer, V. J. (1938). Expansion patterns of protein monolayers on water. *Journal of Physical Chemistry, 42*, 1089-1098.

Schiffer, M., and Edmunson, A. B. (1967). Use of helical wheels to represent the structures of proteins and to identify segments with helical potential. *Biophysical Journal, 7*, 121-135.

Segrest, J. P., Deloof, H., Dohlman, J. G., Brouillette, C. G., and Anantharamaiah, G. M. (1990). Amphipathic helix motif - Classes and properties. *Proteins: Structure Function and Genetics, 8*(2), 103-117.

Stryer, L. (1995). *Biochemistry* (4th ed.), pp. 603-628. W. H. Freeman and Company, New York.

Taylor, G. I. (1934). The formation of emulsions in definable fields of flow. *Proccedings of the Royal Society of London, A146*, 501-523.

Tupy, M. J., Blanch, H. W., and Radke, C. J. (1998). Total internal reflection fluorescence spectrometer to study dynamic adsorption phenomena at liquid/liquid interfaces. *Industrial & Engineering Chemistry Research, 37*(8), 3159-3168.

Walstra, P. (1993). Principles of emulsion formation. *Chemical Engineering Science, 48*(2), 333-349.

Walstra, P. (1996). *Encyclopedia of Emulsion Technology*, Vol. 4(1). Marcel Dekker, New York.

Walstra, P., and Deroos, A. L. (1993). Proteins at air-water and oil-water interfaces - Static and dynamic aspects. *Food Reviews International, 9*(4), 503-525.

Ward, A. F. H., and Tordai, L. (1946). Time-dependence of boundary tensions of solutions. *Journal of Chemical Physics, 14*(7), 453-461.

Wijmans, C. M., and Dickinson, E. (1999). Brownian dynamics simulation of the displacement of a protein monolayer by competitive absorption. *Langmuir, 15*(24), 8344-8348.

Williams, A., Janssen, J. J. M., and Prins, A. (1997). Behaviour of droplets in simple shear flow in the presence of a protein emulsifier. *Colloids and Surfaces A-Physicochemical and Engineering Aspects, 125*(2-3), 189-200.

Williams, A., and Prins, A. (1996). Comparison of the dilational behaviour of adsorbed milk proteins at the air-water and oil-water interfaces. *Colloids and Surfaces A-Physicochemical and Engineering Aspects, 114*, 267-275.

Wolf, B., Byekwaso, E., and Windhab, E. (1996). *Food emulsion processing with optimized rotor/stator dispersing devices.* Paper presented at the 5th World Congress of Chemical Engineering, San Diego, California.

Wustneck, N., Wustneck, R., Fainerman, V. B., Miller, R., and Pison, U. (2001). Interfacial behaviour and mechanical properties of spread lung surfactant protein/lipid layers. *Colloids and Surfaces B-Biointerfaces, 21*(1-3), 191-205.

Xu, G. F., Wang, W. X., Groves, J. T., and Hecht, M. H. (2001). Self-assembled monolayers from a designed combinatorial library of de novo beta-sheet proteins. *Proceedings of the National Academy of Sciences of the United States of America, 98*(7), 3652-3657.

Zayas, J. F. (1997). *Functionality of Proteins in Food*, pp. 139-144. Springer-Verlag, Berlin.

Zhang, S. G., Holmes, T., Lockshin, C., and Rich, A. (1993). Spontaneous assembly of a self-complementary oligopeptide to form a stable macroscopic membrane. *Proceedings of the National Academy of Sciences of the United States of America, 90*(8), 3334-3338.

Zhang, Z., Ferenczi, M. A., and Thomas, C. R. (1992). A micromanipulation technique with a theoretical cell model for determining mechanical-properties of single mammalian-cells. *Chemical Engineering Science, 47*(6), 1347-1354.

Zurowska-Pryczkowska, K., Sznitowska, M., and Janicki, S. (1999). Studies on the effect of pilocarpine incorporation into a submicron emulsion on the stability of the drug and the vehicle. *European Journal of Pharmaceutics and Biopharmaceutics, 47*(3), 255-260.